Australian Government
Bureau of Meteorology

Victorian Climate Initiative annual report 2014-15

Hope, P., Timbal, B., Hendon, H. and Ekström, M. (eds.)

October 2015

Bureau Research Report - 005

Victorian Climate Initiative annual report 2014-15

Hope, P., Timbal, B., Hendon, H. and Ekström, M. (ed.s)

Bureau Research Report No. 005

October 2015

National Library of Australia Cataloguing-in-Publication entry

Editors: Hope, P., Timbal, B., Hendon, H. and Ekström, M.

Authors : Hope, P., Timbal, B., Hendon (Bureau of Meteorology/R&D), H., Ekström, M. (CSIRO/LW), Moran, R. (independent expert), Manton, M. (independent expert), Lucas, C., Nguyen, H., Lim, E-P., Luo, J-J., Liu, G., Zhao, M., (Bureau of Meteorology/R&D), Fiddes S. (Melbourne University), Kirono, D., Wilson, L., (CSIRO/OA), Potter, N. and Teng, J. (CSIRO/LW)

Title: Victorian Climate Initiative annual report 2014-15

ISBN: 978-0-642-70666-9

Series: Bureau Research Report - BRR005

Enquiries should be addressed to:

Bertrand Timbal

Bureau of Meteorology
GPO Box 1289, Melbourne
Victoria 3001, Australia

Contact Email: b.timbal@bom.gov.au

Copyright and Disclaimer

Contents

EXECUTIVE SUMMARY

The Victorian Climate Initiative (VicCI) was established in 2013 as a three-year program of research to inform strategies aimed at ensuring the sustainable management of water resources and the provision of secure water supplies for urban and rural water users and the environment. The program is a partnership between the Victorian Department of Environment Land Water and Planning (DELWP), the Bureau of Meteorology and CSIRO. It builds on the results of the South Eastern Australia Climate Initiative (SEACI), which ran from 2006 to 2012.

There are three themes of research in VicCI aimed at (1) improving seasonal climate prediction for Victoria, (2) improving understanding of past climate variability and change in Victoria, and (3) improving understanding of future climate and the associated risks to water resources in Victoria. Progress has been made in each of the three themes over the first two years of the program, with the key gains made in the second year being:

- improved understanding of decadal-scale variations in the predictability of seasonal rainfall in Victoria;
- increasing understanding of the effects of the changing large-scale atmospheric circulation on Victoria's rainfall; and
- initial projections of future runoff in selected Victorian catchments.

The climate of Victoria is influenced by a number of large-scale factors, such as the El Niño – Southern Oscillation (ENSO), the Indian Ocean Dipole (IOD) and the Southern Annular Mode (SAM), that represent the effects of the Pacific, Indian and Southern Oceans surrounding Australia and internal and externally forced atmospheric variability. Key investigations have clarified, not only the influence of each factor on Victoria's climate, but also the interactions among these factors. For example, the intensity of the flooding rains during La Niña in spring of 2010 was due to the alignment of ENSO, IOD and SAM, together with warmer sea surface temperatures to the north of Australia. The warmer sea surface temperatures at least partly reflect the swing of the Inter-decadal Pacific Oscillation (IPO) to its 'cold' phase since the late 1990s. While the current 'cold' phase of the IPO means that the lead-time for prediction of development of El Niño or La Niña is limited to a season at best, it also means that rainfall in Victoria is more closely related to ENSO and IOD than in periods (such as the 1980s and 1990s) when the IPO is in its 'warm' phase. Hence, the high springtime rainfall associated with the La Niña of 2010 was highly predictable from the preceding winter. While the IPO remains in its 'cold' phase, there is also an increased risk of flooding in spring-summer in Victoria. The onset of the very strong 2015 El Niño has been predicted by the Bureau of Meteorology well ahead of its maturation, which may reflect that the IPO has already swung to its warm phase after the demise of the weak El Niño in 2014.

These large-scale factors will continue to be dominant influences on seasonal and inter-annual rainfall variability for Victoria in the coming decades even in the face of ongoing anthropogenic climate change. The Bureau's seasonal streamflow forecast system includes the influences of these large-scale factors, and the forecasts are potentially useful for informing short-term water management strategies.

The global climate models used to develop future projections of climate change due to anthropogenic activities can be evaluated by comparing their simulations of past climate with observations. Some large-scale factors, such as the IPO, have little or no predictability, which means there is some inherent uncertainty in all long-term climate projections. Models should generally capture the observed relationships between large-scale factors and regional climate but their capabilities are limited. For example, while they have some skill in simulating the observed relationship between SAM and Victorian rainfall, the models yield too large an increase in summer rainfall and too small a decrease in winter rainfall when SAM is increasing. Hence, although a shift to high SAM is a robust projection in response to increasing greenhouse gases, there still remains uncertainty for the impacts in Victoria as a result of systematic model errors in the depiction of key drivers of SEA climate.

Since SEACI, it has been known that the rainfall of Victoria is influenced by the sub-tropical ridge (STR), which is the region of high surface pressure associated with the sinking arm of the Hadley cell that transfers heat from the tropics toward the poles. While some models can simulate the seasonal variations of the STR, they tend to under-estimate the relationship between the STR and Victorian rainfall. Similarly, the models do not capture the full extent of the observed expansion of the Hadley cell in recent decades. Nonetheless, careful analysis suggests that since 1979 about 30% of the expansion is due to natural factors (volcanoes and ENSO), 40% is from stratospheric ozone depletion, and 30% is from increasing greenhouse gases. On a longer time-scale (since the 1960s), anthropogenic forcings (greenhouse gases and stratospheric Ozone) are the dominant drivers.

Despite the limitations in the capability of global climate models, our current understanding of the interactions between the large-scale climate factors and the consistent results from models suggest that there will be a continuing decline in cool-season rainfall and possibly an increase in warm-season rainfall. This suggests that the traditional cool season filling period for water supply systems may not be as reliable into the future, but impacts may be offset by enhanced warm season rainfall. However, in any particular year, the effects of long-term trends will be modulated by the behaviour of the natural large-scale factors, ENSO, IOD and SAM.

While there are clear uncertainties in the projections of global climate models, they do provide the optimal approach to the estimation of future climate change. A range of techniques is being developed to translate model output for application to climate-sensitive activities, such as water management, at local levels. It is found that biases in the output of climate models can be amplified when used in hydrological models to estimate changes in runoff. The removal of bias is therefore an important step in the 'downscaling' of climate model output for application at local or catchment scales. Both statistical and dynamical downscaling techniques can provide useful results for application at local scales.

A simple statistical model, that relates streamflow to local gridded rainfall, has been used successfully to simulate past streamflow in a number of Victorian catchments. This method was applied using downscaled rainfall projections from global climate models to estimate future changes in streamflow in those catchments. Results from this novel approach which incorporate a climate change signal with a high spatial resolution will be compared with the projections

from traditional rainfall-runoff models where the climate change signal inherently remains at a coarse resolution. However, because the key factors in runoff projections are the climate projections from the global climate models and because the rainfall projections used in the runoff projections prepared during SEACI are generally similar to those recently prepared for Victoria by CSIRO and the Bureau of Meteorology, the updated projections arising from VicCI are not expected to be substantially different from the earlier ones from SEACI. The inherent uncertainties in the natural climate system, as well as in the factors leading to anthropogenic climate change, mean that robust and adaptive approaches need to be applied to the planning and management of future water resources.

BACKGROUND

Effective management of the water resources of Victoria is needed to secure sustainable water supplies for urban and rural users and for the environment. Such management is dependent upon knowledge of the availability of water resources over time scales from weeks to decades ahead. In turn, the availability of water resources for Victoria is critically dependent on variations in the climate of the region. The Victorian Climate Initiative (VicCI) was established in 2013 as a three-year program of research to inform Victorian water resource planning and management through:

- improved prediction and understanding of the climate system and its representation by climate models; and,
- improved understanding of the linkages between climate and water availability.

This strategic knowledge provides the basis for improved projections of future climate and associated water availability in Victoria; in particular, it enhances knowledge of the uncertainties in future projections.

The VicCI program is a partnership between the Victorian Department of Environment Land Water and Planning (DELWP), the Bureau of Meteorology and CSIRO. It builds on the results of the South Eastern Australia Climate Initiative (SEACI), which ran from 2006 to 2012. A primary motivation for SEACI was the need to understand the causes of the Millennium Drought (1997–2009), which was the worst drought for south-eastern Australia for more than a hundred years. The Millennium Drought was unusual in its duration, severity and extent. It was unprecedented in being largely restricted to southern Australia, in having a large rainfall decline in autumn, and in having much reduced inter-annual rainfall variability. Moreover, the decline in rainfall led to a larger than anticipated decrease in runoff, which was a challenge for water management and planning.

The rainfall decline in the Millennium Drought extended across the cool season (April–October), and it appeared to be related to changes in the Hadley cell—the large-scale north–south (meridional) atmospheric circulation that transports the sun's energy from equatorial regions to higher latitudes. There was evidence from SEACI that the Hadley cell is expanding at a rate of about 0.5° latitude (50 km) per decade. The extent of the Hadley cell is associated with both the intensity and the position of the sub-tropical ridge. Its expansion leads to an expanded sub-tropical dry zone, pushing mid-latitude storms further south to miss Victoria and

resulting in reduced rainfall across southern Australia. The cool season rainfall deficits were shown to persist even when the drought was broken by spring–summer rainfall in 2010–11. There was also some evidence that the changes in the meridional circulation are at least partly attributable to human activities and so may be likely to continue, but the relative importance of global warming and Antarctic ozone depletion was not resolved.

Research in SEACI included support for the development of the Predictive Ocean Atmosphere Model for Australia (POAMA) modelling system for seasonal climate prediction in the Bureau of Meteorology, and the incorporation of POAMA output into the Bureau's operational seasonal streamflow forecast system. The POAMA model was used for studies on the nature and causes of seasonal and inter-annual variations in the climate of Victoria. From SEACI and related research, it is apparent that these variations are influenced by at least three large-scale features of the global climate system: the El Niño – Southern Oscillation (ENSO), which characterises atmosphere–ocean interactions across the Pacific Ocean; the Indian Ocean Dipole (IOD), which characterises atmosphere–ocean interactions in the Indian Ocean; and the Southern Annular Mode (SAM), which characterises the intensity and position of higher-latitude westerly winds and associated storm systems. While the influence of each feature is well understood individually, much is to be learned about the interactions between them, and between them and global warming.

Climate model simulations from SEACI and related programmes (using a worldwide set of models known as CMIP3, associated with the Fourth Assessment of the IPCC) indicate that, owing to global warming, both rainfall and runoff will decline over future decades in the southern part of south-eastern Australia. However, associated with the Fifth Assessment of the IPCC, a new set of global climate model projections (CMIP5) has been computed by the major modelling centres around the world. It is therefore appropriate to determine whether these new projections will lead to substantial revision of hydro-climate projections for Victoria.

The VicCI program aims to resolve some of the key challenges remaining after SEACI. Its focused research on climate variability, predictability and change will:

- improve predictions of water availability in the short term (seasonal to inter-annual time scales), which have the potential to inform drought response strategies and outlooks for urban supplies, and processes for seasonal determinations for rural supplies and risks of spill for irrigation systems; and
- underpin an improved assessment of the risks to water resources and supplies from changes in climate over the medium to longer term, based on improved understanding of the climate system and its representation by climate models.

The program is composed of seven projects under three broad themes:

- improved seasonal climate predictions
- improved understanding of past climate variability and change
- improved understanding of future climate and associated risks to water resources.

See http://www.cawcr.gov.au/projects/vicci/documents/Science_plan_final.pdf to access the detailed initial science plan for VicCI.

The program is integrated across time scales and themes, so that the work to improve understanding of climate variability feeds directly into the work to assess seasonal to multi-year predictability and into the work to assess climate model simulations, which in turn are used for projections of the future climate of Victoria. The research program has strong connections to related programs being undertaken in Australia and overseas. For example, in south-eastern Australia, results from VicCI complement other regional programs such as NARCliM, Goyder Institute for Water Research, and Climate Futures for Tasmania, which are focused on the development of specific regional climate change projections. Nationally, VicCI is working directly with CSIRO and the Bureau of Meteorology to connect the NRM climate change projections with water resource needs in Victoria. Internationally, the work of VicCI is linked with initiatives of the World Climate Research Programme and with development of modelling capability at the UK Meteorology Office.

This report provides a description of progress over the first two years of VicCI. The Science Plan for VicCI lists a number of key science questions to guide each project. The next section in this report summarises the key findings across the research themes and highlights the implications of the results for water management and planning in Victoria. The following section provides a summary of the progress towards answering the key science questions and lists the direction of research in the third year. The final six sections give detailed descriptions of the research undertaken in year two and results for each of the projects. The key gains during the second year are:

- improved understanding of decadal-scale variations in the predictability of seasonal rainfall in Victoria;
- increasing understanding of the effects of the changing large-scale
- atmospheric circulation on Victoria's rainfall; and
- initial projections of future runoff in selected Victorian catchments.

KEY FINDINGS ACROSS THEMES AND IMPLICATIONS FOR WATER RESOURCES PLANNING AND MANAGEMENT

The Victorian Climate Initiative (VicCI) program has three theme areas of research aimed at improving seasonal climate prediction for Victoria, improving our understanding of past variability and change in Victoria, and improving our understanding of future climate and the associated risks to water resources in Victoria. Each of the seven projects in the program focuses on a particular aspect of the research themes. However, the results of the individual projects can be integrated to provide a comprehensive view of our increasing understanding of the climate of Victoria. The following summary highlights the key findings from the research in VicCI over the last two years. The implications of the research results for water resources planning and management are highlighted in boxes throughout the section.

Improved understanding and prediction of the climate of Victoria

The climate of south-eastern Australia is influenced by several large-scale features of the climate system that operate on time scales from weeks to decades (Figure 1). The Southern Annular Mode (SAM) characterises the intensity and position of higher-latitude westerly winds and associated storm systems, the Indian Ocean Dipole (IOD) characterises atmosphere–ocean interactions in the Indian Ocean, the El Niño – Southern Oscillation (ENSO) characterises atmosphere–ocean interactions across the Pacific Ocean, and the Inter-decadal Pacific Oscillation (IPO) is a sea-surface temperature pattern in the Pacific Ocean related to decadal modulation of ENSO. The demonstrated impacts of ENSO, IOD and SAM on Victorian climate highlight the importance of the three oceans (Pacific, Indian and Southern Oceans) to this region. In addition to these natural features of the climate system, global warming is also a factor affecting the climate of Victoria. Recent research has enhanced our understanding of not just the influences of each factor on the climate of Victoria but more importantly the interactions between these factors.

Interactions between ENSO, IOD and the rainfall of south-eastern Australia vary on decadal time scales. Over the last 40 years, the changes on one hand in the relationship between ENSO and IOD and on the other hand between their impacts on south-eastern Australian rainfall have evolved together. The impacts on rainfall are greatest in the decades when ENSO and IOD have small amplitude and they are weakly related. These variations are related to the phase of the IPO. Unfortunately there appears to be no predictability in the phase swings of the IPO.

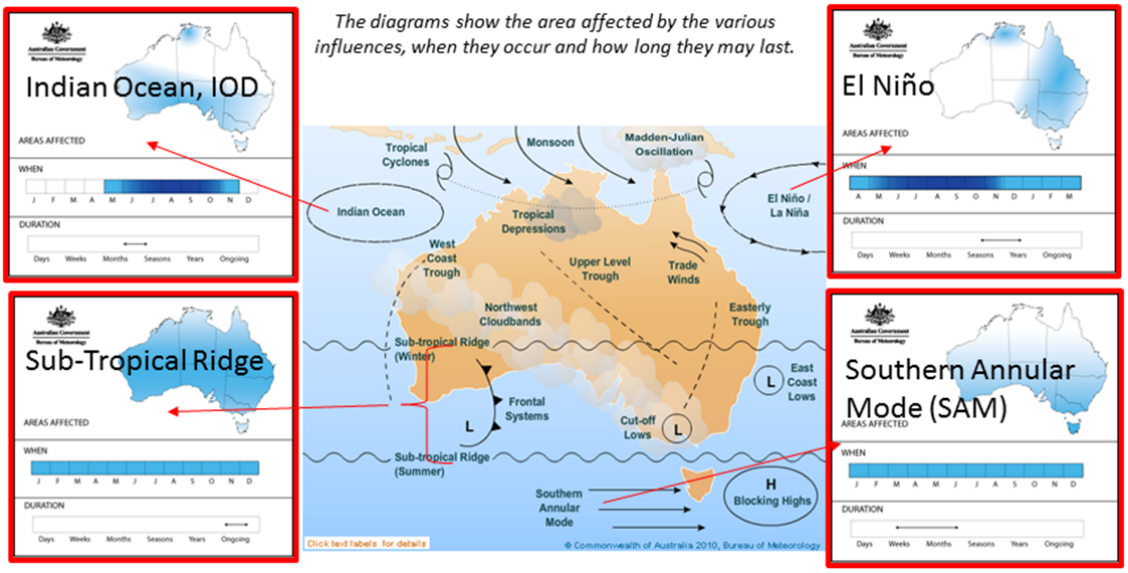

Fig. 1 Key large-scale influences affecting Victorian rainfall: depicted here are four large-scale influences which are particularly important for the climate of Victoria (for each influence, an estimate of the area of influence is depicted on the map and the annual cycle of that influence is indicated as well as the typical duration of that influence) and which are extensively the focus of on-going research in VicCI (sourced from www.bom.gov.au/climate/about).

There has been a swing of the IPO since 1999 to its cold phase (that is, cooler sea-surface temperatures in the east Pacific and warmer in the west). This is associated with reduced variability and predictability of ENSO. A cold IPO phase means a warming of the waters north of Australia. Thus the IPO cold phase has a similar signature to global warming in the sea-surface temperatures north of Australia. These combined factors enhanced the recent La Niña event in the spring of 2010, leading to extreme rainfall in south-eastern Australia in spring and summer. This event was also associated with strongly positive SAM (that is, weaker westerly winds with storm tracks further southward than normal). The alignment of ENSO and SAM at that time not only enhanced rainfall but also increased the predictability of SAM. Thus, although the IPO was in its cold phase, the rain events of spring 2010 could be predicted some months ahead.

While the longer lead-time predictive skill of ENSO has been lower since the late 1990s compared with 1980-1999 when the IPO was in its warm phase, the short lead-time seasonal prediction skill of Victorian rainfall has been higher, especially in spring. This increase in predictability is due to stronger links between ENSO and IOD and Victorian rainfall associated with reduced strengths of ENSO and IOD. These relationships are also consistent with the observation that Victorian rainfall tends to vary more directly with ENSO indicators in La Niña (wet) years than in El Niño (dry) years. These inter-connections further highlight the importance of both the Indian and Pacific Oceans to the climate of Victoria, and so they imply that it is necessary to improve the representation of the Indian Ocean in climate models both for seasonal prediction and for long-term projections.

The relationship between ENSO and SAM is relevant in dry periods as well as wet. The near-record drought over eastern Australia in the spring of 2002 has been shown to be due not only to the moderate El Niño event, which had its maximum sea-surface temperature warming in the central (rather than eastern) Pacific, but also to the stronger negative phase of the SAM at that time.

Importance of the three oceans

The state of the three oceans (represented by ENSO, IOD and SAM) will continue to be a dominant influence on seasonal and inter-annual rainfall variability in Victoria. They have 'dry' and 'wet' phases which may occur in concert with or in opposition to each other.

Given the current negative phase of the IPO it can be expected that:

- the lead time for skilful prediction of ENSO and IOD events will be reduced to around one season due to the reduced amplitude of these events;
- there is a lower likelihood of ENSO and the IOD both being in the same phase (i.e. both dry or both wet) than when the IPO is in a positive phase;
- there will be enhanced influences of ENSO and IOD events on south-eastern Australian rainfall and better predictive skill at short lead times, due to the stronger teleconnections.

La Nina events may be more frequent given the negative phase of the IPO, and their impacts on Victorian rainfall are likely to be enhanced as a result of the additional influence of warming sea surface temperatures to the north of Australia.

Anthropogenic influences (increasing greenhouse gases and stratospheric ozone depletion) are contributing to current positive trends in SAM. This also is expected to enhance spring and summer rainfall.

Overall, this suggests an enhanced risk of flooding in spring and summer, at least while the IPO remains in its negative phase. In the event of the IPO switching to a positive phase, which has increased in likelihood in 2015 due to the large 2015 El Niño on-going, we would expect to see increased lead time for skilful prediction of ENSO and IOD events, enhanced likelihood of 'dry' ('wet') ENSO events occurring in conjunction with 'dry' ('wet') IOD events, but lower predictability of, and weaker, impacts on south- eastern Australian rainfall associated with ENSO/IOD events due to weaker teleconnections.

The Bureau's seasonal streamflow forecasting system captures the influence of the state of the three oceans via the incorporation of various climate indices into the predictive system where they add predictability. These forecasts are potentially useful for informing short-term management strategies in relation to drought response, seasonal allocations, environmental watering, water market planning and in estimating risks of spill.

The large-scale meridional circulation of southern hemisphere climate (Figure 2) is important to the climate of Victoria: convection across the tropics drives the rising arm of the Hadley cell (HC) with its descending arm around 30 degrees from the equator. Averaged around the hemisphere, the HC is expanding at a rate of about 0.5 degree (50 km) per decade. However, the change is not steady: there was a jump in the late 1990s following the major El Niño of 1997-98. Moreover, the expansion varies around the hemisphere, with the greatest expansion in the Australian region where the warm waters of the maritime continent strongly drive the upward arm of the HC. These local variations occur at seasonal as well as inter-annual time scales. The recent expansion of the HC can be linked to the cold phase of the IPO (that is, La Niña-like conditions), with warmer waters to the north of Australia. In turn, the HC expansion is also likely to be associated with the positive phase of the SAM, with the mid-latitude jet-steam shifted poleward.

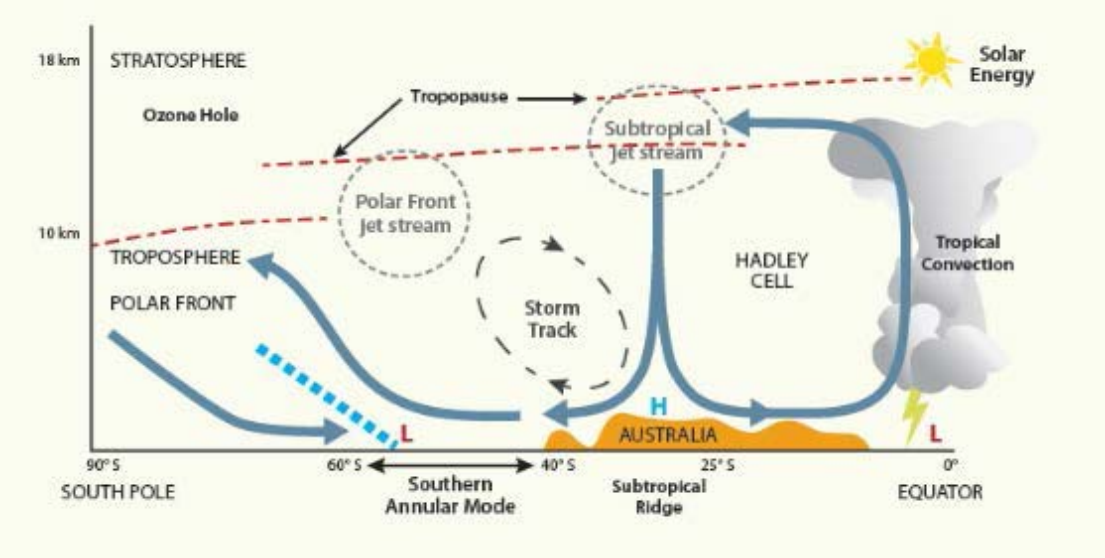

Fig. 2 Mean meridional circulation features of relevance to Victorian climate: as Victoria is located between 34 and 38 degrees south, it is directly influenced by the sub-tropical ridge under the sinking arm of the Hadley cell. Changes in the Hadley cell and Southern Annular Mode (SAM) are related to changes in mid-latitude storm track.

The sub-tropical ridge (STR) is the region of high-pressure at the surface associated with the sinking arm of the HC around 30 degrees south in the Australian region. Variations in the latitude and intensity of the STR over the longitude of eastern Australia have been shown to be associated with the recent drying around Victoria, especially in the cool season (April to October). The variations in the position and intensity of the STR are found to be related to variations in the HC on a hemispheric scale, except in winter. There is evidence that variations in the STR are associated with variations in heating in the tropical Indian Ocean, and that the pathway for these interactions is affected by the intense mid-latitude jet-stream that moves nearer southern Australia in winter. The effects of these interactions on the relationship between the HC and the STR are more complex when analysed on a regional (rather than hemispheric) scale (i.e. Australasian sector).

An initial hypothesis in VicCI was that expansion of the HC leads to a reduction in the cool season rainfall of Victoria. However, recent work suggests that regional (rather than hemispheric) expansion in the HC is more obviously associated with wetter conditions over much of northern and eastern Australia (that is, with southward extension of tropical rainfall) with little impact in Victoria. Further research is needed to clarify the relationship between regional variations in the HC and the STR and their relationship to the local observation based STR, which has been shown to be linked to the cool season rainfall reduction across Victoria.

Analysis of simulations from global climate models shows that they do not capture the full extent of the observed HC expansion. In particular, we know that the recent cold phase of the IPO has contributed to HC expansion, but the variations of the IPO are not captured well by the climate models. It is therefore difficult to accurately attribute the causes of HC expansion from model simulations. On the other hand, simulations with the warmest global mean temperatures (that is, with greenhouse gases forcing but no stratospheric ozone deficit) show the greatest HC expansion and poleward movement in the STR.

It is clear that hemispheric-scale HC expansion is associated with increasing global mean temperature. Models with both greenhouse gases forcing and stratospheric ozone deficit have the largest increase in intensity of the STR. These results again highlight the complexity of the

interactions between the components of the large-scale meridional circulation in the Australian region. Careful analysis of the model simulations suggests that since 1979 about 30% of HC expansion in the Southern Hemisphere is from natural factors (volcanoes and ENSO), 40% from stratospheric ozone depletion, and 30% from greenhouse gases forcing. For the longer trend, since the 1960s, analysis of the single forcing simulations shows that stratospheric ozone depletion and enhanced greenhouse gases are the dominant forcings of tropical expansion.

The poleward shift of the mid-latitude storm track in winter is associated with drier conditions in southern Australia; that is, the positive phase of SAM tends to lead to dry conditions in Victoria. In spring and summer, positive SAM leads to a greater excursion of tropical rainfall into southern Australia and so to wetter conditions in Victoria. To some extent climate models are able to simulate the relationship between SAM and sub-tropical rainfall. However, there is substantial bias, with too large an increase in sub-tropical rainfall in summer when SAM is increased. Moreover, the winter reduction in sub-tropical rainfall with increasing SAM is under-estimated by the models. Similarly, models do not capture the seasonal variations of the correlation between SAM and ENSO; they particularly under-estimate the strength of this relationship in summer.

We have seen that global climate models run over long periods have difficulty in capturing several important factors relevant to the climate of Victoria. However, the Bureau's current seasonal prediction system (POAMA) has useful skill in predicting climate variability a few months ahead. The present situation, with the IPO in a cold phase, means that the predictability of El Niño and La Niña events is limited. On the other hand, POAMA represents the impacts of SAM well, and so it was able to provide useful predictions of the enhanced impacts of recent La Niña events some months ahead. Moreover, because the model is initialised with the present state of the IPO, the background state of the model is properly set for each forecast.

Some trials have been carried with POAMA running multi-year forecasts. However, initial analysis of these forecasts suggests that there is little predictability of the La Niñas of 2010 and 2011 with the current version of the model. Until the Bureau's model is updated, the capability of other overseas models to capture such multi-year events will be monitored and reported by VicCI.

Improved projections of the future climate and water availability for Victoria

In January 2015, CSIRO and the Bureau of Meteorology released a report on climate change in Australia with projections for Australia's natural resource management (NRM) regions. The projections are based on the global climate models used in the Fifth Assessment Report of the IPCC. The overall projections for Victoria from the NRM reports (CSIRO and Bureau of Meteorology, 2015; Timbal et al. 2015; Grose et al. 2015) suggest that:

- warming will continue and the amount of warming after 2050 will primarily depend on the rate of emission of greenhouse gases;
- temperature increases of 0.5 °C to 1.3 °C are expected by 2030 in all future scenarios, with warming of up to 4.6 °C by 2090 for the highest emission scenario;
- the hydrological cycle will change and, although the main drivers of climate variability will continue to exert a strong influence, a rainfall reduction during the cool season is likely;
- extreme hot temperatures will increase and be more frequent, and heavy rainfall extremes are
  likely to increase.

Thus the observed warming trend over the past century will continue. While the pace of the warming, during the second half of the century, will depend primarily on the emissions pathway, uncertainties due to global climate model sensitivities and natural decadal variability will dominate during the first half of the century. Climate change will not be limited to warming trends but will affect the hydrological cycle through changes in rainfall and other climate variables, such as evapotranspiration. It is worth noting as well that natural variability and gradual climate change can combine into abrupt changes for all these variables as observed.

Comparison of SEACI and NRM Rainfall Projections for 2°C Warming

	SEACI PROJECTIONS (2011) (2°C warming 2060 A1B)			**NRM PROJECTIONS (2014)** (~2°C warming 2090 RCP4.5*) [1.9° (1.2° – 2.5°)]		
	Change in future rainfall (%)			**Change in future rainfall (%)****		
	10th%ile Wet	**50th%ile Median**	**90th%ile Dry**	**10th%ile Wet**	**50th%ile Median**	**90th%ile Dry**
Average N Vic Basins (N=8)	0	-9	-17	+4	-6	-16
Average S Vic Basins (N=18)	-2	-9	-16	+3	-3	-10
Average SW Vic Basins (N=9)	-5	-11	-16	+3	-7	-15
Average SE Vic Basins (N=9)	0	-9	-16	+3	-5	-14

*see Figure 3.5.1 Technical Report 'Climate Change in Australia"

** see Appendix in Southern Slopes and MDB Cluster Reports and Summary Brochures

Overall, NRM results for the 'dry' (90th %ile) scenario are very similar to the SEACI projections for both 1° and 2° C warming. Only the 2° C warming results are shown here. Broadly speaking, the NRM results for the 'wet' (10th %ile) scenario are typically around 5% wetter than the SEACI projections, while NRM results for the median scenario are slightly (<5%) less dry than the SEACI projections.

While updated streamflow projections are yet to be generated for Victoria, given the similarity of the rainfall projections between SEACI and NRM, it is expected that updated projected streamflow reductions will generally be similar, noting that streamflow reductions would typically be expected to be two to three times greater than the reductions in rainfall. These rainfall comparisons indicate that, in relation to climate change projections, the context for developing updated strategic plans will not be very different from the case in 2011-2012. It also follows that, as was the case with the SEACI projections, projected future declines in streamflow for around 2065, even for the 'dry' scenario, are likely to be around the same magnitude or less severe than the reductions in streamflow experienced during the Millennium Drought across most of the State.

However, it must be recognised that the projected changes are relative to a specified baseline climate. While the baseline period for SEACI is 1895-2008 and it is 1986-2005 for NRM, the average annual rainfall is similar for both periods. Because there is uncertainty in the degree to which climate change has affected a baseline and because models tend to under-estimate natural variability, it is difficult to select a baseline that is representative of the current climate while also encompassing an appropriate range of natural climate variations.

While these changes are less certain than those for temperature, a convergence is seen amongst models toward a reduction of rainfall during the cool period of the year, with no clear direction for the warm season. These results are similar to those found from models used in the IPCC Fourth Assessment Report, and so it is likely that updated projections of future streamflow will

not be substantially different from those prepared from SEACI research. This conclusion is supported by the comparison of SEACI and NRM rainfall projections in the box below.

Research in VicCI has involved not only work towards revised projections of streamflow for Victorian catchments, but also investigations of the uncertainties associated with climate model projections. In particular, the capacity of the models to simulate the observed relationships between Victorian climate and large-scale factors such as SAM and the STR has been studied.

The climate models predict higher values of SAM in all seasons in the future under global warming; that is, the response is similar to warming temperatures in the western Pacific due to the IPO in its cold phase. This response leads to wetter conditions in spring and summer in Victoria, but drier conditions in winter. The upward trend in SAM is also at least partly associated with stratospheric ozone depletion, and this forcing will reduce as the ozone layer recovers in coming decades. While the impact of SAM on Victorian rainfall may seem to be a robust result from the models, we should bear in mind that this relationship is not properly captured in simulations of the present climate.

Some models are found to simulate the seasonal variations of the intensity and latitude of the STR. However, they tend to under-estimate the relationship between the STR and Victorian rainfall. Further, the models do not simulate well the magnitude of the observed trends in the intensity of the STR and the associated reduction in rainfall in Victoria. Analysis of projections of future climate shows that the STR continues to intensify and to move poleward. However, given the inability of models to capture the magnitude of past trends, it is possible that the projected changes in the STR and the reduced rainfall in Victoria are underestimated.

Continuing Cool Season Rainfall Decline and Enhanced Spring-Summer Rainfall

Current and projected longer-term trends in the STR and SAM suggest the likelihood of a continuing, and possibility intensifying, cool season (April to October) rainfall deficit together with enhanced spring-summer rainfall.

Of concern is the fact that there are a number of reasons to expect that projected cool season rainfall deficits may be underestimated by current climate models, particularly for the winter months:

1. Climate models do not capture the magnitude of observed trends in the STR and the associated magnitude of reductions in rainfall for Victoria and therefore are likely to be under-predicting future trends and their associated impacts on rainfall
2. To date there has not been a statistically significant trend in SAM in winter, so the cool season rainfall deficit that is already occurring is expected to be largely attributable to changes in the sub-tropical ridge. An emerging positive trend in SAM in winter would therefore be likely to further intensify the rainfall decline during winter months.
3. For Victorian latitudes, climate models have been shown to under-predict the rainfall decline associated with SAM in winter.

This suggests that the traditional cool season filling period for water supply systems may not be as reliable into the future, but impacts may be offset by enhanced warm season rainfall. However, in any particular year, the effects of long-term trends will be modulated by the behaviour of the natural large-scale factors, ENSO, IOD and SAM.

The studies of global climate models have been extended to examine the relationship between the sea-surface temperature (SST) patterns to the north of Australia and the rainfall of Victoria. While most models capture some of the relationship between tropical SSTs and Victorian rainfall, the relationship is generally found to be much weaker than the observed correlation. The relationship between SST and rainfall in models is found to be unchanging into the future. Bearing in mind that the relationship has been observed to vary in strength on decadal time-scales in the past, this result suggests these modulating variations are due to natural factors rather than greenhouse gases forcing.

The most notable feature of Victorian climate over the last couple of decades is the Millennium Drought, which extended for over a decade: there were no 'wet' months for a record 121 months. Despite the magnitude of this event, no climate model has captured this feature. Moreover, there is little relationship between the overall skill of a model and its capacity to generate long periods without very wet months. Initial analysis of model projections suggests that the frequency of long spells without very wet months similar to the Millennium drought will not change significantly over the present century. Although the frequency of these very long spells may not vary significantly, the overall frequency and severity of droughts is likely to increase over the century (Timbal et al., 2015). While there are clear uncertainties in the projections of global climate models, they do provide the state-of-the-art estimates of the likely range of future climate change.

A range of techniques is being developed to translate model output for application to climate-sensitive activities, such as agriculture and water management, at local levels. Studies have been carried out in VicCI on the options for translating the climate model output particularly for use in local or catchment scale hydrological models. It is found that bias correction is an important step in preparing climate model output for local-scale applications. Such adjustments are needed because bias in climate model output can be amplified when fed into application models, especially on seasonal time scales.

Analysis of the chain of uncertainty in the development of streamflow simulations shows that the climate models are the main source of uncertainty. Nonetheless, it is difficult for current hydrological models to capture the full range of natural streamflow variability in Victoria which can extend from no-flow drought conditions to flooding conditions. This can lead to either a wet or dry bias in projections of future streamflow, depending on the range of the calibration period.

High-Resolution Downscaling

The results from the regional, high-resolution (convection resolving) downscaling model for the case study periods are promising. However, the fine resolution set-up is resource intensive, implying that with limited computing resources, important choices are required with regard to the simulation period and extent of spatial domain.

The resource intensiveness of such simulations will also constrain the range of scenarios and the number of models for which such downscaling can be performed, thus resulting in a limited representation of the uncertainty associated with projections.

The Simple Statistical Method for Generating Streamflow Projections

The method gave promising results when tested in 27 diverse catchments across Victoria using downscaled rainfall (and temperature) projections derived from 22 climate models as inputs (after a bias correction process was applied) to the statistical model to generate streamflow projections.

The applicability of the approach in catchments other than the 27 utilised in this study is dependent on being able to calibrate a ‘natural’ flow record against catchment rainfall, and derive and suitably bias-correct catchment-averaged downscaled rainfall projections.

The relatively coarse spatial resolution of global climate models means that they are not able to capture the features of many extreme weather events, especially extreme rainfall. Work has been carried out with a regional, high-resolution model, driven by output from a global climate model, to investigate the nature of extreme rainfall events in Victoria under climate change conditions. Three two-week study periods for the model have been chosen to align with flood events during the winter, spring and summer of 2010-2011. Evaluation of the daily rainfall patterns from the regional climate model are found to be sensitive to the representation of microphysical cloud processes in the model as well as the representation of turbulence near the surface.

A simple statistical model of the relationship between streamflow and local temperature and rainfall in several Victorian catchments has been developed. Including decadal variations in rainfall in the model leads to improvement in the estimates of streamflow. The model is able to capture the severity of the Millennium Drought. Based on the capacity of the model to simulate past hydro-climate variations, it has been used to estimate future changes in streamflow in a number of Victorian catchments. Careful statistical adjustments to the output of the global climate models are required to reduce known biases in the climate models. These projections will provide a benchmark for more detailed hydrological projections for Victoria to be carried out in the future

Use of Climate Change Projections for Water Supply Planning

It is important that users understand the limitations of global climate models in realistically representing the behaviour of key influences on Victoria's climate and associated impacts on rainfall. When conducting impact studies, users should

- select a range of climate projections in order to provide an appropriate 'uncertainty space' relevant to the specific application;
- recognise that the apparent precision in currently available relatively fine-resolution (in time and space) data sets doesn't necessarily imply a 'better' answer, but rather still only provides one realisation of all possible outcomes;
- *recognise that the impacts of climate change may manifest as step-changes (as evidenced both in observations and in time series of model projections) rather than gradual trends (see, for example, Jones et al 2013, 'Valuing adaptation under rapid change', National Climate Change Adaptation Research Facility, Gold Coast, 184 pp).*

The Climate Futures Tool enables projection data to be explored and provides guidance on scenario selection and model selection for specific NRM Clusters (see www.climatechangeinaustralia.gov.au/en/climate-projections/climate-futures-tool/introduction-climate-futures/). The associated Technical Report "Climate Change In Australia" (CSIRO, 2015) also contains detailed information about model evaluation.

Knowledge of model performance relative to the key influences on Victoria's climate and associated impacts can be used to guide the development of improved methodologies for developing runoff projections. However, the large uncertainty associated with the magnitude and timing of projected changes in rainfall and runoff means that robust and adaptive planning will continue to be required across a wide range of plausible futures (i.e. it is not possible to characterise a 'most likely' future).

There is now a significant body of literature available that considers methodologies for robust planning and their application in a water supply context (see for example M. Mortanzavi-Naenin et al. (2015) Environ. Modelling & Software, 69, 437-451, and references contained therein).

PROGRESS IN ANSWERING KEY SCIENCE QUESTIONS

The VicCI Science Plan gives detailed descriptions of each of the seven research projects that make up the overall program. Within the descriptions, there are key science questions that aim to guide the research. As results are gradually obtained, it is appropriate to consider progress in each of the projects after year two in answering these questions.

Theme 1 – Improved seasonal prediction

Project 1 – Understanding decadal variations of seasonal climate predictability and potential for multi-year predictions

The climate of south-eastern Australia varies markedly on multi-year and decadal time scales, impacting the capability to make seasonal climate predictions but also obscuring the detection of anthropogenic climate change. Importantly, the capability to make seasonal climate predictions for south-eastern Australia primarily depends on the capability to predict ENSO because ENSO is the most predictable component of the climate system and the most important driver of rainfall variability in Victoria.

However, predictability of ENSO varies on decadal time scales: decades of high prediction skill are associated with high ENSO variability (i.e. when the signal to noise is high), and decades of low skill occur during periods of quiescent ENSO variation (i.e. when the signal to noise is low). The relationship of these variations of ENSO predictability with recent warming trends in the tropical oceans and with varying phases of the Inter-decadal Pacific Oscillation (IPO), which characterises decadal-scale variations in interactions between the ocean and atmosphere across the wider Pacific basin (Figure 3), needs to be determined to inform users of the seasonal predictions. This relationship is further complicated by the observed increase in mean sea-surface temperature (SST) in the tropical oceans. Understanding these relationships will provide more confidence in managing short-term climate variations in the future.

Why has ENSO prediction skill been low since 1999 compared to the previous 20 years (1980-1999)?

The decline in skill for long lead prediction of El Niño and La Niña since 1999 is attributed to a concomitant decline in ENSO activity as a result of a swing of the IPO to its 'cold' phase. The IPO cold phase is characterised by relatively colder temperatures in the eastern equatorial Pacific Ocean and warmer temperatures in the western Pacific. The results of sensitivity tests with the seasonal forecast system confirm that the slow variation in the background climate associated with the swing from positive to negative IPO affected the activity and predictability of ENSO.

Despite continued improvements in forecast systems, skill for prediction of ENSO can be expected to wax and wane decadally in the future as a result of natural variation of the background climate. Although the strength of the teleconnections between ENSO and rainfall in south-eastern Australia are expected to strengthen due to greenhouse warming, changes in predictability of ENSO are uncertain because they will depend crucially on the details of how the climate of the wider Pacific Ocean changes but as yet there is little consensus.

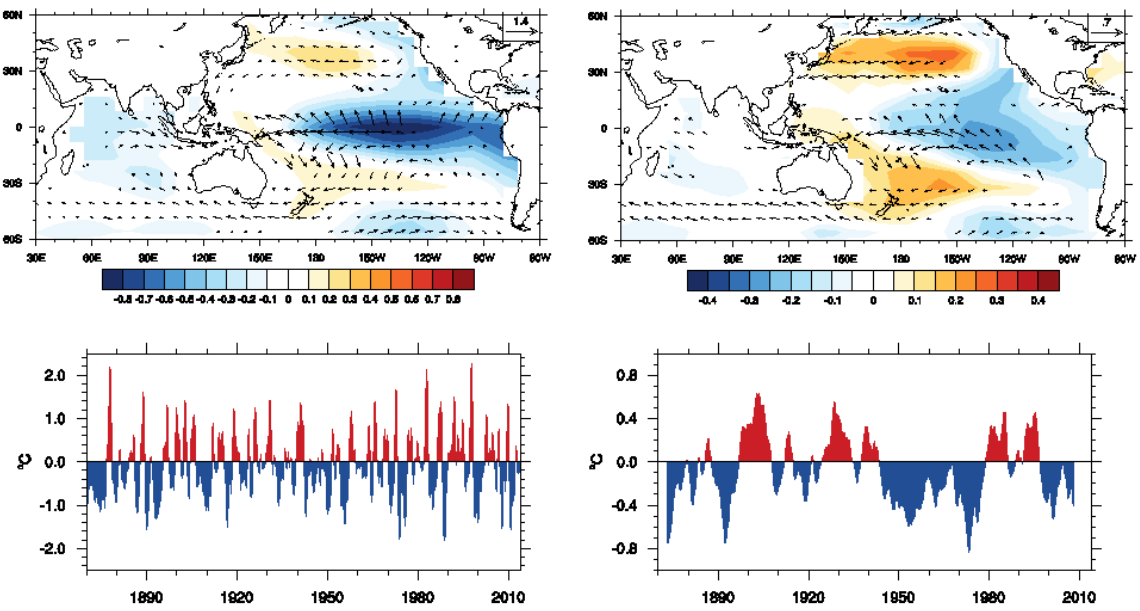

Fig. 3 Left hand panels show time series of the Nino34 index (lower) and a map of the typical surface temperature and wind anomalies (upper) during La Niña phase. The opposite conditions would tend to occur during El Niño. The right hand panels show the same thing but for the IPO using the tri-pole index. ENSO varies monthly with a typical duration of a warm or cold event being about 1 year. The IPO varies decadally with the cold phase of the IPO occurring, for instance, during 1947-1976, the warm phase in 1977-1998, followed again by a cold phase 1999-2014. Although the wind and temperature patterns are similar for ENSO and the IPO, the IPO has a broader meridional structure compared to ENSO, which reflects the longer time scale of the IPO. The surface temperature anomalies in the extratropics are relatively larger in comparison to the tropical anomalies for the IPO. There is also a tendency for high SAM conditions during cold phases of both ENSO and IPO.

Can the drop in ENSO prediction skill be related to changes in the global circulation associated with the expansion of the Hadley cell?

Results indicate that the Southern Hemisphere Hadley cell expansion is associated with a La Niña-like state in the tropical Pacific: cold waters in the eastern equatorial Pacific contrasting with warm waters in the west. That is, tropical expansion has been promoted by the shift to the cold phase of the IPO after 1999. Thus, both the drop in ENSO prediction skill and the recent expansion of the HC have been associated with the same shift to cold IPO after 1999. The implications of this finding are that there is a possibility of a reversed tendency if/when the IPO shifts back to its warm phase; however, this conjecture has not been carefully explored, and cannot be assumed. There are also early indications that the El Niño currently underway in 2015 may be contributing to a reversal of the IPO to the positive phase.

What has been the impact of the recent warming of ocean temperatures to the north of Australia on ENSO and ENSO's impacts on Australian climate?

The recent upward trend in ocean temperatures in the tropical Indian Ocean and western Pacific, due in part to the swing to the cold phase of the IPO, was found to have significantly amplified the springtime rainfall anomaly (10-30%) over eastern Australia during the 2010-11 La Niña event as a result of enhanced promotion of high SAM. To the degree that the upward trend in SST in the tropical Indian and western Pacific is a result of anthropogenic climate change, the risk of extreme rainfall in eastern Australia during La Niña events can be expected to increase in future events. However, some of the recent SST trend appears to be a result of a naturally

occurring swing of the IPO, so we can also expect epochs of reduced impact of La Niña events in the future when the IPO is in a warm phase. Although swings in the IPO are not predictable, persistence of the IPO is long and therefore its impact (and other ongoing trends) should be captured in the Bureau's POAMA seasonal forecast model because forecasts are initialised from observed ocean state. As a consequence, the extreme rainfall in spring 2010 was largely predictable at least one season in advance and it is reasonable to expect that significant events of similar magnitudes may also benefit from this increase predictability.

Furthermore, IPO in its negative phase may have contributed to the asymmetry in the cool season rainfall deficit observed across Victoria between autumn and spring as the IPO influence is not felt in the early part of the cool season (autumn and early winter) but only in the later part (late winter and spring).

What are the mechanisms of the observed multi-year variations of climate in south-eastern Australia?

The strength of the teleconnection of ENSO and the Indian Ocean Dipole (IOD) to SEA rainfall strongly varies on decadal timescales. Paradoxically, the teleconnection tends to be strong in decades when ENSO and the IOD have weak amplitude and when the covariation between ENSO and the IOD is weak. These decadal changes in the covariance of ENSO and the IOD, in the amplitudes of ENSO and the IOD and in the strength of the teleconnections of ENSO and the IOD to SEA rainfall are highly coherent in the last 40 years.
The decadal change of the Indo-Pacific background climate associated with the swing to the cold phase of the IPO after 1999 can account for some of the decadal change in amplitude and predictability of IOD. However, it does not account for the reduced short lead forecast skill of SEA rainfall in spring when the relationships between ENSO/IOD and SEA climate are strongest. We postulate this is because the impacts of the change in mean state, while in the right direction to account for the changes in observed ENSO-IOD variability, are small and so are not expressed strongly in the initial months of the forecast. Hence, it is difficult to detect an appreciable change or impact on the rainfall teleconnection as a result of changes in background climate.

Why did the last two La Niñas (2010-11 and 2011-12) bring a lot of rainfall to Australia, but the 2007-09 La Niña did not?

The IOD-SEA rainfall relationship is found to be stronger when the IOD-ENSO connection is weak. This helps explain why SEA was drier than usual during the 2007-2009 La Niña because it co-occurred with the positive phase of IOD in an epoch when the IOD-ENSO connection was weak. When the IOD-ENSO connection is strong, La Niña would tend to co-occur with negative IOD, which would cooperatively act to increase rainfall in SEA. In contrast during 2010-11, all large-scale influences (ENSO, IOD, SAM) aligned to contribute to the very large observed rainfall in Victoria.

How predictable are the multi-year La Niña episodes that are the primary drivers of water resource replenishments (e.g. mid 1970s, late 1980s, 2010-2012)?

The potential for multi-year prediction of El Niño and La Niña was explored by extending an ensemble of POAMA forecasts out to 2 years for two case studies. This was motivated by the observations that some El Niño/La Niña events exhibit multi-year persistence. Although the limit of predictive skilful El Niño/La Niña using the full hindcast set is ~9 months, exploration of longer lead prediction for a selection of events is warranted in order to reveal possible sources of predictability and to give a glimpse of what might be possible in the future with

improved models. Two extended La Niña episodes (2007-2009 and 2010-12) were targeted. Forecasts were initialized monthly from the peak of the preceding El Niño in each case (i.e. 2006 and 2009) and run for 2 years. Preliminary results indicate some predictability for the 2008/09 event but no indication of predictability for the 2011/12. Based on the inconclusive results, we decide not to pursue this issue any further with POAMA. However, similar forecasts using the SINTEX-F model in Japan are more promising and follow up evaluation of those runs is being pursued.

While there has been some progress on the following questions, they will be considered in more detail in the future:

- *What role does global warming play in multi-year wet or dry periods?*
- *What is the relationship between changes in ENSO activity and forecast skill due to the IPO and epochs of enhanced global warming and strengthening of the sub-tropical ridge?*

During 2015/16, Project 1 will continue to further understanding of the causes of why the teleconnections of ENSO and the IOD to Australian rainfall become stronger when the ENSO and IOD amplitudes themselves are weaker, and vice versa. Preliminary assessments suggest that the strength of the rainfall teleconnection could be sensitive to the spatial variation of SST anomaly during ENSO/IOD, thus causing changes in the pattern of tropical convection that acts as the Rossby wave source, and therefore the source of anomalous circulation over SEA. Given that the teleconnection strength of ENSO and the IOD to SEA rainfall is a more important factor than the change of the mean state these sorts of sensitivity experiments with the seasonal prediction system will not be pursued further.

Theme 2 - Improved understanding of past climate variability and change

Projects 2 and 4 – Understanding the mean meridional circulation and its relevance to Victoria and Exploration of the causes of tropical expansion

A key outcome of SEACI was the confirmation that the Hadley cell is expanding and this expansion could be playing a key role in the recent climate variability of south-eastern Australia (SEA). Projections of future climate indicate a continued expansion of the Hadley cell, so it is imperative to understand its impact on the climate of the region and the mechanism for, and likely limits to, the expansion. An important development in VicCI has been to develop regional indices for the Hadley cell as well as the surface signature of the sub-tropical ridge. In this report three different measures of the subtropical ridge are considered: global across the entire southern hemisphere, regional (60°E to 175°W) and local (140°E to 150°E). The first two are computed using re-analyses while the last one can either be computed using reanalyses or MSLP observations from the Bureau of Meteorology.

Recent results indicated that the recent expansion of the Hadley cell has been relatively greater over Australia compared to the rest of the hemisphere. However, the seasonal variation of the expansion is complex: investigation of reanalysis data suggests that the expansion averaged around the hemisphere has a maximum in summer and autumn, but analysis of radiosonde data in the region of Australia and New Zealand shows little seasonal variation. The seasonality of the expansion bears on the issue of what is driving the expansion and on understanding the observed autumnal rainfall decline and how rainfall may respond to future changes.

Climate model simulations can best represent observed recent changes in the mean meridional circulation and the expansion of the tropics when ozone depletion and other anthropogenic external forcings are used, suggesting at least a partial human influence on recent changes. However, simulations of the tropical expansion are typically weaker than observed. It is thus critical to understand what is actually driving the changes and why the models are underestimating the change?

What mechanism explains the relationship between the expansion of the Hadley cell and the intensification of the sub-tropical ridge? What is the role of extra-tropical dynamics compared with low-latitude forcing?

Australian rainfall shows significant correlations with the Hadley cell extent in the Asia-Pacific sector: poleward expansion correlates positively with higher tropical/sub-tropical rainfall totals. In winter and spring there are significant positive correlations across east Australia while in summer they are mainly in the west of the continent. Only in autumn is there a hint of dry conditions in the south-east associated with the expansion of the regional index of Hadley cell.

In contrast, across south-eastern Australia, correlations between rainfall and the regional sub-tropical ridge intensity and position in all seasons are highly similar to the correlations obtained using the local, observation-based, STR which was used in SEACI. The main differences are seen across large areas of eastern and northern Australia where correlations between rainfall and regional STR indices are significantly positive and are similar to the correlations obtained using the regional HC indices. No such areas of positive relationship were observed using the local observation-based STR indices. These two quantities have markedly different annual cycles in both position and intensity which help explain the different relationship with Australian rainfall. The relationship between these quantities (hemispheric, regional and local) in a warming world is not straightforward and requires further investigations.

How do relationships between the Hadley cell and the sub-tropical ridge vary on inter-annual and decadal time scales?

An expanded Hadley cell both hemispherically and regionally in the Asia-Pacific sector is associated with a poleward expansion of the tropical wet zone but does not strongly affect the intensity of the regional sub-tropical ridge which in turn means that the regional Hadley cell index does not relate with rainfall across southern Australia during the cool season. Hadley cell expansion is promoted by La Niña conditions and the cold phase of the IPO. A possible mechanism to explain the association of an expanded Hadley cell with La Niña conditions is via the Southern Annular Mode: a poleward shift of the mid-latitude jet is favoured by La Niña conditions in the tropics, which results in an expansion of the Hadley cell.

On the other hand, variation of the intensity and position of the local sub-tropical ridge which was shown on decadal time-scale to evolve with global warming, on shorter time-scale is mainly driven by random mid-latitude processes and also as a remote response to tropical diabatic heating in the Indian Ocean that has characteristics of the IOD. This association of the STR with the Indian Ocean is mainly a cool season response.

What are the relative roles of greenhouse gases, stratospheric ozone depletion, and anthropogenic aerosols in producing the observed expansion of the Hadley cell and the associated impact on sub-tropical rainfall?

A critical comparison of metrics (or indicators) of tropical expansion reveals that the consensus observed expansion rate since 1979 is on the order of 0.5 degrees of latitude per decade (about 50 km/decade) in each hemisphere. Attribution analysis using both statistical analysis of

observations and single forcing climate model simulations indicates that Southern Hemisphere tropical expansion is attributable to a combination of factors: Since 1979, the partition of forcing factors for Southern Hemisphere tropical expansion is 30% resulting from natural factors (volcanoes and ENSO), 40% resulting from stratospheric ozone depletion and 30% resulting from increasing greenhouse gases, with an error range roughly estimated at ± 10%. Since 1979, natural factors (ENSO, IPO, volcanoes) have been of increased importance. For the longer trend, since the 1960s, analysis of the single forcing simulations shows that O3 and GHG are the dominant forcings of tropical expansion.

If the Hadley cell expansion is primarily driven by variations in tropical sea surface temperatures (especially those associated with ENSO), how will the expansion vary in the future?

An expanded Hadley cell is found to be promoted by La Niña and the large trend in Hadley cell expansion during the last 15 years is concomitant with the negative phase of the IPO. However, anthropogenic climate change is expected to lead to an El Niño-like SST pattern of warming in the tropics, so we can expect a promotion of Hadley cell contraction due to the SST-forced component. However, Hadley cell expansion can also be driven directly by CO2 increases and global warming, which would work against an SST-driven component. The mechanisms by which increased greenhouse gases drive Hadley cell expansion are being investigated.

Why do current models under-estimate the observed Hadley cell changes?

An ensemble mean from climate model simulations will not capture recent trend to negative IPO, and this accounts for some of the reduced tropical expansion in the models compared to the observations. Climate model simulations of the past 50 years do not capture the observed timing of ENSO or changes in the wider state of the Pacific, thus ENSO will not form an important part of the expansion seen in an ensemble mean of model simulations. The results from 10 CMIP5 models all show that models largely underestimate the observed amount of tropical expansion, thus the contribution from various forcing factors is also likely to be small. However, it is clear that the simulations with the warmest global mean temperatures (i.e. the simulations with prescribed greenhouse gases increasing but without stratospheric ozone depletion) are also those with both hemispheric HCE and STRP markedly poleward compared to the other simulations. This result highlights that the extent of the hemispheric-wide Hadley cell corresponds closely with global mean temperature, and it seems that factors that act to cool the globe in climate models (e.g. volcanoes) work to reduce the expansion of the tropics.

Can we reconcile the seasonality of observed tropical expansion as given by different methodologies?

A critical comparison of metrics (or indicators) of tropical expansion reveals that the consensus expansion rate since 1979 is on the order of 0.5 degrees of latitude per decade (about 50 km/decade) in each hemisphere. In the Southern Hemisphere, statistically significant tropical expansion and associated changes to the sub-tropical ridge are detectable from the late-1960s. However, the expansion is not steady; for example, there were abrupt jumps following the major ENSO event of 1997-98 and the major volcanic eruption of Mt Pinatubo in 1991.

Analysis in the Australian region shows the regional expansion to be greater than the hemispheric average (about 65 km/decade). It is also found that the expansion and intensification of the Hadley cell is greatest in autumn, which is consistent with the earlier-observed local intensification and poleward shift in the sub-tropical ridge in autumn. The difference in conclusions on the local seasonality of the expansion between SEACI and VicCI is

due to the improved analysis techniques that now provide a detailed picture of regional variations around the hemisphere.

Can new tools and methods be developed to assess regional expansion in the Australian sector?

A method to diagnose the regional Hadley cell in the Australian sector has been developed. A clear and significant expansion and intensification of the regional Hadley cell is observed that is consistent with, but slightly larger (about 0.65 degrees per decade) than, the hemispheric-wide expansion. The expansion is most prominent in autumn (MAM) and is concomitant with the intensification and poleward shift of the local observation-based sub-tropical ridge and observed decline in rainfall in south-eastern Australia. The larger regional expansion over the Australian sector may be the reason that Victorian climate has exhibited a stronger rainfall decline than that recorded at comparable latitudes around the hemisphere. However the correlation of the regional Hadley cell indices with Australian rainfall does not revealed the expected relationship. Further analysis is being carried out to fully reconcile the relationships between variations in Victorian rainfall, the STR and the HC at hemispheric and regional scales.

Software to compute the characteristics of the mean meridional circulation in isentropic coordinates (which essentially follow the trajectories of the air) has been developed. This isentropic analysis will be a potent tool to diagnose forced and naturally occurring interactions of the mid-latitude circulation with the low-latitude Hadley cell.

Further science questions to be considered later in VicCI

Overall, the computation of the Hadley circulation in regional components has revealed that the regional component in the Asia-Pacific prevails in terms of the mean climate. Furthermore, it is also the regional component in the Asia-Pacific region which has seen the largest expansion. However, this cannot be inferred to explain why a cool season rainfall deficit is being experienced across southern Australia. Indeed, on a regional basis, the relationship between the Hadley circulation and the STR is non-existent in the winter. On the contrary, the regional Hadley cell analysis has revealed that the expanded regional Hadley cell is more likely to explain the on-going warm season rainfall increase across most of northern Australia. It remains the case that the local STR, which relates very well to the observed on-going cool season rainfall deficit (spatially and in terms of timing in the annual cycle) has been observed to strengthen in conjunction with global warming. Further, climate models confirm that global Hadley circulation expansion and STR strengthening are to be expected in response to anthropogenic forcings, albeit at a much lower rate than observed. The modelled lower rates are somewhat consistent with this year's finding that internally generated natural variability in the form of a shift in the last 30 years from the warm to the cold phase of the IPO has promoted the regional Hadley circulation expansion (the main component of the global Hadley circulation expansion). Overall, the regional analysis of Hadley circulation has not offered a simple mechanism by which the local sub-tropical ridge strengthening could be causally linked to the global warming. It will therefore remain an active area of research for VicCI in the third year.

The following questions will also be considered in the future:

- *If ozone depletion is an important factor, what are the implications of the expected recovery of stratospheric ozone for projections at different time scales (e.g. 2020, 2050, etc.) and how well is this captured in existing projections?*
- *If the Hadley cell expansion is driven primarily by carbon dioxide and other greenhouse gases, how will the expansion continue in the future?*
- *What are the underlying factors that determine the seasonality of the expansion of the Hadley cell, and how are they affected by climate change?*

- *What role does the Australian land mass (including the maritime continent) play in the regional enhancement of the expansion of the Hadley cell, and why is the enhancement different over South America and South Africa? How will regional effects apply in a changing climate?*
- *What are the implications of the possibility of attributing part of the observed changes to external factors for our best estimate of the current climate baseline?*

During 2015/16, Project 2 will aim to quantify the regional tropical expansion from all metrics and investigate their impacts on Australian climate variability. There will also be investigation of the causes of the zonal variations in changes in the Hadley cell.

Project 3 – Understanding sub-tropical – extra-tropical interactions and their relevance to Victoria

Evidence is emerging that variations in extra-tropical circulations associated with the SAM play a significant role in driving variations of the Hadley cell, and especially rainfall on the poleward edge of the Hadley cell: high SAM (i.e. a poleward shift in the polar front jet) is associated with a poleward-expanded Hadley cell and increased rainfall in sub-tropical latitudes in the warm season and decreased rainfall in the higher southern latitudes (i.e. across Victoria but especially along the Great Dividing Range) in the cool season. This relationship is captured in climate models to varying degrees. The shift to high SAM is especially promoted by ozone depletion, but increased carbon dioxide is also known to drive SAM to its high phase. Understanding the cause of this relationship between SAM and changes in the extent of the Hadley cell is crucial to understanding the behaviour of the Hadley cell in the future. It furthermore bears on the ability to predict regional climate seasonally. There is strong evidence that tropical SSTs during ENSO directly affect the Hadley cell, which then affects the SAM. These variations should be highly predictable. But, because SAM is primarily an internal mode of variability, predictability of Hadley cell variations will be limited by predictability of the SAM.

What is the nature and mechanism of the interaction of the SAM with the Hadley cell? What determines the seasonality of the interaction?

The positive phase of the SAM (high SAM) is associated with a poleward shifted mid-latitude storm track in all seasons. In winter when the mid-latitude storm track plays an important role in the climate of the southern part of Australia, the poleward shift of the storm track results in drier conditions across SEA. In contrast, during spring-summer, the high phase of the SAM increases rainfall in SEA because it causes the poleward edge of the tropics to shift poleward to the latitudes of Victoria. Forced upward trends of the SAM in response to increasing GHGs and ozone depletion are thus expected to act to dry southern portions of Australia during winter but moisten sub-tropical latitudes during spring-summer.

What are the implications of the interaction of the SAM with the hemispheric mean meridional circulation (including the Hadley cell), especially the seasonality of the interaction, for predictability of sub-tropical rainfall?

Future forced upward trends of the SAM in response to increasing greenhouse gases and ozone depletion will be expected to result in drying across the southern-most portions of Australia during winter but moistening across sub-tropical eastern Australia during spring and summer. The near-record high SAM in 2010 was found to have played a primary role for the extremity of the wet conditions over south-eastern Australia during spring in 2010. This swing to high SAM and the occurrence of extreme rainfall was found to be largely predictable at least one season in advance because it was promoted by the strong La Niña conditions in the tropics that were acting on top of the recent upward trend in tropical SST. We further identified the recent trend

in SST to the north of Australia, in part due to the swing to the negative phase of the IPO and in part due to a broader scale warming trend in the tropics, to have played a key role in promoting the extreme positive SAM in 2010. Thus, the warming trend in SST to the north of Australia significantly contributed to the extreme wet conditions in 2010.

What role does ENSO or other tropical sea-surface temperature anomalies play in promoting the interactions between SAM and the Hadley cell? What is the best diagnostic to represent and understand these interactions?

Near record strength of drought over eastern Australia in 2002 spring was found to be driven not only by the moderate El Niño event whose maximum SST warming was shifted to the central Pacific but also the strong negative phase of the SAM (low SAM), which highlights the important role of the SAM in the occurrence of extreme climate events and also in the limitation on long-lead predictability of extreme climate events.

Similarly, the near-record high SAM in 2010 was found to have played a primary role for the extremity of the wet conditions over south-eastern Australia during spring in 2010. La Niña promotes high SAM by acting to weaken the equatorward flank of the sub-tropical jet, thereby shifting poleward the critical line for poleward propagating mid-latitude eddies. Hence, a meridional circulation is induced that acts to shift the mid latitude jet poleward, thus resulting in high SAM. However, the warm SST to the north of Australia as a result of the cold phase of the IPO acted in conjunction with the extreme La Niña event in 2010 to further promote high SAM by a different mechanism, which was more akin to the response to increased greenhouse gases: the mid-latitude jet was accelerated by an increased equator to pole temperature difference, thereby resulting in faster eddies that break further poleward, hence acting to shift SAM to its high phase. Whether such an interaction occurs in the future will depend on the ongoing trend in SST to the north of Australia.

How will these interactions change in future climates, and what is the implication for the future climate of Victoria?

The climate models of CMIP5 with historical forcing correctly simulate the positive relationship between the SAM and sub-tropical rainfall (i.e. high SAM and increased rainfall) in summer and the absence of such positive relationship in winter, which explains the expanded dry zone to the north of Victoria during high SAM in winter, although this impact is underestimated.
However, the models show significant biases in the teleconnection between the SAM and tropical rainfall (i.e. too much rainfall during high SAM) and between the SAM and ENSO in austral warm seasons when these teleconnections are strong in the observations. Hence, the reliability of projected climate for SEA is limited by the bias in this interaction of the SAM and the Hadley cell in the CMIP models. Work is under way to sort the models by the bias in these relationships so as to see whether a more consistent picture emerges for SEA climate if only the models that faithfully represent the SAM-HC interaction are used.

Can the interaction of extra-tropical circulations and the mean meridional circulation explain the link between the Hadley cell expansion and the intensification of the sub-tropical ridge, associated with the deficit in cool season rainfall in south-eastern Australia?

Results suggest that HC expansion has been promoted by cold IPO and should be associated with cyclonic circulation over SEA with increased rainfall over most of the country (except in MAM in SEA). The results so far do not provide a path to relate the observed intensification of

the local STR and the subsequent rainfall reduction to the overall HC expansion globally or regionally.

What is the best diagnostic to represent and understand these interactions?

Software to compute the characteristics of the mean meridional circulation in isentropic coordinates has continued to be developed. This alternate method for investigating the mean meridional circulation will provide added insight into the possible links between the tropical expansion, the intensification of the sub-tropical ridge and forcing by ENSO, and also into the observed south-eastern Australia cool season rainfall deficit. The calculation of the MMC in isentropic streamfunction is a complex calculation, and current results based on monthly quantities do not fully capture the 'geostrophic' part of the isentropic flow which is dominant in the extratropics. Investigation is still ongoing to explore further the issue using daily quantities to obtain more accurate results.

The calculations using monthly data do seem to agree with what is expected regarding inter-annual variability. In response to El Niño, a narrowing and intensification of the tropics and the Hadley cell is observed. In terms of the SAM response, the variability appears correct: the storm track is further poleward during the positive phase. Over the longer term, computed trends indicate changes to the MMC. The outflow regions of the upper arm of the Hadley cell may be changing. In the Southern Hemisphere, the sub-tropical 'downward' branch appears to be moving more poleward. The calculations suggested that the biggest changes may lie in MAM, although an expansion in most seasons is seen. These results are subject to change, particularly in the extratropics, because of the largely missing 'geostrophic' component of the MMC which is currently under investigation.

Further science questions to be considered later in VicCI

During 2015/16, research will continue to improve the isentropic stream function code by acquiring model level data and daily data to explore tropical – extra-tropical interactions of relevance to Victorian climate. The linkage between the SAM and Australian climate in the present and future climate will be investigated by assessing the CMIP5 models for their capability to simulate the seasonality of the response of the SAM to ENSO. The relationship between the misrepresentation of the SAM-rainfall teleconnection and biases in the model's mean state, especially the separation of the mid and high latitude jets will be explored.

Theme 3 – Improved understanding of future climate and associated risks to water resources

Project 5 – Critical assessment of climate model projections from a rainfall perspective

Climate model projections from CMIP3 (those used in IPCC Fourth Assessment report in 2007 and SEACI) for the climate of south-eastern Australia show some consistent behaviour (e.g. drier to the south and wetter to the north) and some inconsistent behaviour (the magnitude of future rainfall change). Some of this uncertainty is linked to the models' ability to represent important links between climate variables at one location and those at another (i.e. teleconnections) (e.g. the influence of the SAM on the Hadley cell), and key modes of variability that directly influence the climate of south-eastern Australia (e.g. stationary high pressure systems). In order to provide greater confidence for projections of future climate (with

a particular focus on subsequent impacts on water availability), we need to assess models for the capability to simulate these key teleconnections and processes.

Is the relationship between the sub-tropical ridge (STR) and rainfall across south-eastern Australia, which underpins the secular changes in rainfall across the region but which was poorly represented in CMIP3 models, better represented in the CMIP5 models (those used in the IPCC Fifth Assessment report) in 2013. What are the reasons for the poor representation? What implication does the poor representation of the STR-rainfall relationship have for future projections?

Simulations of the Australian sub-tropical ridge (STR) in 50 latest-generation climate models were analysed. Many models were found to reproduce the broad character of the STR similar to that observed, but some models simulate the STR too far to the west, and some simulate it too wide. Some models also have a different relationship between the STR intensity and rainfall over Victoria, with either too broad an extent of the region of negative rainfall – STR intensity relationship over Victoria, or too restricted a region. These biases are an issue for making regional climate projections for Victoria and hence a narrower and more reliable range of projections may be obtained by omitting some models.

Future projections of the STR and rainfall under a high emissions scenario were analysed. Most models showed an intensification of the STR over recent decades, but not all showed the observed southerly trend in its position. However, all models showed the STR to intensify and move south over this century. This confirms that changes to atmospheric circulation are generally projected to lead to reduced rainfall in Victoria in the cool season (April to October). Models with a poor simulation of the STR have a distinct rainfall projection for certain regions, suggesting that it may be possible to select models for future projections based on some constraints on their representation of the STR and its relationship to rainfall. . However, given the inability of models to capture the magnitude of past trends, it is possible that the projected changes in the STR and the reduced rainfall in Victoria are underestimated.

How are model projections for either wet or dry tendencies related to the model's projections of tropical ocean warming (especially the relative warming between the Pacific and Indian Oceans)?

Following on from the analysis of Australian Sub-tropical Ridge (STR) and its relationship with Victorian rainfall in climate models, the influence of the tropical sea surface temperatures (SSTs) to Australia's north was examined. It was found that while the CMIP5 models capture a part of the observed relationship between tropical SSTs and SEA rainfall with a reasonable annual cycle, the magnitude of the correlation varies strongly from one model to the next and is weaker than observed. In that respect, while models' future warming projected on the tropical tripole index varies considerably amongst models, it does not relate as expected to the range of rainfall projections across Victoria.

The relationship between SEA rainfall and the tripole index which has been observed to vary markedly on decadal timescale appears stable in response to external anthropogenic forcings. While individual models have differences over 50 years period, they show a remarkably stable picture for the past and current centuries; suggesting no change in the magnitude of this relationship due to response to anthropogenic forcing.

The Millennium drought had the longest spell of months in the historical record (121 months) during which no 'very wet' months occurred. The CMIP5 models do not capture spells of this duration; nor do they indicate any likely change in frequency of these prolonged no 'very wet' month spells over the coming century.

Further science questions to be considered later in VicCI

The following questions will also be considered in the future:

- *Should the capability of models to simulate observed trends attributable to external forcings be used to confirm or invalidate future projections of these models? What is the best probabilistic approach to reconcile observed trends with model trends, and so to estimate future trends?*

During 2015/16, Project 5 will, in consultation with DELWP, prepare documentation on findings obtained through the NRM national projections specifically focused on Victoria. Additional work will aim to increase the confidence in the projections for rainfall by evaluating the uncertainties in the modelled relationship between rainfall and large-scale climate factors, with a particular focus on the effects of warming of the tropical ocean around Australia. An investigation will also be carried out to determine how the overall projected mean rainfall reduction may affect the potential for prolonged drought in the future (similar to what was experienced during the Millennium Drought). A new small component will aim to provide updated monitoring of SEA rainfall anomalies over the last 20 and 30 years and the implication in defining a new climate baseline for water managers.

Project 6 – Convection-resolving dynamical downscaling

Statistical downscaling methodologies of varying complexity were investigated in SEACI in order to provide projections of future climate at the local scale. A key weakness in all methods used within SEACI was the underestimation of extreme rainfall events, which leads to underestimation of high runoff events, thereby also underestimating mean runoff. Improved spatial and temporal characteristics of rainfall can be obtained when using convection-resolving high-resolution regional climate models (RCMs) to downscale predictions and projections to regional scales.

What are the optimum physical parameterisation settings and grid resolution that best capture the key synoptic processes associated with heavy rainfall? Can a high-resolution RCM be configured for regional Victoria that provides faithful representation of key physical processes that drive extreme rainfall and runoff?

The Advanced Weather and Research Forecasting (WRF) modelling system was configured using three nested domains, with the innermost nest focused on a region of about 450 by 600 km along the Great Dividing Range. Three 15-day case study periods with contrasting synoptic conditions were identified during the 2010-11 La Niña event when south-eastern Australia experienced flooding events. Simulations for case study 1 were completed and the sensitivity to a range of model physics options is being assessed. Progress to date suggests that the properly-configured RCM will be able to well simulate key precipitation processes relevant to rainfall and runoff in Victoria.

In the second year, model simulations using the selected 6 WRF configurations were completed for all case study periods. Suspected spurious simulated rainfall patterns identified in year one were addressed in part by model upgrade but also through some modification of model dynamics and model structure settings. An evaluation of daily rainfall patterns in the fine resolution domain against observed gridded rainfall data showed a somewhat better performance (as judged by spatial skill metrics) by simulations using microphysics scheme WDM6 in combination with the planetary boundary layer scheme MYNN.

The results are promising, but the fine resolution set-up is resource intensive, implying that with limited computing resources, important choices are required with regard to simulation period and extent of spatial domain. For the final year, a multi-year example is scheduled to investigate if very fine resolution convective permitting simulations are computationally justified from a water resource perspective.

During 2015/16 the multi-year experiment will be conducted and followed by an analysis of output of the 2 and 10 km fields to assess whether there are quantifiable differences in rainfall simulations that are of significant importance when downscaling for the purpose of water resource impact and adaptation work.

Project 7 – Identification and application of improved methodologies for water availability projections

The aim of this project is to provide information about the behaviour of the latest generation of climate models and methodological choices that can improve the reliability and usefulness of runoff projections for mid- to long-term future time horizons (out to about 2065). In comparison with CMIP3, CMIP5 comprises a larger data set, with more models operating at higher resolution and with more complex physics.

Which existing bias-correction methods are best suited to adjust statistical characteristics of climate model output to observed data, in order to use model output directly in hydrological models?

A literature review was undertaken on regional climate model (RCM) bias correction methods. The best performing bias correction technique – distribution mapping – was assessed using daily precipitation series simulated by the Weather Research and Forecasting (WRF) model for eight Victorian catchments.

The results confirmed the usefulness of distribution-based methods but also highlighted that, since not all errors are necessarily biases, none of these methods which aim to remove errors can lead to a perfect result. Although bias correction does not seem to alter the change with time in RCM precipitation, it does introduce extra uncertainty in the change in runoff. Consistent with other studies, bias from hydrological models is much smaller than bias from downscaling.

Empirically downscaling 'perfect' GCM results, examined by downscaling observed rainfall data aggregated to GCM scale, suggests that the scale effect (i.e. the loss of fine scale information at the larger spatial scale) by itself produces little bias, with the exception of spring rainfall and the number of dry days. This result indicates that most of the error from empirical downscaling comes from the GCM itself rather than the downscaling method.

How can outputs from different CMIP5 models and subsequent downscaling methods be most appropriately merged into projections of future streamflow?

A proof-of-concept of the ability to produce values of catchment-scale monthly streamflow from rainfall and temperature fields was demonstrated in the first year of the program. That simple method was extensively tested across a diverse set of catchments (in terms of size, elevation, mean streamflow, mean runoff). The method was updated with the inclusion of ten year antecedent rainfall which a small improvement consistent across almost all catchments. The model was able to capture the magnitude of streamflow reductions during the Millennium Drought, something which has proven difficult to achieve with many hydrological models. Having now demonstrated the performance of the simple method across a diverse set of catchments, it was applied to downscaled GCM outputs. Two variations of the linear

reconstruction of streamflows were applied to 22 downscaled CMIP5 GCMs with and without the temperature influence. Results suggest there is very little difference in these two sets of projections as expected from the validation phase. The dataset has been handed to DELWP. These projections are being analysed as part of the third year of the program.

As part of the validation of the simple approach across Victorian selected catchments, a further analysis of the drivers of the declining trend in streamflow from 1977-2012 at 27 catchments across the State was conducted. The response of streamflow across the State is strongly related to the mean runoff rather than to the pattern of rainfall reduction. The elasticity term varied from catchment to catchment. In terms of large-scale climate forcings, strong correlations were found during the cool season with the sub-tropical ridge intensity and, to a lesser extent, with its position. Tropical modes of variability are important in catchments other than those on the southern flank of the Great Dividing Range; however, they do not explain the streamflow reduction during the Millennium drought. Instead they continue to relate well to high and low streamflow years (albeit relative to lower mean streamflows) since the mid-1990s.

Further science questions to be considered later in VicCI

The following questions will also be considered in the future:

- *Can statistical downscaling provide useful insight into the source and associated uncertainties of the wide range of projections from CMIP5 models?*
- *Which CMIP5 models show best skill in reproducing rainfall characteristics that define regional streamflow characteristics, accounting for the spatial and temporal behaviour of streamflow across different meteorological seasons and time frames?*
- *Which are the best methods for generating updated streamflow projections for periods around 2040 and 2065?*

During 2015/16, Project 7 will deliver streamflow projections for selected catchments across Victoria for the twenty-first century based on the latest IPCC science and the simple statistical method developed in the first year, and extended in the second year of VicCI for predicting streamflow from rainfall. In addition, a broader application of some commonly used approaches that provide future climate projections for hydrological modelling (e.g. empirical scaling from global climate models, empirical scaling informed by regional climate models, bias correcting of regional climate model simulations, bias correcting of analogue downscaling) will be performed in order to compare the results with the simple method. The strengths and weaknesses of each method will be assessed, with a view to recommending methods for different applications.

PROJECT 1: UNDERSTANDING DECADAL VARIATION OF SEASONAL CLIMATE PREDICTABILITY AND THE POTENTIAL FOR MULTI-YEAR PREDICTIONS

Harry H. Hendon, Eun-Pa Lim, Jing-Jia Luo, Mei Zhao and Guo Liu
R&D Branch, Bureau of Meteorology

Key Findings

- The strength of the teleconnection of ENSO and the IOD to SEA rainfall varies decadally. Paradoxically, the teleconnection tends to be strong in decades when ENSO and the IOD have weak amplitude and when the covariation of ENSO and the IOD is weak. These decadal changes in the covariance of ENSO and the IOD, in the amplitudes of ENSO and the IOD and in the teleconnections of ENSO and the IOD to SEA rainfall are highly coherent in the last 40 years.
- Although longer-lead predictive skill of the occurrence of El Niño has been shown to be lower since ~2000 compared to 1980-1999, short-lead seasonal prediction skill of SEA rainfall has been higher, especially in the spring season. This is attributed to the strengthening of teleconnections of ENSO and the IOD to SEA rainfall in the recent decade despite reduced ENSO/IOD amplitude and covariance that appears to result largely from natural variability. This highlights that similar variation of predictive skill for ENSO/IOD/SEA rainfall might occur in the future and also stresses the importance of improved representation of the Indian Ocean for improved prediction of SEA climate.
- The decadal change of the Indo-Pacific background climate can account for some of the decadal change in amplitude and predictability of IOD. However, it does not account for the change in short lead forecast skill of SEA rainfall in spring when the relationships between ENSO/IOD and SEA climate are strongest. We postulate this is because the impacts of the change in mean state, while in the right direction to account for the changes in observed ENSO-IOD variability, are small and so are not expressed strongly in the initial months of the forecast. Hence, it is difficult to detect an appreciable change or impact on the rainfall teleconnection as a result of changes in background climate. This line of research (i.e. conducting sensitivity experiments with the Bureau of Meteorology's seasonal forecast model (POAMA)) appears not to be able to reveal further insight as to why SEA rainfall forecast skill increases when ENSO/IOD amplitude is reduced, and so will not be further pursued.

Background

Climate in SEA varies markedly on multi-year and decadal time scales, impacting the capability to make seasonal climate predictions but also obscuring detection of anthropogenic climate change (ACC). Importantly, the capability to make predictions of seasonal climate variability in SEA varies decadally in association with changes of ENSO, the IOD, and their teleconnections. Based on published findings, the epoch 1960-1979 exhibited relatively low ENSO variability, 1980-1998 exhibited high ENSO variability and since 1999 ENSO variability has been low. Together with these variations in ENSO variability, since 1999 ENSO activity has been observed to shift west in the Pacific. The relationship of these variations of ENSO variability and predictability with epochs of increased global warming and intensification of the sub-tropical ridge needs to be explored. Furthermore, the epochs of high/low ENSO variability may be related to warm/cold phases of the Interdecadal Pacific Oscillation (IPO, noting that the IPO is not an oscillation in the true sense because its behaviour is more episodic without exhibiting a prominent periodicity). Furthermore, there is clear evidence that some specific ENSO events are

predictable for 1-2 years in advance but many are only predictable 2-3 seasons in advance. Further, ENSO variability today is acting on a warmer mean state and this warming may have played a role in changing both the behaviour of ENSO and the ENSO teleconnection to SEA (e.g. there is some evidence to suggest that the La Niña pluvial phase may be more intense now than previously; e.g., Kumar et al. 2010). Understanding these changes will provide more confidence for predictions of short term climate variations in the future.

Objectives

1. Gain new insight into how ENSO and IOD behaviours have varied decadally and have impacted SEA climate.
2. Gain new insights into how mean state change affects the predictability, predictive skill and interactions of ENSO, IOD and associated SEA climate.

Activity 1: Decadal variation in ENSO-IOD co-variability

A literature review (included here as Appendix 1) and a draft paper (Lim, 2015) have been produced to help answer the question posed by Objective 1. The climate of the early 21st century exhibited the cold phase of the Interdecadal Pacific Oscillation (IPO; e.g. England et al. 2013, Kosaka and Xie 2013), which is characterised by a "La Niña-like" sea surface temperature (SST) anomaly pattern with cold anomalies in the tropical central-eastern Pacific flanked by a boomerang shape of warm anomalies in the far western Pacific and the North and the South Pacific. In contrast, the 1980s and 1990s were the decades of the warm phase of the IPO (e.g. Parker et al. 2007). Although it is under investigation as to whether the IPO could modulate the frequency of El Niño or La Niña, several studies suggest that the IPO modulates the strength of El Niño/La Niña: when the IPO is in its cold phase (negative IPO), the amplitude of El Niño/La Niña reduces, and the amplitude increases when the IPO is in its warm phase (positive IPO; e.g. Parker et al. 2007, Zhao et al. 2015). Zhao et al. (2015) showed that the variance of the SSTs over the tropical eastern Pacific was large in the 1980s and 1990s but substantially reduced in the 2000's. They demonstrated that a significant portion of this difference of El Niño/La Niña variance was due to the mean state difference between the two epochs (i.e. negative IPO in the recent epoch vs. positive IPO in the earlier epoch). They further argued that reduced variance of El Niño/La Niña explained the reduced predictability and lower predictive skill of El Niño/La Niña events in the recent decade.

Such inter-decadal changes in the strength and frequency of El Niño and the Southern Oscillation (ENSO) significantly affect ENSO's teleconnections to many parts of the globe. For instance, Chowdary et al. (2012) showed that during the decades when the ENSO variability was high (low), its influence on the northern Indian Ocean and the North West Pacific climate was strengthened (weakened). Jia et al. (2014) found a similar relationship between the strength of ENSO and the North Pacific and North American (NPNA) climate. As a result, climate over the northern tropics and NPNA was more predictable in the 1980s and 1990s when the ENSO variability was large, compared to the 1960s and 1970s when the ENSO variability was small. On the contrary, the response of Australian rainfall to ENSO appears to be stronger when the IPO is in its negative phase and ENSO variability is reduced (e.g. Power et al. 1999, King et al. 2013). Power et al. (1999) analysed observational data over 1911-1995 and showed that when the IPO was negative, the variance of Australian rainfall was nearly doubled, and the rainfall correlation with ENSO increased. In explaining the stronger relationship between Australian rainfall and ENSO during negative IPO, Power et al. (2006) noted that La Niña generally had a stronger relationship with Australian rainfall than El Niño, and La Niña was more frequent during negative IPO (e.g. Kiem et al. 2003). This implies that Australian rainfall should have had a stronger relationship with ENSO and also a higher variance post-2000, which has

experienced the negative phase of the IPO, compared to the 1980's and 90's which experienced the positive phase of the IPO, but this has yet to be demonstrated.

> ***'Prediction skill'*** is the capability of the forecast system to predict observed events. It is measured with methods such as correlation, correct forecast rates, and root-mean-square error between forecasts and observations.
>
> ***'Potential predictability'*** is the predictable fraction of the climate system. Heightened predictability can be due to forcing such as slowly evolving ocean sates, land surface states, greenhouse gas changes, or ozone depletion. Potential predictability is measured as the ratio of forced variance to total variance. For example, if ENSO related climate variability is larger than the uncertainty measured by the spread of ensemble forecasts, the potential predictability is regarded to be high.

Interannual variation of Australian rainfall, especially, over the southern part of the country is also strongly affected by the Indian Ocean Dipole mode (IOD; Saji et al. 1999) in austral winter to spring seasons (Meyer et al. 2007, Lim et al. 2009, Risbey et al. 2009). The positive phase of IOD (positive IOD) is characterised by cold SST anomalies in the tropical eastern Indian Ocean concurrent with warm SST anomalies in the tropical western Indian Ocean, and it exerts its strong influence on the Australian climate because its eastern and western poles serve as diabatic heat sources that excite equivalent barotropic Rossby wave trains resulting in high pressure anomalies over southern Australia (Cai et al. 2011). Consequently, warm and dry conditions prevail over southern Australia during the positive IOD. In general, the IOD and ENSO correlation peaks in austral spring (e.g. Annamalai et al. 2005, Lim et al. 2009, Cai et al. 2011), and Cai et al. (2011) indicate that the impact of ENSO on SEA rainfall is via the association with the IOD in that season. Earlier studies show that the strength of the ENSO-IOD connection varies on inter-decadal time scales (e.g. Annamalai et al. 2005, Abram et al. 2008, Ihara et al. 2008, Weller et al. 2014). For example, the relationship between the IOD and ENSO was found to be very strong after 1960 especially in the 1980's-90's (Annamalai et al. 2005, Abram et al. 2008, Ihara et al. 2008). Ummenhofer et al. (2009) and Cai et al. (2012) argued that the skewness towards the positive IOD in the 1990's to 2000's, which was concurrent with the skewness towards El Niño, played a key role in the millennium drought over south-eastern Australia in that period.

Motivated by these earlier studies of impact of the IPO on changes in the variance and predictability of ENSO and ENSO's teleconnections, this study investigates the impact of the inter-decadal changes of ENSO amplitude on the co-variation of ENSO with the IOD and resultant changes in the predictability and prediction skill of the IOD and south-eastern Australian rainfall. Our focus will be on the past 30 year period (1985-2014) during which time a full swing from positive to negative IPO occurred and for which we have a comprehensive hindcast set from the Bureau of Meteorology's seasonal prediction model (POAMA).

Observations

The 15 year sliding correlations of the Nino3 index with the DMI and the eastern and western poles of the IOD; of the western pole of the IOD with the eastern pole of the IOD; and of SEA rainfall with the DMI and the Nino3 index are shown in Figure 1.1 for the period 1951-2014 (each correlation is plotted at the end of the 15 year window). For plotting clarity, we used the inverse of the eastern pole SST of the IOD and SEA rainfall. In these calculations, anomalies of SST and rainfall were obtained from the respective climatologies of 1951-2014.

Firstly, the positive relation between the ENSO and IOD has been significant since the early 1960's but displays some decadal wobbles. The correlation of ENSO with the IOD is mainly

governed by the correlation of ENSO with the western pole of the IOD, which is consistent with the finding of Cole et al. (2000). However, for the last 35 years (i.e. from around 1980?), the relation between ENSO and the eastern pole of the IOD has also been strong and in unison with the strong co-variation of the two poles during this time (e.g. Annamalai et al. 2005). Also, during this 35 year period the strength of the ENSO-IOD correlation is closely related to the amplitude of ENSO: the correlation is strong when ENSO amplitude is high in the 1980s and 1990s, and weakened when ENSO amplitude is weak in the 2000's. The strong relationship of ENSO and IOD in the 1980's and 90's coincides with increased DMI amplitude, largely due to increased amplitude of the eastern pole, which is more directly associated with the change of ENSO than is the western pole. The amplitudes of ENSO and the IOD and the strength of the ENSO and IOD relationship have reduced somewhat abruptly in the last 20 years (i.e. from the 15 year period ending in 2012).

Moreover, it is interesting to note that the inter-decadal variation of the correlation between the IOD and SEA rainfall (Figure 1.1c) is out of phase with that of the ENSO-IOD correlation. That is, when the ENSO-IOD relation is strong, the IOD and SEA rainfall relation is weak, and vice versa. This out-of-phase relationship is clear through the past 40 years. A similar feature is found for the relation between the ENSO (strictly speaking, the eastern Pacific ENSO monitored by the Nino3 SST anomalies) and SEA rainfall, but the variation of the rainfall association with ENSO is generally weaker than that of the IOD. Consequently, variation of SEA rainfall was strongly driven by the IOD and ENSO in the recent 15 years (i.e. from 1997 to 2014) despite the fact that the strengths of both ENSO and IOD were substantially reduced and the IOD and ENSO were only weakly correlated to each other. On the contrary, in the 1980's-90's when the amplitudes of ENSO and the IOD were large and the ENSO and IOD were strongly tied to each other, the influence of IOD and ENSO on SEA rainfall was much weaker. Lastly, the inter-decadal variation of the variance of SEA rainfall (Figure 1.1b) is not related to the fluctuations of the ENSO and IOD amplitudes, which is different from the finding of Power et al. (1999) but who used annual mean-all Australia rainfall that is dominated by the summer wet season in tropical northern Australia.

So, how are these variations in the amplitudes of the ENSO and IOD and their interaction reflected in the predictability and prediction skill of the IOD and SEA rainfall in the past 30 years?

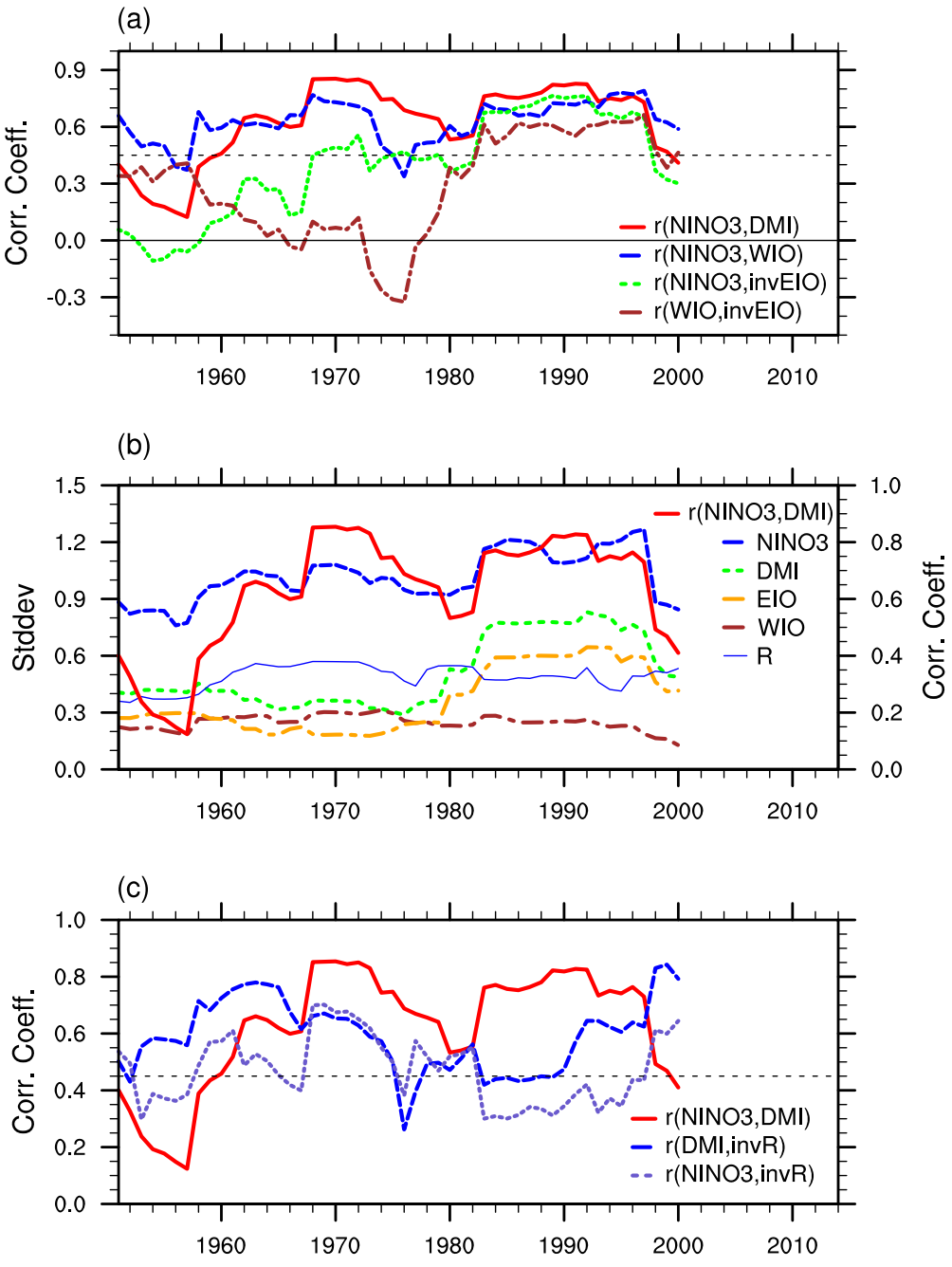

Figure 1.1:(a) The 15-year sliding correlation coefficients during 1951-2014 for September-November means of the Nino3 index with the Indian ocean dipole mode index (DMI; red line), Nino3 with the western pole SST of the IOD (WIO; blue line), Nino3 with the inverted eastern pole SST of the IOD (EIO; green line) and the western pole of the IOD with the eastern pole of the IOD (brown line). (b) The standard deviations of the Nino3 index (long dashed blue line), DMI (dotted green line), EIO (orange line), WIO (brown line), and south-eastern Australian (SEA) rainfall (33°-45°S, 135°-156°E) (solid thin blue line). (c) The correlation coefficients of the inverted SEA rainfall index with DMI (long dashed blue line) and with Nino3 index (dotted light blue line). The solid red line in (b) and (c) is the same as in (a). Correlation coefficients and standard deviations are displayed at the first data points of each 15 year block. Correlations greater than ~0.45 are assumed to be significantly different from zero at the 90% confidence level.

Predictability and Prediction skill of the IOD and SEA rainfall

The POAMA hindcasts correctly predict the differences of the amplitude of the IOD between 1985-99 (stronger) and 2000-14 (weaker) out to a lead time of 6 months (Figure 1.2a). However, the model systematically underestimates the amplitude of the IOD (e.g. Zhao and Hendon 2009) especially in the earlier 15 years. Similarly, the epochal difference of the strength of the correlation of the IOD and ENSO (strong during 1985-99 and weaker during 2000-14) is also reasonably well maintained out to 6 month lead (Figure 1.2b). Considering that the correlation of the IOD with ENSO and the amplitude of the IOD are reduced during 2000-14, potential predictability (Figure 1.2c) and prediction skill (Figure 1.2d) of the IOD are also significantly reduced in post-2000. A drop in skill of a persistence forecast (Figure 1.2d) is consistent with this drop in predictability and predictive skill of the IOD since 2000.

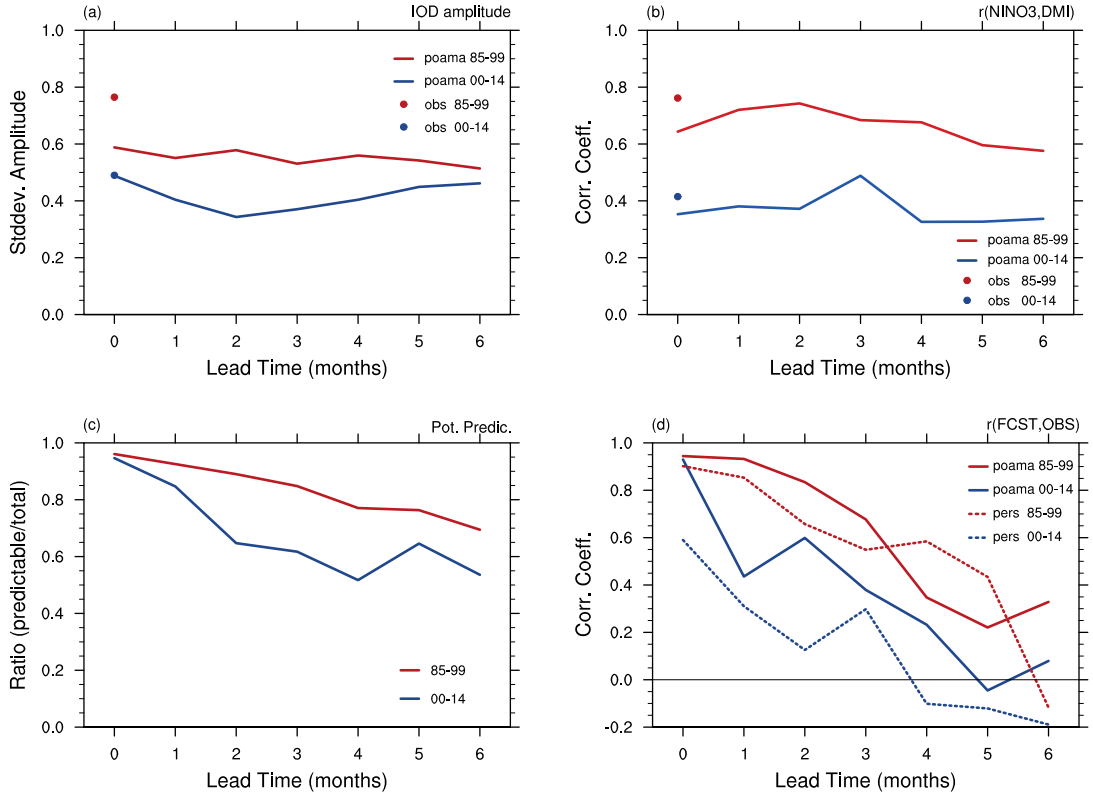

Figure 1.2: Predictability and prediction skill of the IOD in the 15 years before (red lines) and after (blue lines) 2000: (a) observed and predicted standard deviation of DMI, (b) observed and predicted correlation between the DMI and the Nino3 index, (c) potential predictability of the DMI, and (d) prediction skill of the DMI as a function of forecast lead time. Persistence forecasts in (d) were made with the state of the IOD in the previous months as a predictor for the IOD in austral spring (e.g. persistence forecast at lead time 0 was made by using August DMI to predict September-November mean DMI in each year). Predicted standard deviation of the DMI and the correlation of the DMI with the Nino3 index in the model were computed for each ensemble member, and the means of standard deviations and correlations are displayed in (a) and (b). Prediction skill of the DMI in (d) was computed with ensemble mean forecasts.

Despite the decrease of predictability and prediction skill of the IOD since 2000, the prediction skill for SEA rainfall since 2000, at least for lead time to 4 months, was higher (Figure 1.3a).

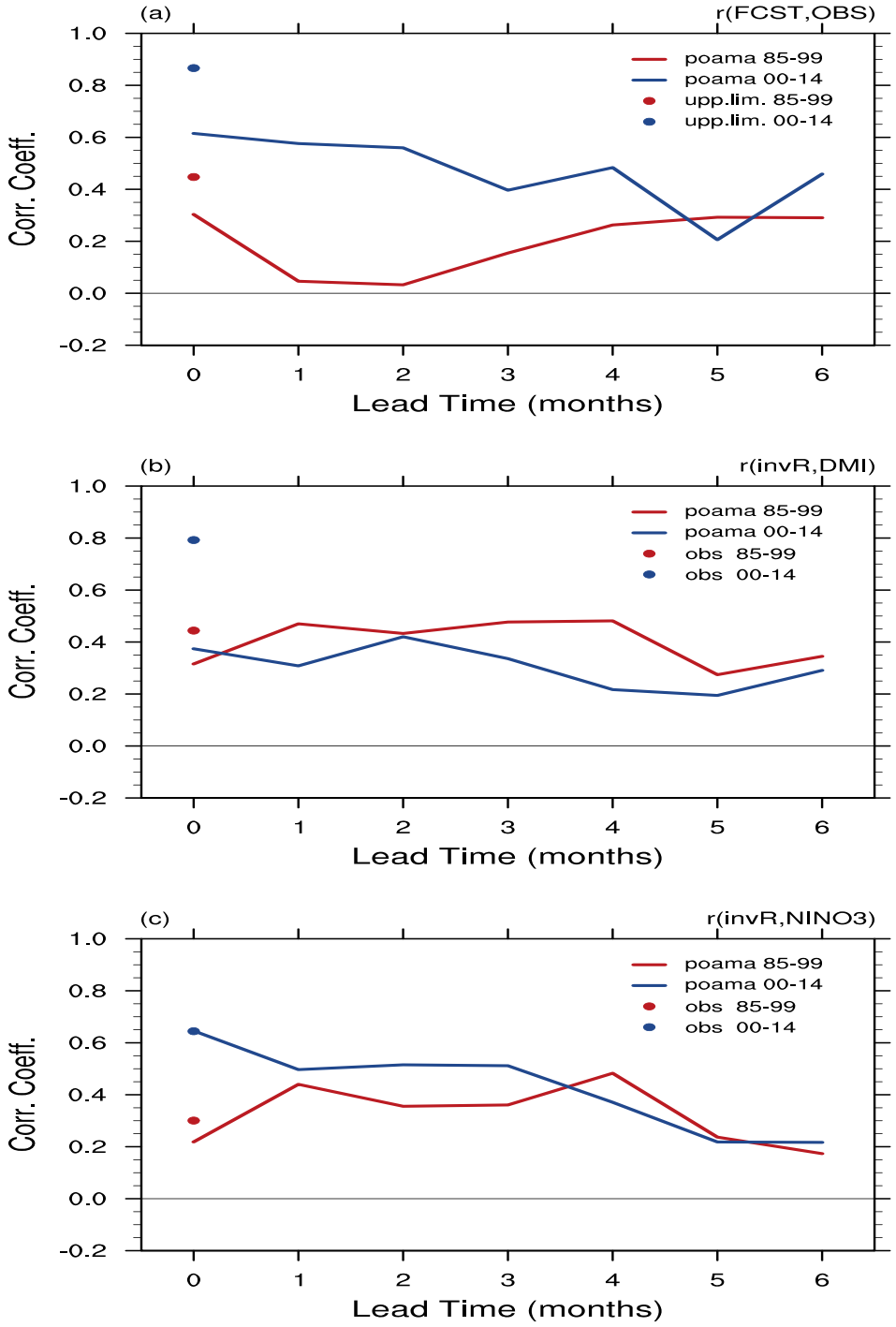

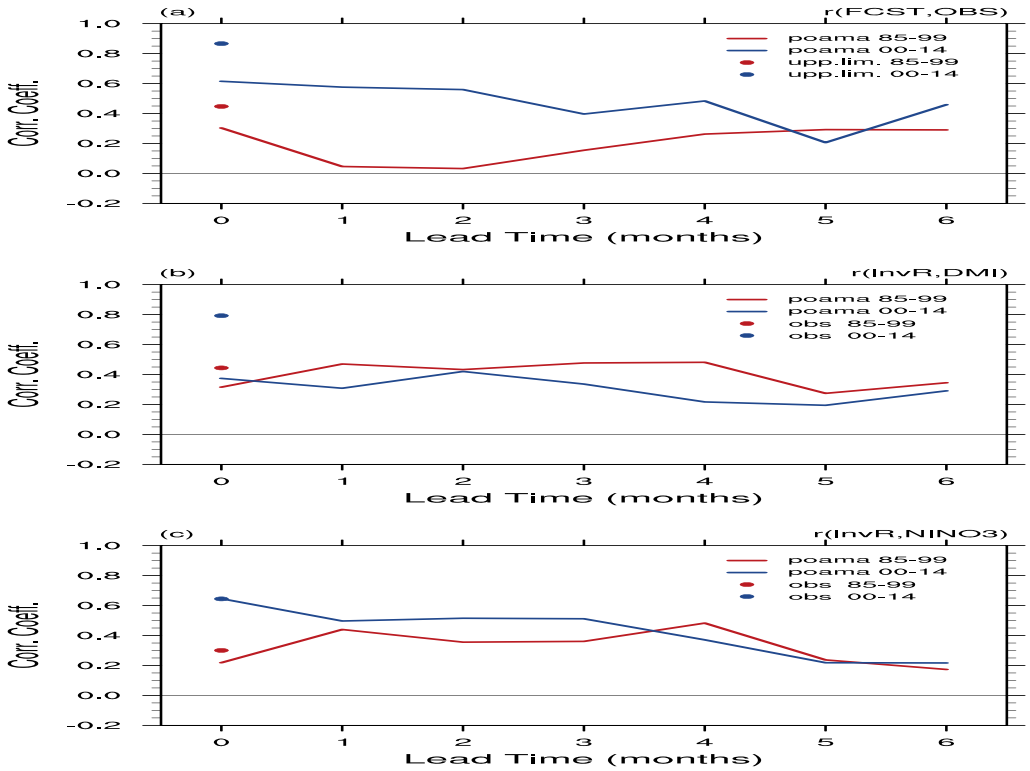

Figure 1.3: Predictability and prediction skill of SEA rainfall in the 15 years before (red lines) and after (blue lines) 2000: (a) prediction skill (lines) and the upper limit of predictability estimated by the multiple linear regression using SEA rainfall as a predictand and the DMI and the Nino3 index as predictors (dots), (b) observed and predicted correlation of inverted south-eastern Australian rainfall with the DMI, (c) observed and predicted correlation of inverted SEA rainfall with the Nino3 index as a function of forecast lead time. Prediction skill in (a) was computed with ensemble mean forecasts whereas the correlation SEA rainfall with the DMI and the Nino3 index of the model was computed for each ensemble member, and the mean of correlations is displayed in (b) and (c).

A plausible explanation is the strengthened teleconnection between SEA rainfall and tropical Indo-Pacific SSTs since 2000 as discussed earlier. However, the model is unable to capture the increased strength of the IOD and SEA rainfall relation during 2000-14 (Figure 1.3b). On the other hand, the model does capture the strengthened relation of SEA rainfall with ENSO since 2000 (Figure 1.3c). The lack of distinction in correlation between SEA rainfall and the IOD between the two epochs suggests that the forecast model is underperforming for prediction of SEA rainfall. Indeed, the rainfall prediction skill in both epochs is much lower than the upper limit of predictability of SEA rainfall estimated by the multiple linear regression of observed SEA rainfall with the IOD and ENSO (shown with dots in Figure 1.3a). This underperformance is likely due to the model's biases in the IOD teleconnections to SEA rainfall. Although the epochal difference of the strength of the relationship between ENSO and SEA rainfall is better represented in the model, the ENSO teleconnection also suffers from biases of the overestimation of the teleconnection strength in the earlier period and the underestimation of it in the later period (Fig 3c).

Activity 2: Impact of mean state on predictability, predictive skill and interactions of ENSO, IOD and associated SEA climate

Impact of mean state on the predictability and predictive skill of IOD

Zhao et al. (2015) showed that the observed decrease of ENSO amplitude since 2000 is attributable to decadal variations of the mean state of the tropical Pacific: the recent decades have experienced a shift toward the cold phase of the IPO which has acted to weaken the coupling in the eastern Pacific thereby resulting in weakened ENSO activity that is less predictable. Activity 1 revealed that the amplitude of the IOD also decreased in the recent decade due to its tight linkage with the amplitude of ENSO. Moreover, the relationship between ENSO and the IOD has recently weakened, and this lack of tight coupling between the IOD and ENSO was evident in the occurrence of a positive IOD event (which typically acts to dry Victoria) during the 2007-2009 La Niña episode. Therefore, in Activity 2, we have explored the impact of the decadally-varying background mean state upon the amplitude, potential predictability and prediction skill of the IOD and its covariability with ENSO.

For this activity, forecast sensitivity experiments were performed using the Bureau of Meteorology dynamical seasonal forecast system, POAMA. POAMA is an atmosphere and ocean coupled-model forecast system (Wang et al. 2005). The atmospheric model of POAMA is the BoM's Atmospheric Model version 3 (BAM3; Colman et al. 2005). The ocean component of POAMA is the Australian Community Ocean Model version 2 (ACOM2) (Schiller et al. 2002, Oke et al. 2005). The atmosphere and ocean component models are coupled by the Ocean Atmosphere Sea Ice Soil (OASIS) software (Valke et al. 2000).

The seasonal forecasts for the later epoch (2000-10) were re-run, but the mean state (2000-2010) was removed from the ocean initial conditions and replaced with a mean state from 1985-95. The anomalies still held information from the particular start month from 2000-2010. A similar method was used to assess forecasts from the earlier period (1981-99) with a background climate of 1985-95 replaced with that of 2000-2010. Forecasts from these mean state swapped experiments were compared to the standard forecasts for the same period to detect the differences caused by the change of the mean state.

The results suggest that the decadal change of the Indo-Pacific background climate accounts for only a small portion of the decadal change in amplitude and predictability of IOD (Figure 1.4 a and b). And, in particular, it does not account for the change in the teleconnection between the IOD and ENSO or the forecast skill of the IOD (Figure 1.4c). Consequently, the change of mean state does not appear to impact the forecast skill of SEA rainfall, and therefore, the change of the strength of the teleconnection of SEA rainfall with the IOD and ENSO, which seem more important for the predictability of SEA rainfall than the state of the IPO. We postulate this is because the impacts of the change in mean state in the forecast sensitivity experiments, while in the right direction to account for some changes in the strength and predictability of the IOD, are small in the initial months of the forecast. Hence, it is difficult to detect an appreciable change or impact on the rainfall teleconnection as a result of changes in background climate. Given the findings from these experiments, this analysis will not be pursued further.

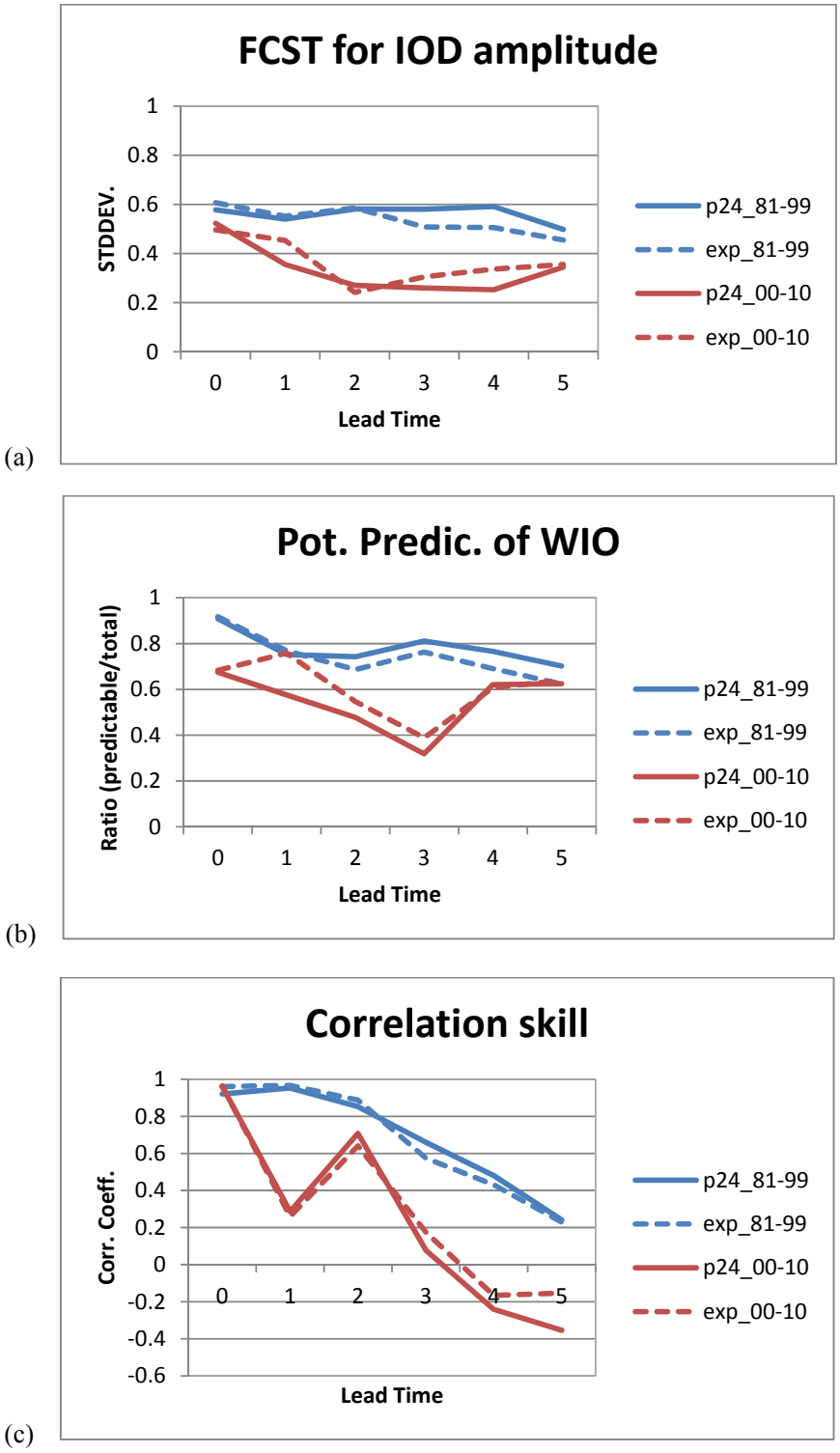

Figure 1.4: Comparisons of the amplitude, predictability and prediction skill of the IOD between the standard hindcasts (p24; solid lines) and the forecast sensitivity experiments where forecasts of the earlier epoch (1981-99) were initialised with the mean state of the later epoch (2000-10) and forecasts of the later epoch (2000-10) were initialised with the mean state of the earlier epoch (1985-95) (dotted lines).

Multi-year prediction of ENSO

The potential for multi-year prediction of El Niño and La Niña was also further explored by extending an ensemble of POAMA forecasts out to 2 years for two case studies. This was motivated by the observations that some El Niño/La Niña events exhibit multi-year persistence. Although the limit of predictive skilful El Niño/La Niña based on the POAMA hindcast set for 1981-2014 is ~9 months, exploration of longer lead prediction for a selection of El Niño/La Niña events is warranted in order to reveal possible sources of predictability and to give a glimpse of what might be possible in the future with improved models. Two extended La Niña episodes (2007-2009 and 2010-12) were targeted. Forecasts were initialized monthly from the peak of the preceding El Niño in each case (i.e. 2006 and 2009) and run for 2 years.

Preliminary results indicate some predictability for the back to back La Niñas in 2008/09 but no indication of predictability is indicated for the 2011/12 case. Based on the inconclusive results, we decided not to pursue this issue any further with POAMA. We note that severe model drift in POAMA after 1 year of forecast probably limits any predictive capability after 1 year, and so multiyear predictability of El Niño/La Niña should be revisited once the new prediction model (ACCESS-S is implemented at BoM. Similar forecasts using the SINTEX-F model in Japan, which exhibits much less drift, have been conducted and do indicate potential for prediction of La Niña in year 2 for both cases (Luo et al. 2015). This source of predictability is being pursued with JAMSTEC/Japan and will be reported in due course.

Conclusions and future perspectives

In Activity 1, we showed that when the mean state of the tropical Pacific SST is in the cold phase of the IPO (La Niña-like), the amplitude of ENSO and the IOD tend to decrease, the linkage between ENSO and the IOD weakens, and the predictability and prediction skill of ENSO and the IOD decrease. However, the teleconnections of ENSO and the IOD to SEA rainfall tend to become stronger, which results in the increased seasonal predictability and prediction skill of SEA rainfall in austral spring season. When the mean state of the tropical Pacific SST is in the positive phase of the IPO (El Niño-like), the opposite changes tend to occur. Consequently, during 1985-1999 when the IPO was positive, ENSO and the IOD amplitudes were large and the ENSO-IOD correlation was high; hence predictability and prediction skill of the IOD were high. However, as the teleconnections of ENSO and the IOD to SEA rainfall were weak, the predictability and prediction skill of SEA rainfall was low. In contrast, during 2000-2014 when the IPO was negative, ENSO and IOD amplitudes were reduced and their interaction was weak, hence predictability and prediction skill of the IOD was reduced. But, skill for prediction of SEA rainfall increased.

This study did not tackle some key dynamical questions such as why the teleconnections of ENSO and the IOD to Australian rainfall become stronger when the ENSO and IOD amplitudes themselves are weaker, and vice versa, which is somewhat counter-intuitive and in contrast to the NH cases with changes of the ENSO amplitude discussed above. Preliminary assessments suggest that the strength of the rainfall teleconnection could be sensitive to the spatial variation of SST anomalies during ENSO/IOD, thus causing changes in the pattern of tropical convection that acts as a Rossby wave source, and therefore the source of anomalous circulation over SEA. Further investigations to address this question are underway.

In Activity 2, we investigated the impact of the decadal variation of the mean state of climate system on the strength of the IOD, its relationship with ENSO, and its predictability and prediction skill. The impact was found to minimal compared to the impact of the decadal mean state change on ENSO. The impact of the mean state change on SEA rainfall was small as well. We identified that the teleconnection strengths of ENSO and the IOD to SEA rainfall are more

important factors than the change of the mean state and associated changes in ENSO and IOD amplitudes. Given the inconclusive findings from these experiments as to why the teleconnections to Australian rainfall are stronger when ENSO/IOD are weak, these sorts of sensitivity experiments with the POAMA seasonal prediction system will not be pursued further.

PROJECT 2 & 4: UNDERSTANDING THE MEAN MERIDIONAL CIRCULATION (MMC) AND ITS RELEVANCE TO VICTORIA AND EXPLORATION OF THE CAUSES OF TROPICAL EXPANSION

Hanh Nguyen, Chris Lucas, Harry H. Hendon, Bertrand Timbal
R&D Branch, Bureau of Meteorology

Key findings

- Model simulations of the historical era do not capture the full extent of the observed hemispheric Hadley cell expansion. The results from 10 CMIP5 models all show that models largely underestimate the observed amount of tropical expansion. Thus the contribution from various forcing factors is also small in these models. The simulations associated with the warmest global mean temperatures (i.e. the simulations with prescribed GHG-forcing but without ozone changes) are also those depicting the largest Southern Hemisphere expansion of the Hadley and poleward shift of the sub-tropical ridge. This confirms that Hadley cell expansion is closely associated with global warming. Factors that act to cool the globe in climate models (e.g. volcanoes) are expected to reduce the expansion of the tropics.
- An analysis of the Hadley cell in three separate sectors (the Asia-Pacific, Europe-Africa, and America (north and south)or regions) indicates that the Southern Hemisphere Hadley cell expansion is mainly happening in the Asia-Pacific sector, both for annual and individual seasonal means. This expansion is associated with the negative phase of the IPO (La Niña-like state in the tropical Pacific): cold waters in the eastern equatorial Pacific contrasting with warm waters in the western Pacific and Indian Oceans.
- Attribution analysis using both statistical analysis of observations and single forcing climate model simulations indicates that Southern Hemisphere tropical expansion is attributable to a combination of factors: Since 1979, the partition of forcing factors for Southern Hemisphere tropical expansion is 30% resulting from natural factors (volcanoes and ENSO), 40% resulting from stratospheric ozone depletion and 30% resulting from increasing greenhouse gases, with an error range roughly estimated at ± 10%. Since 1979, natural factors (ENSO, IPO, volcanoes) have been of increased importance. The recent trend toward negative IPO/strong La Niña conditions would not be simulated by an ensemble mean from climate model simulations and this accounts for some of the reduced tropical expansion in the models compared to the observations. On a longer time-scale (since the 1960s), anthropogenic forcings (greenhouse gases and stratospheric Ozone) are the dominant drivers.
- An expanded Hadley cell both hemispherically and regionally in the Asia-Pacific sector is associated with a poleward expansion of the tropical wet zone but does not relate during the peak of the cool season to the intensity or position of the regional sub-tropical ridge in the Asia-Pacific sector nor the southeast Australia (SEA) observation-based sub-tropical ridge. A possible mechanism to explain the association of an expanded Hadley cell with La Niña conditions is via the Southern Annular Mode: a poleward shift of the mid-latitude jet is favoured by La Niña conditions in the tropics, which results in an expansion of the Hadley cell.
- As regional Hadley cell expansion relates primarily to wet conditions over Australia, it cannot explain directly the on-going cool season deficit over south-east Australia. Variation of the intensity and position of the regional sub-tropical ridge is connected by a remote response to tropical diabatic heating in the Indian Ocean that has characteristics of the Indian Ocean Dipole but this is mainly operating in the later part of the cool season on inter-

annual time-scales. However, due to the absence of a marked trend in the dipole and the lack of relationship during the earlier part of the cool season where most of the on-going deficit has been observed, it cannot explain the bulk of the on-going cool season rainfall deficit.

- The significant correlations of Australian rainfall with the regional Hadley cell extent indicate that a poleward expansion induces higher tropical/sub-tropical rainfall totals. In winter and spring there are significant positive correlations across east Australia while in summer they are mainly in the west of the continent. In contrast, across south-eastern Australia, correlations between rainfall and the regional sub-tropical ridge intensity and position in all seasons are highly similar to the correlations obtained using the local, observation-based, STR which was used in SEACI. The main differences are seen across large areas of eastern and northern Australia where correlations between rainfall and regional STR indices are significantly positive and are similar to the correlations obtained using the regional HC indices. No such areas of strong positive relationship were observed using the local observation-based STR indices.
- Overall, the computation of the Hadley circulation in regional components has revealed that the regional component in the Asia-Pacific prevails in terms of the mean climate. Furthermore, it is also the regional component in the Asia-Pacific region which has seen the largest expansion. However, this cannot be inferred to explain why a cool season rainfall deficit is being experienced across southern Australia. Indeed, on a regional basis, the relationship between the Hadley circulation and the STR is non-existent in the winter. On the contrary, the regional Hadley cell analysis has revealed that the expanded regional Hadley cell is more likely to explain the on-going warm season rainfall increase across most of northern Australia. It remains the case that the local STR, which relates very well to the observed on-going cool season rainfall deficit (spatially and in terms of timing in the annual cycle) has been observed to strengthen in conjunction with global warming. Further, climate models confirm that global Hadley circulation expansion and STR strengthening are to be expected in response to anthropogenic forcings, albeit at a much lower rate than observed. The modelled lower rates are somewhat consistent with this year's finding that internally generated natural variability in the form of a shift in the last 30 years from the warm to the cold phase of the IPO has promoted the regional Hadley circulation expansion (the main component of the global Hadley circulation expansion). Overall, the regional analysis of Hadley circulation has not offered a simple mechanism by which the local sub-tropical ridge strengthening could be causally linked to the global warming. It will therefore remain an active area of research for VicCI in the third year.

Background

The topics of research in Topics 2 and 4 have become very closely aligned as research has progressed, and thus will be reported together in this annual report.

Estimates of tropical expansion vary greatly in their magnitude and seasonality, depending on the metric and dataset used. A range of metrics of tropical expansion were reported in the 2013-14 annual report (Murphy et al., 2014), and were presented as a poster at the 5th SPARC General Assembly (Stratosphere-Troposphere Processes And their Role in Climate) in 2014 'A Critical Comparison of Tropical Expansion Metrics'. Further exploration of the extension of the methods to regional estimates has been undertaken this year

Climate model simulations best represent observed recent changes in the mean meridional circulation (MMC), especially its expansion, when ozone depletion and other anthropogenic external forcings are used, suggesting at least a partial human influence on recent changes. However, the expansion in the models is typically much weaker when compared to

observations. Stratospheric ozone depletion, often poorly represented in GCMs, may play a significant role in the southern hemisphere circulation, including the tropics and subtropics. It is thus critical to understand what is actually driving the changes in the MMC and why the models are underestimating the changes.

Objectives

These objectives have been re-ordered to start with the analysis of the hemispheric situation, before moving onto the regional response:

1. (Project 2, Activity 2) To further compare estimates of tropical expansion.
2. (Project 4, Activity 1) To quantify the relative roles of the factors that are hypothesized to drive tropical expansion. Greenhouse, ozone, aerosol and natural forcing.
3. (Project 4, Activity 2) To gain insight on how ozone depletion is contributing to changes in regional HC.
4. (Project 2, Activity 1) Define a regional streamfunction of the HC, relevant to the Australian sector, and evaluate the relationship between changes in the regional HC and Victorian rainfall.

Project 2, Activity 2: Tropical expansion metrics

After an exhaustive comparison reported on in Murphy et al. (2014), the most likely rate of tropical expansion, since 1979, is of the order of 0.5 deg.decade^{-1} in each hemisphere. However, this trend is not continuous, in part due to natural variability caused by large volcanic eruptions (e.g. Mt. Pinatubo 1991) and ENSO. A shift in the position of the tropical edge in the late 1990s across all the metrics analysed here is suggestive of abrupt change to the circulation. This comparison was presented at the 5th SPARC General Assembly (Stratosphere-Troposphere Processes And their Role in Climate) in 2014: 'A Critical Comparison of Tropical Expansion Metrics: Lucas et al'. Further extension of this work has focussed on the regional signature of this expansion and further extension of the isentropic method which is being reported in project 3.

Project 4, Activity 1: Attribute relative roles of climate forcings in the observed tropical expansion

This work was reported in last year's annual report (Murphy et al. 2014) in some length and only a brief summary of the key findings in light of some recent additional work follows. Two approaches were used. One was a statistical regression analysis relating the Southern Hemisphere tropical expansion results of Lucas et al. (2012) to indices of known large-scale climate drivers, including internally generated variability (ENSO), the sporadic and unpredictable forcing from volcanoes, and externally forced factors known to have an anthropogenic contribution to their time evolution (Global or Southern Hemisphere temperature anomaly, and Antarctic ozone hole area). The other method was assessing the contribution to the trend of single-forcing simulations of the CCSM4 coupled climate model. Trends in the tropical edge were examined over the whole period (1960-2005) or from 1979.

Of this trend, the statistical analysis reveals that approximately 10% is due to ENSO and 20% due to volcanoes. This is simply a matter of the timing of the period over which the trend is computed. There are more La Niña events during more recent years than earlier in the record, and La Niña is associated with tropical expansion. Similarly, the significant volcanic eruptions

occur earlier in the record (1982, 1991). The remaining 70% of the trend is due to anthropogenic forcing: ozone depletion and rising temperatures (presumably due to greenhouse gas increase). The exact partition between these two variables is unclear in the statistical analysis, due to the strong correlation between the two variables. We can use the two realizations of the regression to assign a range: 10-40% of total trend is due to global temperature (i.e. GHG increase), while the remainder (60%-30%) is due to ozone depletion.

The modelling simulations have their own internal variability and are unlikely to align with the observed ENSO timing. Of the trend 1960-2005, analysis of the single forcing simulations (see Table 2.1 for explanation of the forcings) shows that O3 and GHG are the dominant forcings of tropical expansion. Trends in the tropical edge in the NAT and AER simulations are small over this time frame. From 1979, the picture is quite different, with NAT producing the largest trend. This is largely due to the strong contraction of the tropics associated with the El Chicon and Mt Pinatubo eruptions in 1982 and 1991, respectively. This contraction is considerably stronger than what is seen in the observed record. The only significant trend identified from 1979 is in the O3 experiments.

Table 2.1: Overview of CCSM4 coupled model simulations.

ALL	Full forcings
NAT	Natural forcings only– volcanic aerosol and solar variability
GHG	Greenhouse gas forcing only
O3	tropospheric and stratospheric ozone only
AER	Anthropogenic aerosol (direct effects) only

Combining results from the two approaches, the best estimate is that since 1979, the partition of forcing factors for Southern Hemisphere tropical expansion is 30% resulting from natural factors (volcanoes and ENSO), 40% resulting from stratospheric ozone depletion and 30% resulting from increasing greenhouse gases, with an error range *roughly* estimated at ± 10%. The strong role of natural factors is largely the result of the choice of starting point of the analysis. The longer analysis suggests that natural variability plays a smaller role. The role of aerosol remains unclear. The CCSM4 simulations suggest that aerosols are unimportant for Southern Hemisphere tropical expansion, but this may be the result of the type of aerosols specified in the CCSM4 and requires further investigation to determine if this is a robust result. While our results suggest that O3 has been dominant in the recent past, its role is expected to diminish as the ozone hole recovers; GHG is expected to be more dominant in the future. How exactly the tropical edge will evolve over the next 20-30 years is unclear.

Further work in this topic has progressed to an early draft paper and this will be completed in the coming year. The important role of ozone forcing on the trend since 1979 has been examined using CMIP5 models in Project 4, Activity 2 below.

Project 4, Activity 2: The response to Antarctic stratospheric ozone depletion in CMIP5 model simulations

It was found that since 1979, the growing Antarctic ozone hole has contributed to the expansion of the tropics in the Southern Hemisphere. Climate modelling groups implement the response to changing stratospheric ozone in a range of ways, and thus it is worthwhile exploring this

question in a range of models beyond just CCSM4. The CMIP5 suite provides this opportunity. Unfortunately, only one of the models examined was found to have a single forcing run that included only the variability of stratospheric ozone. However, of the 10 models examined, it was found that of the simulations forced only by greenhouse gases, half also included the forcing from Antarctic stratospheric ozone variability. This provided an opportunity to explore not only the contribution from the changes in the ozone hole alone, but also the impact after including the non-linear interaction with growing greenhouse gas levels. Aspects of this work were reported in the annual report of VicCI last year, and that work and this extension is now in a submitted paper, Nguyen et al. 2015a, and the publication of this work will be pursued in Year 3.

Method to define the Hadley cell Edge (HCE), Hadley cell Intensity (HCI), and sub-tropical ridge intensity (STRI) and position (STRP)

The hemispheric Hadley cell is identified using the zonal mean meridional streamfunction Ψ, representing streamlines of mass transport in pressure coordinates. The Hadley cell Edge (HCE) is defined as the location of the sub-tropical zero contour of Ψ averaged between 600-400 hPa, The Hadley cell Intensity (HCI) is the average of the peak Ψ values from between 900 to 200 hPa. Full details on the computation are described in Nguyen et al. (2013). The zonal mean sub-tropical ridge (STR) is characterized by its intensity (STRI) and position (STRP) and is here assumed to be associated with the absolute maximum zonal average mean sea level pressure (MSLP). Therefore STRI and STRP can be defined by identifying the amplitude and location of the MSLP peak. Here data from the 20CR reanalysis and from the 10 CMIP5 ensemble model mean of the historical all forcings (HIS), greenhouse gas forcing with and without ozone (GHG+O3 / GHG) and natural forcing (NAT) simulations are used. We compare the different simulations with the 20CR in the attempt to attribute the changes in HC and STR to anthropogenic forcing.

The time series of annual mean indices from the multi-model average is shown in Figure 2.1. As expected the warming trend is reproduced only in anthropogenic GHG-induced (i.e. historical forcing (HIS) and GHG-forcing with or without ozone) time series. The main difference in these latter time series resides in the mean values, with the GHG being about 0.25 and 0.5K warmer than the GHG with ozone and the all forcing, respectively. This highlights that the forcing from the growing ozone hole from the early 1980s to the early 2000s can have an observable impact on the global temperature. The ensemble mean global temperature series simulated under natural forcing (NAT) is marked by three sharp cooling periods in 1963, 1982, 1991 in response to major volcanic eruptions of Mount Agung, El Chichón and Pinatubo, respectively. These cooling episodes are also seen in the all forcing time series, but with reduced intensity. Both the GHG-induced time series exhibit a steady increase in temperature over the whole period.

The mean edge and intensity of the Hadley cell in the CMIP5 models ensemble mean are relatively similar to those from 20CR, except in the last 20 years when the variability of 20CR HCE is larger than the modelled variability and 20CR HCE shows a strong southward shift which is not evident in the modelled time series. However, a long-term, subtle trend to HC expansion is seen in the series with only GHG forcing. Like for 20CR, this expansion is concomitant with a tendency for a poleward shift of the STRP. This is associated with more intense mean STRI in the CMIP5 models ensemble mean (~1hPa). Note however that at annual mean, 20CR STRI is at odds with the model simulations (Fig. 2.1, bottom), depicting a generally weaker intensity.

The simulations with the warmest global temperatures (GHG-forcing without ozone) are also those with both HCE and STRP markedly poleward compared to the other simulations.

However, when GHG and ozone work together, the intensity of the STR is increased. Since this aspect of the MMC most strongly impacts upon Victorian rainfall, if the ozone hole reduces in size over coming decades, as it is projected to do, the action of this component to increase the pressure of the STR and reduce rainfall might be reversed. From the results here, it may also contribute an extra layer of global warming that we have thus far been 'protected' from. The impacts from the ozone hole are likely to be felt in spring and summer.

The association of trends in Hadley cell or STR indicators between themselves and with trends in global temperature are shown in Figure 2.2. Some of these regressions are problematic in the case of the 20CR as they imply trends in STR even in the absence of warming trends. The issue with these reanalyses is discussed in more details in Nguyen et al. (2015a).

Results

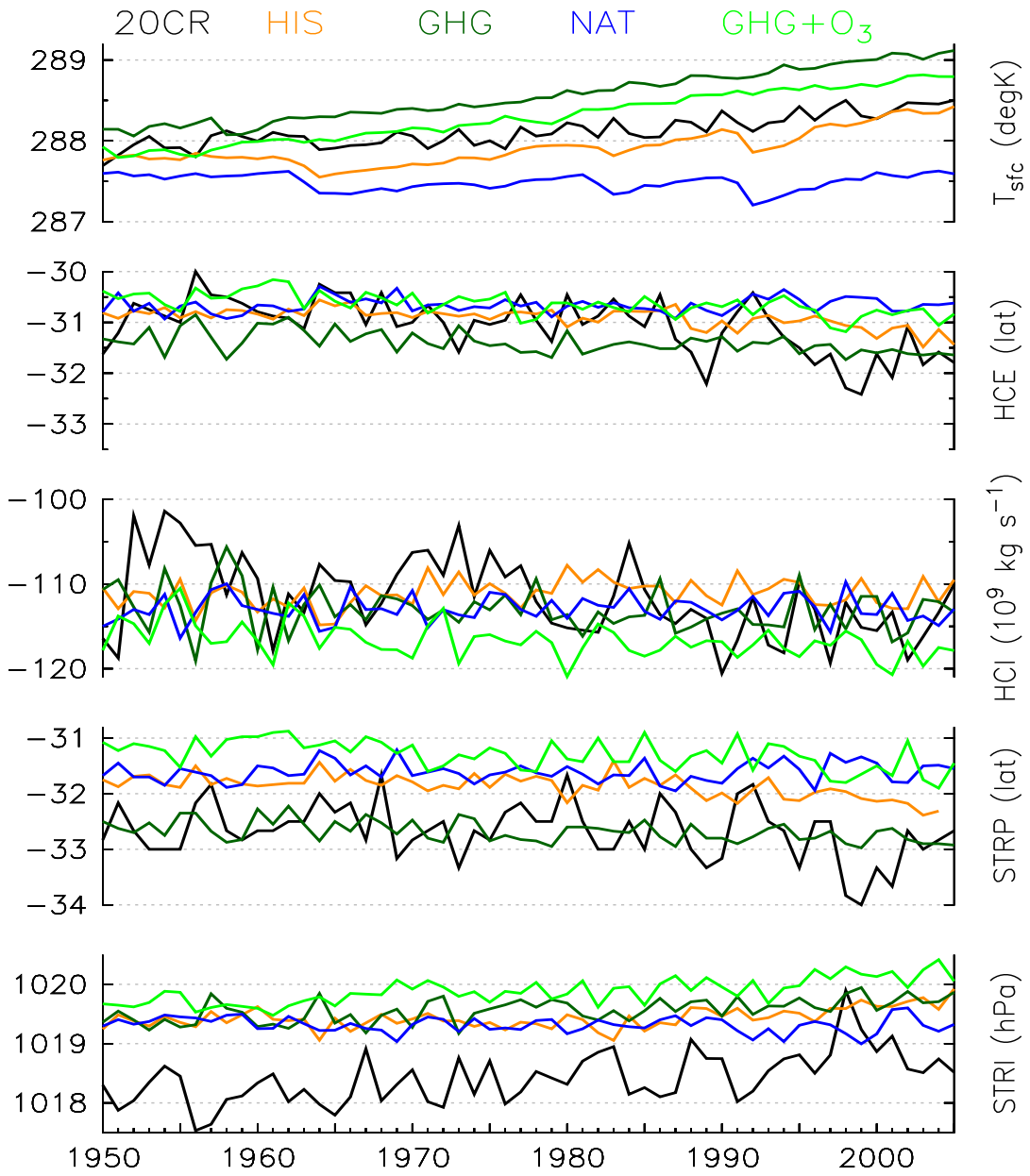

Figure 2.1: Annual mean and standardized annual anomalies indices from 20CR (black) and CMIP5 multi-model average (HIS: orange, GHG only: dark green, GHG with O_3 included: light green, NAT: blue,) from top to bottom: Global Temperature, HCE, HCI, STRP and STRI. See Table 2.1 for the forcing in the model simulations.

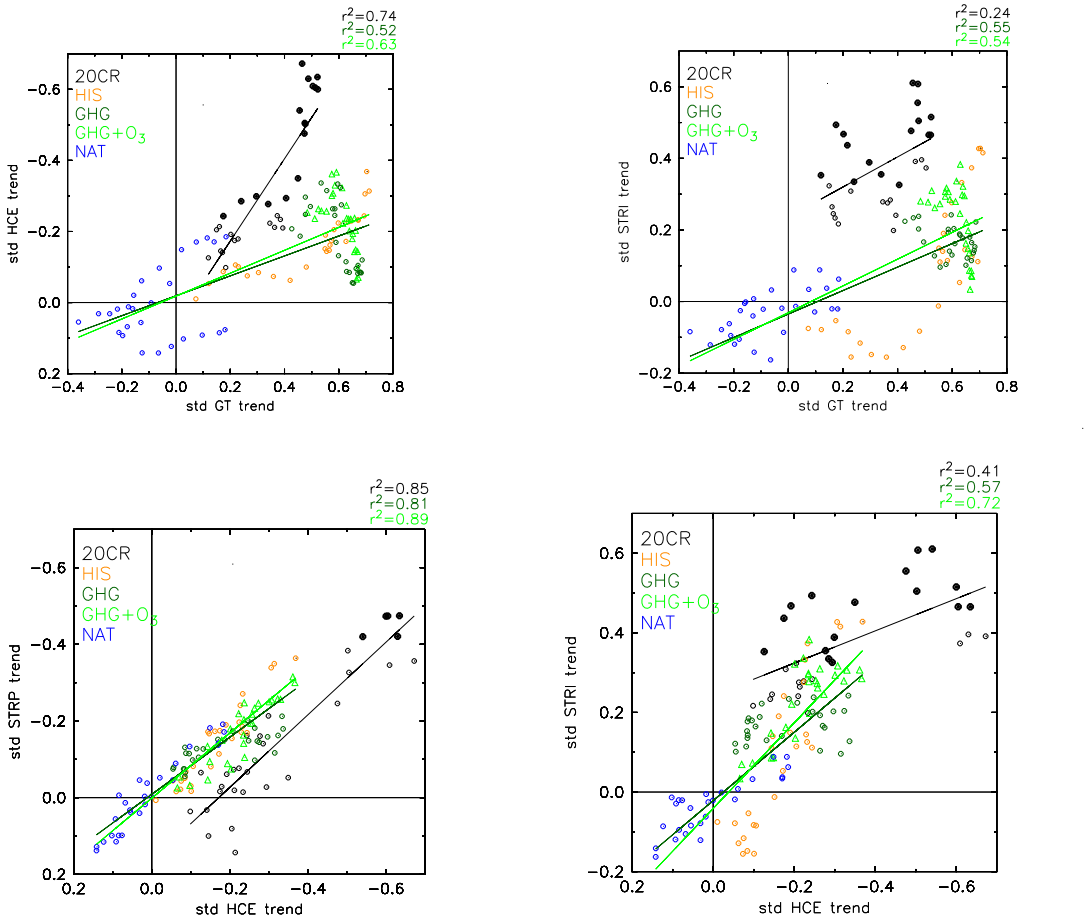

Figure 1.2: The comparison of the rate of change of global temperature and indicators of Hadley cell or STR. Each symbol represents the comparison of two 30 year linear trends. Data are: 20CR (black) and CMIP5 (HIS: orange, GHG only: dark green, GHG with O3 included: light green triangles, NAT: blue). Top row is the trends in standardized (std) GT compared with HCE (top left) and STRI (top right). Bottom row is the comparison between the standardized (std) HCE trend and STRP (bottom left) and STRI (bottom right). Values statistically significant at the 95% level are indicated with closed symbols and the variance explained are shown

Note the reversed vertical axis on the left-hand plots, where more negative numbers (higher on the graph) mean poleward expansion in the Southern Hemisphere. As the rate of global temperature change (rise) increases, so does the rate of Hadley cell expansion. This relationship is strong in the observations, and less strong, but evident in the all-forcing simulation. Changes in the intensity of STR can be rapid, even when the global temperature is changing only slowly, although there is a suggestion of a non-linear relationship. When the global warming trend is small or negative in the models, changes in the STRI can be negative. This situation is not evident in the observations. There is limited distinction between the GHG and GHG+O3 simulations, with both showing only strong trends in global temperatures, but a range of rates of change in HCE or STRI. There is an association between the trends in HCE and STRI (lower right panel of Fig. 2.2), with the rate of poleward expansion being associated with stronger intensification of the STR.

This association is stronger in the models than in the observations, and the simulations with O3 included alongside GHG have a stronger association than GHG forcing alone.

These results differ from those found for the Asia-Pacific sector in Project 2, Activity 1 described below, where the HCE is positively correlated with the position but not the intensity of the STR. This highlights the complexity of understanding how the hemispheric Hadley cell expansion relates to climate indicators across SEA. Further work is warranted to explore these contradictions between hemispheric and regional Hadley cell indicators.

Project 2, Activity 1: Regional Hadley cell expansion and relationship to Australian rainfall

Topical expansion previously reported was estimated assuming zonal symmetry. In reality the tropical edge is marked by longitude dependence (CSIRO, 2012 and Lucas et al. 2012). In particular, Lucas et al. (2012) reported marked variability in tropical expansion for the three southern hemisphere continental longitudes, with the Australian sector exhibiting the largest expansionary trend. This result, combined with conclusions from last year (Lucas and Nguyen 2015), lead us to the question of how the Hadley circulation can be defined regionally and how it impacts the different regions beneath it. This could be key in explaining how the Victorian rainfall response differs from other sub-tropical regions. In Part A we extend the streamfunction method to define and evaluate the regional Hadley cell over Australia. In Part B we will explore the global and Australian responses to variability in the Hadley cell in the Australian sector.

Defining the Hadley cell from the regional perspective relevant to Australia

On a global scale, Nguyen et al. (2015a) have shown that in the Southern Hemisphere both the intensification and shift poleward of the STR relate well to the HC expansion. However the missing link to tie HC expansion to regional changes in climate and especially the local STRI as used in SEACI is the difficulty in computing a regional index of the HC. Previous results (CSIRO 2012) highlighted the strong relationship between the SEA rainfall decline and intensification of the local STR. We showed above that zonal mean (global average) HC expansion was strongly associated with zonal mean STR intensification. Here we want to quantify the regional and local aspect of both HC expansion and STR intensification and determine whether their relationship at the global mean still holds at the regional/local scale. By nature of the computation using the Stokes streamfunction and in order to conserve the mass flux in the zonal direction, the HC is defined globally only from a hemispheric perspective. Schwendike et al. (2014) proposed the partitioning of the overturning circulation into the meridional (Hadley) and zonal (Walker) component using vertical velocity, where the regional Hadley circulation is defined by the vertical mass flux and the divergent component of the circulation in the meridional plane. However this only reflects the ascent and descent characterising the vertical velocity at mid-levels and the circulation described by the $(\vec{v}, \vec{\omega})$ components. Here we propose to diagnose the regional Hadley circulation in the same way as for the global view using an overturning streamfunction, but with the conservation of mass flux in the zonal direction. This way, direct comparison can be objectively made between the global HC and the regional contribution.

Data

The reanalysis dataset used is the ERA-Interim (ERAI) from the ECMWF (Dee et al. 2011). The observational data include the rainfall dataset Version 2.2 from the Global Precipitation Climatology Project (GPCP, Huffman et al. 2009). In addition to the GPCP, the high resolution Australian Water Availability Project (AWAP) gridded rainfall dataset (Jones et al. 2009) is

used to assess the changes in Australian rainfall. The sea surface temperature (SST) used in the study is the Version 1.1 of the Hadley Centre Sea Ice and Sea Surface Temperature (HadISST) from the Met Office Hadley Centre (Rayner et al. 2002). All the data used for the study are monthly means and the common period chosen is 1979-2010.

Method

The Hadley circulation can be quantified by using the Stokes streamfunction that expresses the fact that for a two-dimensional flow the conservation of mass equation couples motion in one direction with motion in the other direction. Hence, a streamfunction can fully describe the flow. The conservation of mass (continuity equation) requires an average over longitude around the entire globe so that the net divergence over the depth of the atmosphere at each latitude is zero (i.e. there is no net flow across latitude). The regional streamfunction is derived from the irrotational part of the meridional wind averaged over a range of longitudes. By definition, only this part of the meridional wind contributes to the meridional circulation, without any zonal mass transport in and out of a limited domain. The Helmoltz theorem (Arfken 1985) is used to partition the horizontal wind $\vec{V}$ fields into rotational $\overrightarrow{V_r}$ and divergent $\overrightarrow{V_d}$ components:

$$\vec{V} = \overrightarrow{V_r} + \overrightarrow{V_d} = \hat{k} \times \vec{\nabla}\psi + \vec{\nabla}\chi$$

Where ψ is the streamfunction, χ is the velocity potential, and $\hat{k}$ is a unit vector in the vertical direction. The Hadley circulation is contained in the divergent wind fields $\overrightarrow{V_d}$ and regional representation of the Hadley circulation can be obtained by the meridional mass streamfunction derived from the divergent wind fields:

$$\psi_d(\phi, p) = \frac{2\pi a \cos\phi}{g} \int_0^p [V_d(\phi, p)] dp$$

Where ϕ is latitude, p pressure, a the earth's radius, g the acceleration due to gravity.
From the annual mean climatology of the divergent wind fields in the upper (200 hPa) and lower (850) troposphere from the ERA-Interim reanalysis for the period of study (1979-2010), there are clearly three centres of divergence along the equator in the upper troposphere: South Africa, South America and the largest one in the Asia/Maritime Continent region over the Indo-Pacific tropical warm pool.
Therefore three (unequal) longitude bands can be determined based on these centres of divergence:

(i) the Europe-Africa sector (EA = 25°W-60°E) comprises Europe and Africa
(ii) the Asia-Pacific sector (AP = 60°E-175°W) comprises Asia and Australia-New Zealand
(iii) the Americas sector (AA = 175°W-25°W) comprises both North and South America.

Unlike the usual characterization of the zonal mean (hemispheric) Hadley cell, where its edge is defined as the poleward extent of the descending branch as given by where the streamfunction goes to zero, the regional cell does not necessarily reach the zero value at its poleward edge. Therefore we define the edge of the regional Hadley cells when streamfunction decreases from its peak to 25% of that peak between 700-400 hPa.

With the same regions defined above, we also quantify the regional sub-tropical ridge, which is expected to lay at the poleward edge of the HC, using its position (STRP) and intensity (STRI). Position and intensity are determined by the latitude and magnitude, respectively, of the maximum mean sea level pressure (MSLP) averaged zonally for each region.

Regional Hadley cell

The streamfunctions computed from the divergent meridional wind for the three regions are shown in Figure 2.3. The Hadley cell extends much farther poleward in the Asia-Pacific sector than over Europe-Africa and the Americas, which is expected given the strongest convective forcing in this sector, with the global maximum of upper-level outflow being over the Maritime Continent-south Asian sector or warm pool, commonly referred to as the boiler room of the climate.

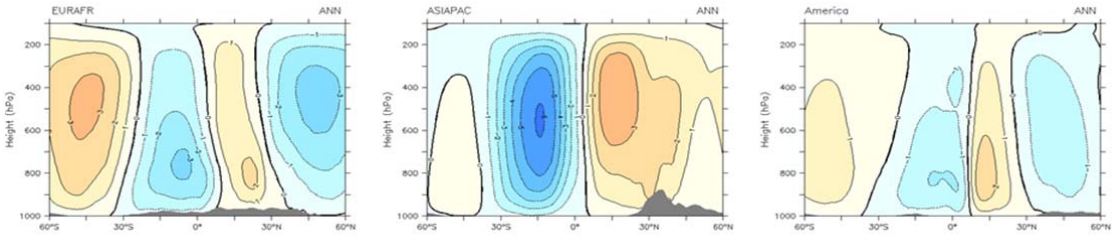

Figure 2.3. Annual mean climatology of the mass streamfunction derived from the divergent wind fields for the Europe-Africa sector (left), the Asia-Pacific sector (middle) and the Americas (right) from the ERAI reanalysis, 1979-2010 (taken from Nguyen et al. 2015b).

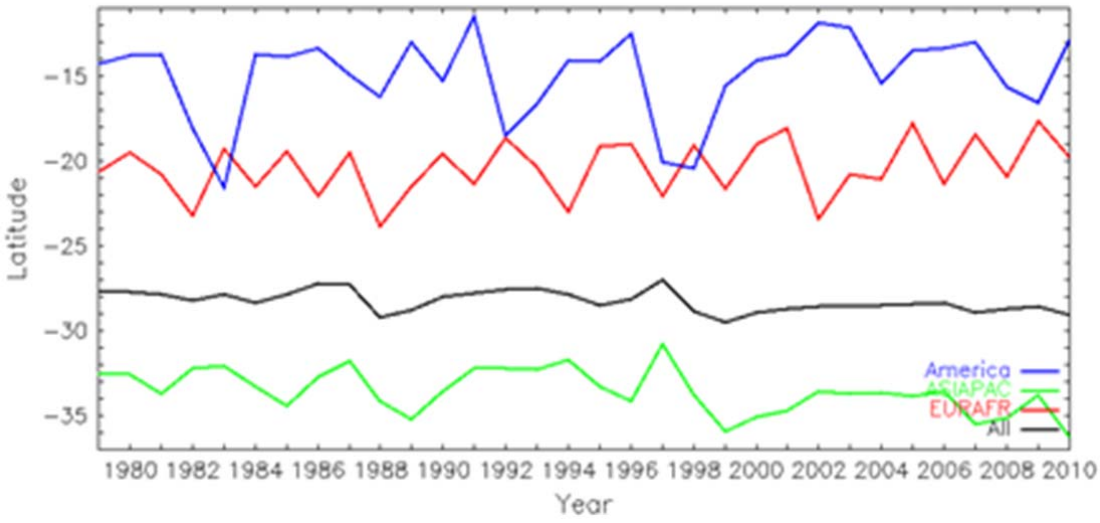

Figure 2.4: Time series of the annual mean of the hemispheric ('All', in black: HE_{SH}) and three regional Hadley cell edges (Europe-Africa, red: HE_{EA}; Asia-Pacific, green: HE_{AP}; and Americas, blue: HE_{AA}) in the Southern Hemisphere from the ERAI reanalysis for 1979-2010 (taken from Nguyen et al., 2015b).

Annual mean time series of the position of the edge of the Hadley cells are shown in Figure 2.4. The latitude of the southern edge of the Hadley cell in the Asia-Pacific sector is consistently further south than in the other two sectors in the Southern Hemisphere. Despite the strong influence on inter-annual timescale of ENSO in that part of the world, the interannual variability is also lower in that sector. Trends from 1979 to 2010 of the Hadley cell extent in the Asia-Pacific sector by season are shown in Table 2.2. In all seasons the Asia-Pacific Hadley cell has expanded.

***Table 2.2**: Long term linear trends of the ERAI HC edge (HE_{AP}), sub-tropical ridge intensity ($STRI_{AP}$) and position ($STRP_{AP}$) for the Asia-Pacific sector for 1979-2010. Trends significant at the 90%, 95% and 99% level are indicated by one, two and three stars respectively. Correlation coefficients between the HE_{AP} and $STRI_{AP}$ and $STRP_{AP}$ are indicated in the right column with the same significance levels marked (taken from Nguyen et al. 2015b).*

	Trend HE_{AP}	Trend $STRI_{AP}$	Trend $STRP_{AP}$	r(HE_{AP}-$STRI_{AP}$)	r(HE_{AP}-$STRP_{AP}$)
ANN	0.71***	0.18*	0.16	-0.13	0.54***
DJF	0.67*	0.16	0.25	-0.02	0.68***
MAM	0.71**	0	-0.06	-0.17	0.56***
JJA	0.53**	0.18	0.08	-0.24	-0.15
SON	0.69	0.37**	0.31*	0.02	0.53***

There is an association between the hemispheric Hadley cell extent and STRI (e.g. Nguyen et al., 2015), whereby the STRI is stronger as the Hadley cell expands. However, in this study, the relationship is not strong in the Asia-Pacific sector (Table 2.2). This may be in part because the STR is mainly driven as a remote response to tropical diabatic heating in the Indian Ocean that has characteristics of the Indian Ocean Dipole and is mainly a cool season response (as suggested in the different regression patterns onto HE_{AP} and STRI shown in Nguyen et al. 2015b). In addition, note the correlation between HE_{AP} and $STRP_{AP}$ breaks down in JJA (Table 2.2).

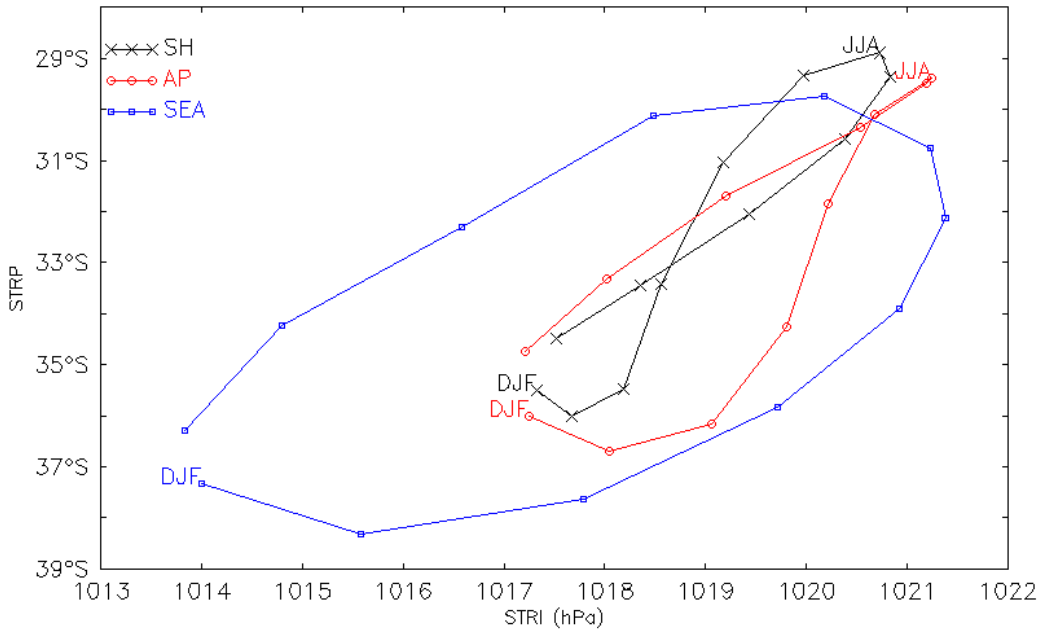

Figure 2.5: Annual cycle of the three month averages (centred on the central month: i.e. DJF for the month of January) mean hemispheric (Southern Hemisphere), Asia-Pacific (AP) and southeast Australia (SEA) STR derived from the MSLP field from ERAI reanalyses.

These results show a complex picture in particular in the early part of the cool season (autumn and winter) where, despite a strong regional Hadley cell expansion based on regional indices, it does not follow that the regional STR is intensifying or moving poleward (these trends are weak and non-significant in both seasons, consistent with lack of relationship indicated by the correlation coefficients).

To clarify the differences between hemispheric, regional and local STRs, the annual cycle of these STRI and STRP are shown in Figure 2.5. The data used is ERAI for the period 1979-2010. The local STR describes an annual cycle very consistent with the observations (from SEACI 2012). However it is markedly different from the regional STR_{AP} and the hemispheric STR_{SH}. Its oval shape is marked by larger seasonal amplitude for both intensity and position. In contrast the other two cycles can be described by a lemniscate with the hemispheric being more symmetrical than the regional. The different relationships between Hadley cell and STR at global and regional scales especially in winter (JJA) can be explained in terms of MSLP patterns associated with variability of these indices as depicted in Figure 2.6.

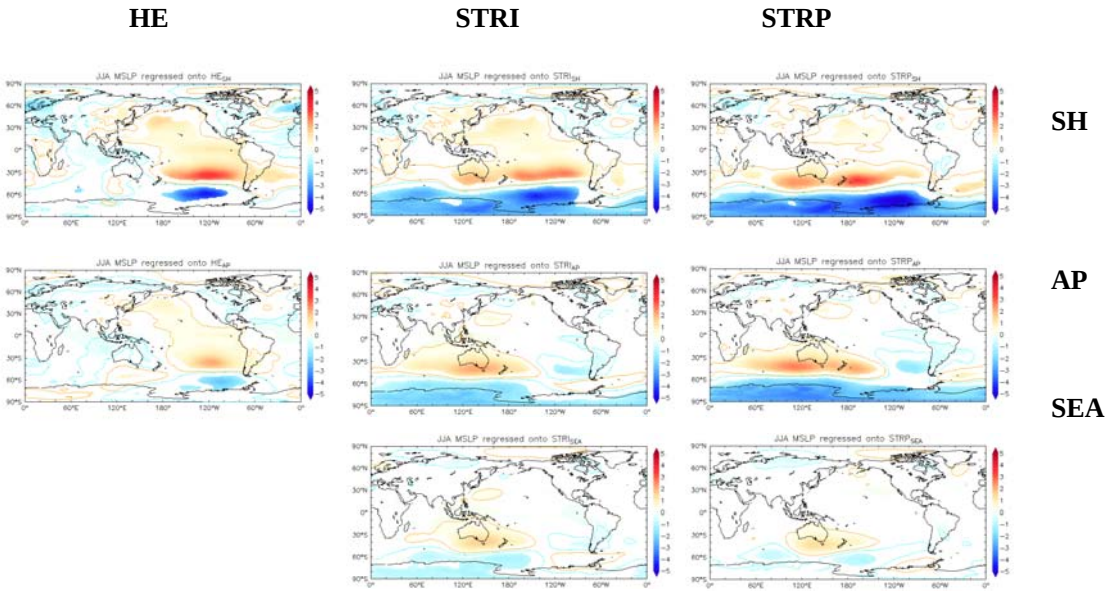

Figure 2.6: JJA mean ERAI MSLP regressed onto HE (left column), STRI (middle column) and STRP (right column) for the Southern Hemisphere (SH, top row), the Asia-Pacific (AP, middle row) and Southeast Australia (SEA, right row). For SEA only STR indices are defined,

The high correlations between HE_{SH} and $STRI_{SH}$ and $STRP_{SH}$ seen in Nguyen et al. (2015a) are here reflected in the similar MSLP regression patterns (top row in Fig. 2.6). All three panels are marked by low MSLP anomalies poleward of 60°S and high MSLP anomalies equatorward, reminiscent of a positive southern oscillation, enhanced by a Pacific-South American (PSA) equivalent barotropic wave train pattern most salient in the regression pattern onto HE_{SH}. However, the MSLP patterns over Australia are really different and explain the lack of relationship between the Hadley cell indices and Australian rainfall in winter (presented in the next section). A quadrupole of pressure anomalies is evident in the pattern of MSLP regressed onto HE_{SH}, with a low pressure anomaly over Australia associated with expanded HE_{SH} and high pressure to the south of Australia, a high across the tropical Pacific and low pressure in the southern high-latitude Pacific. In contrast, the opposite pattern can be drawn from the regressed MSLP onto $STRI_{SH}$ and $STRP_{SH,}$ with high pressure over Australia. Regressions using AP sector indices are very similar to those with HC indices but are generally weaker (second row versus first row in Figure 2.6). The regressed MSLP onto the local STR_{SEA} (bottom row in Figure 2.6) is similar to those with the regional STR_{AP}, but it highlights a much more localised relationship as expected, with high MSLP anomalies centred over southeast Australia, consistent with drier conditions there associated with poleward shift and intensified local STR_{SEA}.

Evaluate the relationship between changes in regional HC and Victorian rainfall

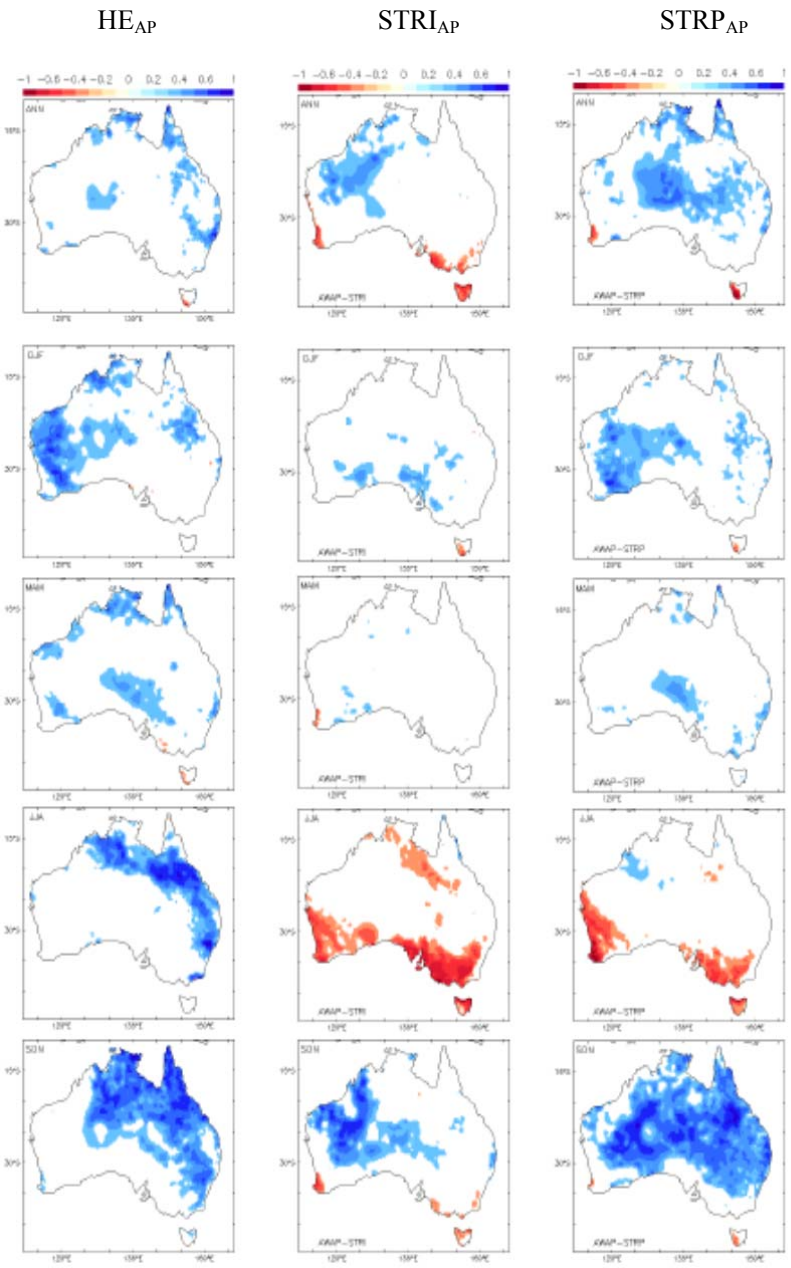

Figure 2.7: Annual and seasonal mean correlation between AWAP rainfall and ERAI (left) HE_{AP}, and (middle) $STRI_{AP}$ and (right) $STRP_{AP}$ for 1979-2010

The regression of the HE_{AP} with climate variables reveals part of the story of what is driving variability in Australian rainfall. Correlations between the Asia-Pacific Hadley cell extent (HE_{AP}) and the $STRP_{AP}$ are positive and strong in all seasons except winter, where the correlation becomes weakly (insignificant) negative (Table 2.2) as discussed above.

Annually, an expanded HC both hemispherically and in the Asia-Pacific sector is associated with lower pressure and wet conditions over Australia (Figure 2.7), especially in the east, and typically occurs in association with La Niña in the tropics (as reflected in both the DJF and JJA conditions in Figures 2.8).

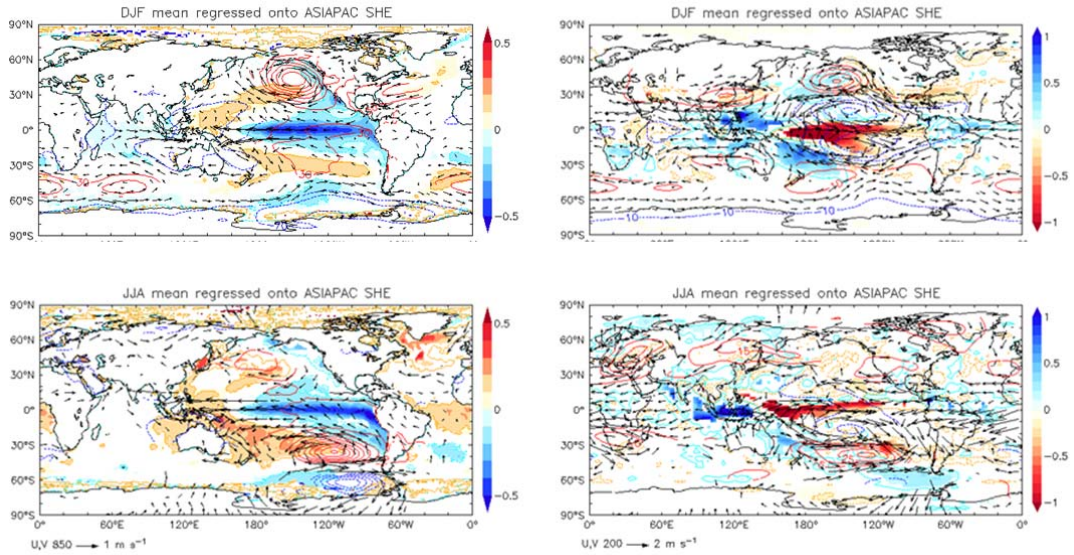

Figure 2.8: *DJF (top row) and JJA (lower row) climate variables regressed against HE_{AP} for 1979-2010. Left column: HadISST (shading, with ±0.1K contoured) and ERAI MSLP (contours, Pa) and horizontal wind at 850 hPa (vectors, m s-1); and Right column: GPCP rainfall (shading, with ±0.1 mm day-1 contoured), and ERAI geopotential height (contours, m) and horizontal wind (vectors, m s-1) at 200 hPa. Only values statistically significant at the 90% level are plotted.*

In light of Figure 2.7 regressions it is not surprising that Australian rainfall shows significant correlations with the HE_{AP} predominantly in the tropics, with southward expansion correlating positively with higher rainfall totals (Figure 2.7). By season, winter and spring show the strongest correlations across east Australia, while in DJF it is Western Australia that has the strongest correlations. Only in MAM are dry conditions correlated with high values of HE_{AP}, over a limited area of the westward facing coasts of Tasmania and Victoria. These relationships with rainfall across Australia are very different when the regional STR indices are considered instead of Hadley cell indices (left two columns in Figure 2.7). These result aligns very well across SEA with the correlations obtained using the local STR (Timbal and Drosdowsky, 2013, their figure 3). It is worth noting than the negative relationship in the south-west corner of W.A. is stronger with the regional STR indices which make sense since it is a broader measure which does cover that part of the Australian continent while the local STR was computed using observations along the eastern part of the continent only. Otherwise, the most significant differences are the large areas of positive relationship with rainfall (particularly in spring but also to a lesser extent in summer and autumn) with both the STR intensity and position when the regional indices are used, which were not observed with the local STR indices.

Since at times similar areas of positive correlations are noted when Hadley cell regional indices are used, they are related to that broader measure of the circulation instead of the STR. These areas of positive correlations, although not necessarily directly relevant to Victoria, require further investigations to understand how regional Hadley cell changes impact Australian climate.

Conclusions and future perspectives

Attribution analysis indicates that qualitatively Southern Hemisphere tropical expansion in the historical simulations is attributable to a combination of factors, since 1979, the partition of forcing factors for Southern Hemisphere tropical expansion is 30% resulting from natural

factors (volcanoes and ENSO), 40% resulting from stratospheric ozone depletion and 30% resulting from increasing greenhouse gases, with an error range *roughly* estimated at ± 10%. Since 1979, natural factors (e.g. ENSO, IPO, volcanoes) have been of increased importance, which means the reduced forcing seen in climate models (e.g. Lucas and Nguyen, 2015) is about right. Accounting for these factors is crucial for understanding the drivers of tropical expansion, and for resolving the differences between model simulations and observations and for estimating its future impacts.

The above results combined with results from 10 CMIP5 models all show that models largely underestimate the observed amount of tropical expansion making the quantification of the attribution from different forcings difficult. However, the simulations with the warmest global temperatures (GHG-forcing without ozone) are also those with both HCE and STRP markedly poleward compared to the other simulations. This result highlights that the extent of the hemispheric-wide Hadley cell corresponds closely with mean global temperature, and it seems that factors that act to cool the globe in climate models (Antarctic ozone hole, volcanoes) work to reduce the expansion of the tropics. However, models forced with the expanding ozone hole and increasing GHG, act to increase the pressure of the STR at a greater rate when the Hadley cell expands than those simulations with GHG forcing alone.

Analysis of the regional contributions to changes in the Hadley circulation indicates that the Southern Hemisphere *Hadley* circulation *expansion* is largely driven by the expansion in the Asia-Pacific sector, and this is at both annual and seasonal timescales. This expansion is associated with a La Niña-like state in the tropical Pacific: cold waters in the eastern equatorial Pacific contrasting with warm waters in the west. This association with La Niña (or a shift to cold IPO since end of 1990's), may explain why historical simulations underestimate the expansion: the observed shift to cold IPO is not reproduced in historical simulations.

An expanded Hadley circulation both hemispherically and locally in the Asia-Pacific is associated with a poleward expansion of the tropical wet zone but does not relate well with the intensity of the regional sub-tropical ridge. A possible mechanism to explain the association of an expanded Hadley circulation with La Niña conditions is via the Southern Annular Mode: a poleward shift of the mid-latitude jet is favoured by La Niña conditions in the tropics, which results in an expansion of the Hadley circulation. Moving into Year 3, this work will be submitted as a paper and revisions completed. This signal in coupled climate models is likely to be small, given the importance of natural variability in the observed changes in indicators of the tropical expansion reported in Murphy et al. (2014), so this is unlikely to be fruitfully pursued using models. There may be the potential to explore these associations in a suite of AMIP-style simulations; however, their availability is still uncertain at this stage.

Australian rainfall shows significant correlations with the Hadley cell extent in the Asia-Pacific sector HE_{AP}, with southward expansion correlating positively with higher rainfall totals. In winter and spring there are significant positive correlations across east Australia while in summer they are on the west. Only in autumn is there a hint of dry conditions in the south-east associated with higher values of HE_{AP}.
There are also links with Project 3 which examines the role of tropical-extratropical interactions. As the stratospheric ozone hole, a polar phenomenon appears to be a driver of tropical expansion in the Southern Hemisphere, there must be a link between the two regions. The teleconnection links with tropical expansion also shed light on these interactions. Future work with this project will focus on applying the knowledge gained to better identify likely impacts of specific regions such as Victoria and southeast Australia.

PROJECT 3: UNDERSTANDING SUB-TROPICAL-EXTRATROPICAL INTERACTIONS AND THEIR RELEVANCE TO VICTORIA

Eun-Pa Lim, Harry H. Hendon, Chris Lucas and Hanh Nguyen
R&D Branch, Bureau of Meteorology

Key Findings

- The positive phase of the SAM (high SAM) is associated with a poleward shifted mid-latitude storm track in all seasons. In winter when the mid-latitude storm track plays an important role in the climate of the southern part of Australia, the poleward shift of the storm track results in drier conditions across south-eastern Australia. In contrast, during spring-summer, the high phase of the SAM increases rainfall in south-eastern Australia because it causes the poleward edge of the tropics to shift poleward to the latitudes of Victoria. Forced upward trends of the SAM in response to increasing GHGs and ozone depletion are thus expected to act to dry southern portions of Australia during winter but moisten sub-tropical latitudes during spring-summer.
- The climate models of CMIP5 with historical forcing correctly simulate the positive relationship between the SAM and sub-tropical rainfall in summer (i.e. high SAM and increased rainfall) and the absence of such a positive relationship in winter, which explains the expanded dry zone to the north of Victoria during high SAM in winter. However, the models show significant biases in the teleconnection between the SAM and tropical rainfall (i.e. too much rainfall during high SAM) and between the SAM and ENSO in austral warm seasons when these teleconnections are strong in the observations.
- Near record drought over eastern Australia in 2002 spring was found to be driven not only by the moderate El Niño event whose maximum SST warming was shifted to the central Pacific but also the strong negative phase of the SAM (low SAM), which highlights the important role of the SAM in the occurrence of extreme climate events and also in the limitation on long-lead predictability of extreme climate events as SAM generally has less predictability than ENSO. Realistic atmospheric initial conditions and good representation of air-sea interaction are found to be important for the skilful prediction of the strong negative SAM during spring 2002.
- Software to compute the characteristics of the mean meridional circulation in isentropic coordinates has continued to be developed. This alternate method for investigating the mean meridional circulation will provide added insight into the possible links between the tropical expansion, the intensification of the sub-tropical ridge and forcing by ENSO, and also into the observed south-eastern Australia cool season rainfall deficit. The calculation of the MMC in isentropic streamfunction is a complex calculation, and current results based on monthly quantities do not fully capture the 'geostrophic' part of the isentropic flow which is dominant in the extratropics. Investigation is still ongoing to explore further the issue using daily quantities to obtain more accurate results.
- The calculations using monthly data do seem to agree with what is expected regarding inter-annual variability. In response to El Niño, a narrowing and intensification of the tropics and the Hadley cell is observed. In terms of the SAM response, the variability appears correct: the storm track is further poleward during the positive phase. Over the longer term, computed trends indicate changes to the MMC. The outflow regions of the upper arm of the Hadley cell may be changing. In the Southern Hemisphere, the sub-tropical 'downward' branch appears to be moving more poleward. The calculations suggested that the biggest

changes may lie in MAM, although an expansion in most seasons is seen. These results are subject to change, particularly in the extratropics, because of the largely missing 'geostrophic' component of the MMC which is currently under investigation.

Background

Evidence is emerging that variations in extratropical circulation associated with the Southern Annular Mode (SAM) play a significant role in driving variations in lower latitude circulation (e.g. the Hadley circulation), and especially rainfall on the poleward edge of the Hadley circulation: High SAM (i.e. a poleward shifted mid-latitude jet) is associated with an expanded Hadley cell (HC) that results in increased rainfall in sub-tropical latitudes during summer. This relationship during summer is captured in climate models to varying degrees. It is especially promoted by ozone depletion, but increased CO2 is also known to drive SAM to its high phase. Understanding the cause of this relationship between SAM and the HC is crucial to understanding the behaviour of the HC in the future. It furthermore bears on the ability to predict regional climate seasonally. In addition to forcing by greenhouse gases and ozone depletion, there is strong evidence that tropical SSTs during ENSO directly affect the HC, which then affects the SAM (e.g., the HC contracts toward the equator during El Niño thereby resulting in a shift toward low SAM). These variations should be highly predictable. But, SAM is primarily an internal mode of variability. So, the limits of predictability of HC variations will be set by the degree that the internal variations of the SAM determine the poleward extent of the HC.

Objectives

1. Further development of the equations to calculate isentropic mass streamfunction. Association of this view of the MMC with ENSO and SAM
2. Investigate seasonal variations of sub-tropical precipitation associated with the Southern Annular Mode in CMIP5.

Activity 1: Isentropic Stream Function

Introduction

The mean meridional circulation (MMC) acts to transfer excess heat from warm, moist tropical regions to cooler, drier regions nears the pole. Evaluation of this circulation and its response to natural variability and anthropogenic climate change is important for exploring the impacts of climate change.

A common method of measuring the MMC is through the use of the isobaric mass streamfunction, a transformation of the zonal mean meridional mass flux in the pressure-latitude plane into a circulation pattern. With use of the hydrostatic equation, this calculation reduces to a vertical integral of the meridional wind component in pressure. This yields the familiar three-cell model of the MMC, as can be seen in numerous papers (e.g. Nguyen et al. 2013).

An alternate picture of the MMC can be created by performing the calculation in an isentropic coordinate system, using potential temperature (θ) as its vertical coordinate. On a latitude-θ cross-section, vertical displacements are directly linked to diabatic heating; horizontal displacements represent adiabatic flow. However, the spatial variability of the isentropes can be problematic; near the surface the isentropes can disappear below ground level. Layers that have constant θ with height or pressure are also difficult to interpret; in this case, a given θ-level can represent some depth in physical space.

The isentropic mass streamfunction is computed analogously to the isobaric example (e.g. Townsend and Johnson 1985). The zonal mean meridional mass flux in the latitude-θ plane is computed and vertically integrated with the appropriate constants to produce streamlines describing the MMC. This isentropic view of the MMC shows important differences from the isobaric version (e.g. Schneider 2006). The circulation shows linkages between the tropics and extratropics. The Hadley cell is present as in the isobaric view, but linked in the near surface with an extratropical cell, analogous to the polar cells of the isobaric view, but often stronger. This isentropic view suggests a more dynamic MMC that is a continuous hemispheric circulation where tropical-extratropical interactions are important, rather than three largely independent cells.

Another benefit of isentropic analysis is the ability to directly diagnose diabatic heating in the atmosphere. In these coordinates, the 'upward' transport of mass corresponds to heating and vice versa. The 'vertical' mass transport value can be easily converted into a heating rate. Horizontal flow corresponds to adiabatic motion within the atmosphere. Identification of these flows can generate insight into important atmospheric processes.

In the next section, brief notes on the data and method will be provided and some results will be shown, although there are still some concerns with aspects of the method. This view of the MMC will then be regressed against ENSO and SAM indices.

Isentropic MMC calculation

The data used in this investigate come from the ERA Interim Reanalysis (Dee et al. 2012). The data are monthly, extending from January 1979 through December 2010. In the vertical, the data have been interpolated onto 37 pressure levels. For this analysis, the meteorological data described above are interpolated to a coordinate system that uses potential temperature (θ) as a vertical coordinate. Potential temperature is defined as the temperature that a parcel of would obtain after moving adiabatically to a reference pressure.

The key quantity of interest here is the meridional mass flux/transport. This requires an estimate of the meridional wind v and the amount of mass at a given isentropic level. This latter quantity is called the 'isentropic density' ρ_θ, and is defined by applying the appropriate Jacobian transformation to the ordinary density (Townsend and Johnson 1985). Mathematically, it is given by:

$$\rho_\theta = -\frac{1}{g}\frac{\partial p}{\partial \theta}$$

This term is computed onto the isentropic grid from the pressure values on the half levels. Centred differences are used to compute the derivative. Also note that the isentropic density is the inverse of static stability. An isentropic streamfunction can be defined

$$\Psi = -2\pi a \cos\phi \int_{\theta_b}^{\theta} \overline{v\rho_\theta} d\theta$$

That describes streamlines of mass flux/transport within the isentropic coordinate system, where the overbar indicates the zonal mean. To accurately compute ψ, the vertical mean mass flux is removed at each latitude, ensuring there is no net meridional flow (through depth of atmosphere, or chosen domain) across a line of latitude

Results

A selection of results showing the basic fields is presented. The presentation here will focus on the solstice seasons (i.e. June-July-August (JJA) and December-January-February (DJF)). These fields presented are time averages from 1979-2010. The purpose here is not to fully document the annual cycle, but to present information to assist in the evaluation of the calculation. Figure 3.1 shows the streamfunction for JJA and DJF. The dominant feature on the plot is the Southern Hemisphere winter Hadley cell. The intensity of this cell is in excess of 200 x 10^9 kg s^{-1}. During this season, the Hadley circulation has an 'extension' in the NH near 310 K, suggesting a quasi-adiabatic flow from 15-30°N. This is likely cross-equatorial flow, possibly the Somali jet, associated with the strong Asian monsoon, which peaks during this season. This extension breaks up the weak NH summer cell. In the mid-latitudes, particularly in the Southern Hemisphere, a pattern reminiscent of the isobaric three cell structure is obvious. A Ferrel Cell analogue is apparent at 45°S, along with a polar cell at 70°S is obvious. The expected 'linkage' between the polar cell and Hadley cell is not present. There are hints of it, as the two parts of the negative streamfunction try to join, but in the mean they do not. A weaker Ferrel cell type structure is also apparent in the NH. Overall the NH circulation is quite weak during JJA.

In DJF, many similarities with the three cell modes are still apparent, in both hemispheres. The dominant feature is the NH winter Hadley cell. It is slightly weaker that the JJA winter cell, but its intensity is still in excess of 170 x 10^9 kg s^{-1}. Unlike in JJA, a linkage between the NH extratropical mode and the Hadley cell is apparent. The hemisphere wide circulation is apparent in the NH during this season. A Ferrel type circulation is also evident in the NH. The Southern Hemisphere summer Hadley cell is stronger than the NH summer cell, but is considerably weaker than the winter cell. A strong Ferrel cell-type structure remains evident in the Southern Hemisphere. As during JJA, there are hints of the hemisphere-wide circulation, but it is not fully manifest. There are deficiencies found in the streamfunction calculation compared with results from other studies. The tropical features seem generally correct compared with the ψ patterns from the ERA-40 Atlas and Schneider et al. (2006); the magnitudes and positions are broadly correct. Diabatic heating values in the Hadley cell ascending regions are of the order of 1-2 K day-1, in line with what is expected. However, the extratropical flows in our calculation are obviously deficient. A closer examination of the differences indicates that our calculation is not resolving the near surface mass flux values correctly, say within 10-15 K either side of the median surface values. Our calculations indicate that we are underestimating this term by a considerable fraction (~80%).

In terms of the paradigm of Townsend and Johnson (1985) noted in the introduction, we are not adequately capturing the asymmetric, 'geostrophic' component of the flow that represents the influence of the baroclinic waves in the extratropics. This is the part of the circulation estimated from the covariance of density and v anomalies along a latitude circle. By using the monthly mean data instead of daily data, we have 'smoothed out' the short-lived but strong (in terms of mass-weighted velocity) equatorward transports of colder air that make up the mass transport at the near surface (e.g. Held and Schneider 1999). With daily data, the flow at the lower isentropic levels is captured in a way that it cannot be when a monthly mean is used. Fundamentally, the calculation is correct, but the data we have used are inadequate. Fortunately, this can be easily rectified.

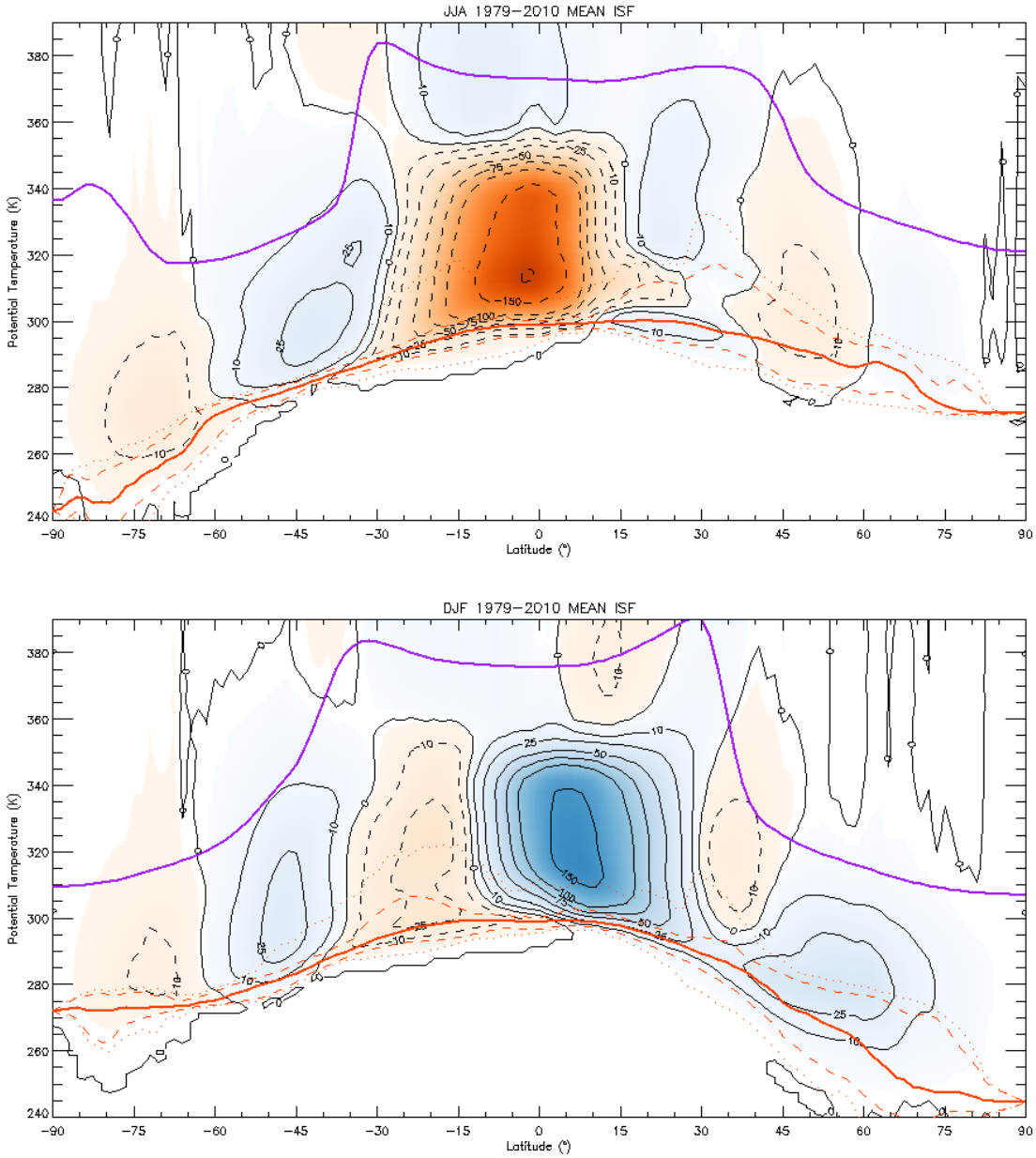

Figure 3.1: Average ψ (10^9 kg/s) for JJA (top) and DJF (bottom). Flow is counter clockwise around negative (orange and brown) contours.

Regression plots for ENSO are shown for January and July (Figure 3.2). The response of ψ to ENSO is stronger in January, typically when El Niño conditions are near their peak. The response is largely tropical, affecting the margins of the Hadley cell. In both months, the results indicate a slight narrowing of the Hadley cell and an intensification of the overall circulation. In the weaker summer cell during these months, a change is indicated generally a reduction in the downward branch. During January, an equatorward shift of the Ferrel Cell type circulation is indicated. Overall, these results are consistent with what has been shown in Oort and Yienger (1996) and Nguyen et al. (2013).

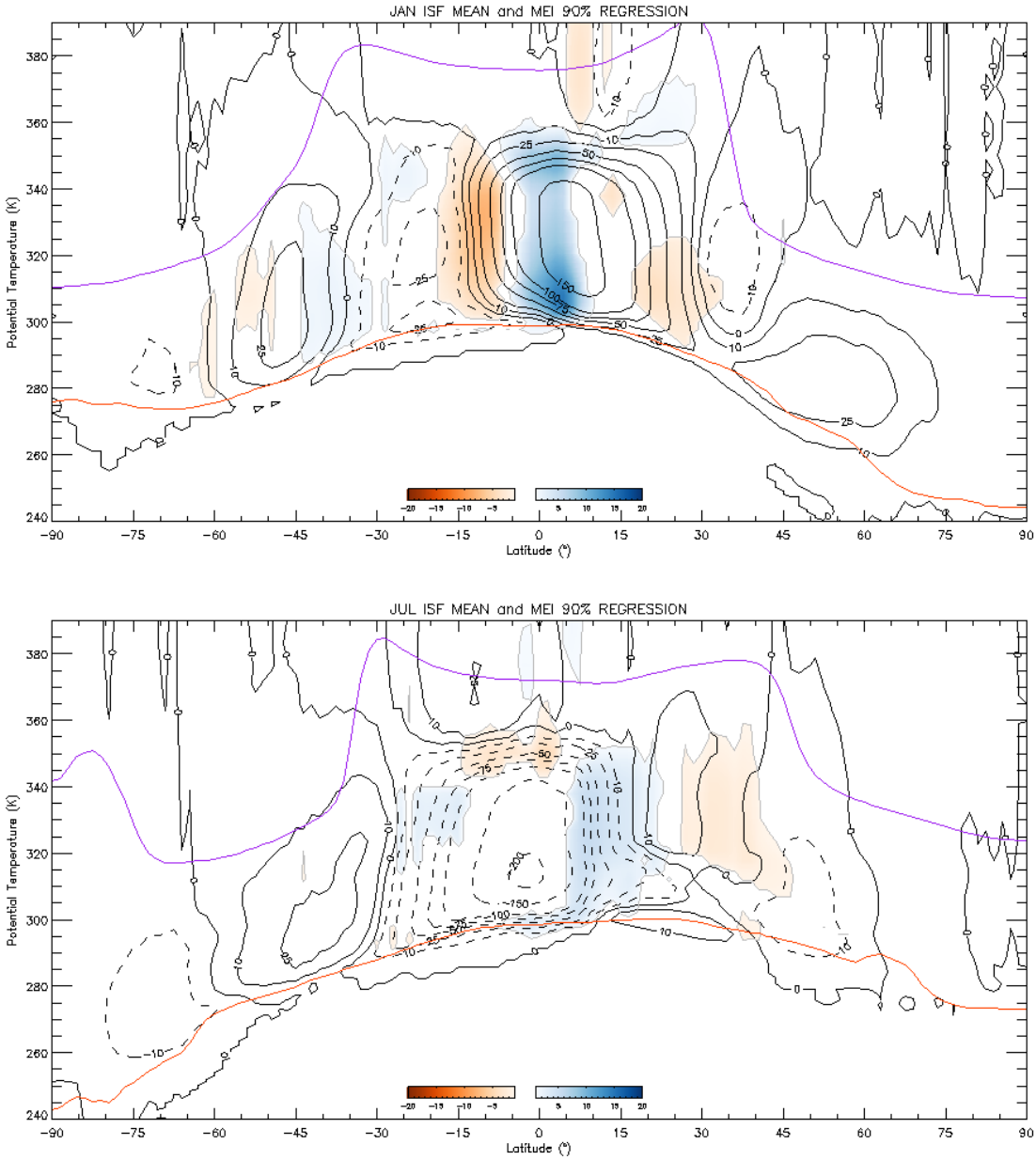

Figure 3.2: January (top) and July (bottom) regression of onto the Multivariate ENSO Index. This corresponds to moderate El Niño response. Magnitude of changes is given by colour scale. Positive changes are blue.

The regressions onto the SAM index are shown for January and July (Figure 3.3). In January, the regression magnitude is generally quite weak, with some positive anomalies in the storm track region near 55°S. This suggests a poleward movement of the storm track, consistent with what is expected with positive SAM. In July, The pattern is similar, but more widespread. A decrease is also seen in the descending part of the Hadley cell. Both of these are consistent with a poleward shift in the storm track. While the magnitudes are relative small here, we note that the circulations themselves are somewhat weak, and that the regressions represent a large relative change in the circulation.

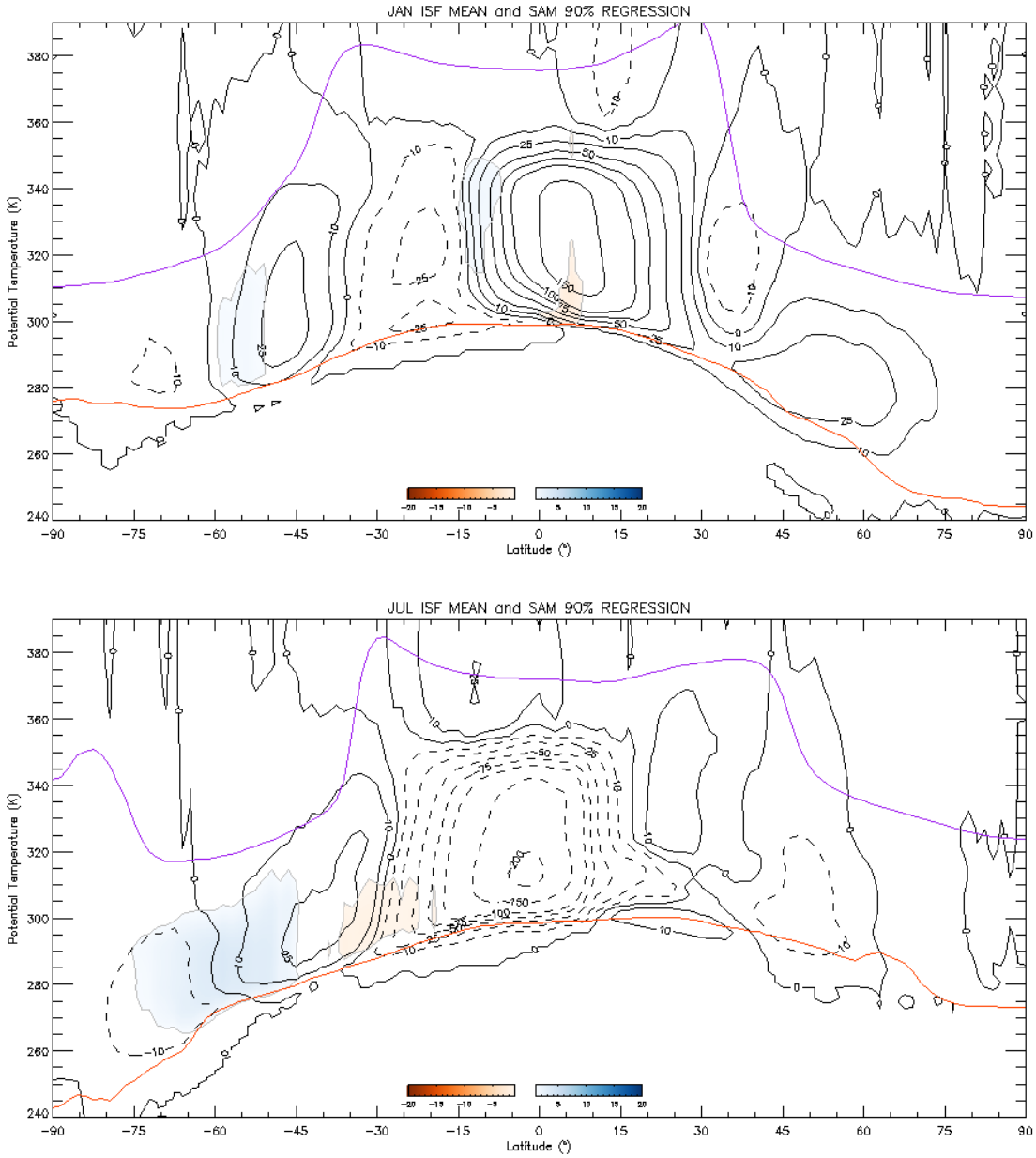

Figure 3.3: As in Figure 3.2, except for the SAM index.

In both examples shown here, the meaningfulness of the regressions remains to be determined, given the issues described above with the calculations. For the ENSO case, the strongest regressions are found in the tropics, where the calculation is more correct; there is more confidence place in relationships. That they are similar to what has been seen in previous studies is also encouraging. The SAM regressions should be viewed with more caution, although the fact that the regressions occur where a relationship might reasonably be expected is a positive. Ultimately, however, the validity of these relationships must be more carefully considered with the correctly calculations.

Activity 2: Understanding tropical -extratropical interactions over the Southern Hemisphere

Seasonal variations of sub-tropical precipitation associated with the Southern Annular Mode simulated in CMIP5 historical simulations

The Southern Annular Mode (SAM) is the leading mode of the variability of the Southern Hemisphere extratropical circulations at time scales beyond 1 week. The SAM is understood to originate as an internal mode of extratropical variability, but variations of the SAM are also promoted by El Niño -La Niña and by increasing greenhouse gases and ozone depletion. In its high-polarity phase (high SAM), the mid-latitude westerlies associated with the polar front jet are shifted poleward, and surface pressure is anomalously low over the polar region and high in the mid-latitudes (Figure 3.4).

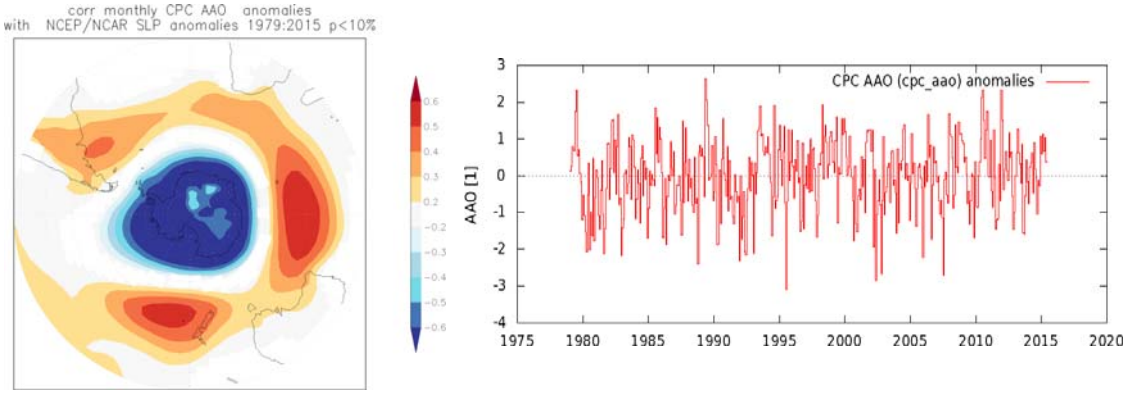

Figure 3.4: Spatial pattern of the Southern Annular Mode (left), which is obtained by regressing monthly mean sea level pressure anomalies on the 1st principal component time series of 700 hPa level geopotential height anomalies over the period 1979-2015 (right), using the NCEP-NCAR reanalysis (Kalnay et al. 2007). The annual cycle was removed, and the data were weighted by cosine latitude.

The associated latitudinal shift of the mid-latitude storm tracks results in changes in rainfall, air and sea surface temperatures, and ocean surface currents throughout the extratropics of the Southern Hemisphere. Specifically, high SAM is associated with decreased rainfall across southern latitudes of Australia in winter but increased rainfall across sub-tropical Australia during austral spring and summer (e.g. Hendon et al. 2007, Risbey et al. 2009). Hendon et al. (2014) showed that high SAM is associated with a poleward shift of mid-latitude storm tracks in all seasons and a shift of rainfall away from the mid-latitudes to higher latitudes. This results in decreased rainfall from 40º-50ºS but in winter this zone of anomalously drier conditions extends as far north as ~35ºS. The promotion of sub-tropical rainfall during high SAM that occurs in summer and spring does not occur in winter. Therefore, the net impact of high SAM in winter is best described as a poleward expansion of the sub-tropical dry zone and Victoria is generally drier during high SAM. During spring and summer, high SAM induces increased rainfall in the subtropics (22º-35ºS) and so makes Victoria (at least the northern parts) wetter. During summer the net impact of high SAM is thus best described as a poleward shift of the sub-tropical dry zone (the mid-latitude storm track moves further away to the south from Victoria but the wet tropics to the north also move further south).

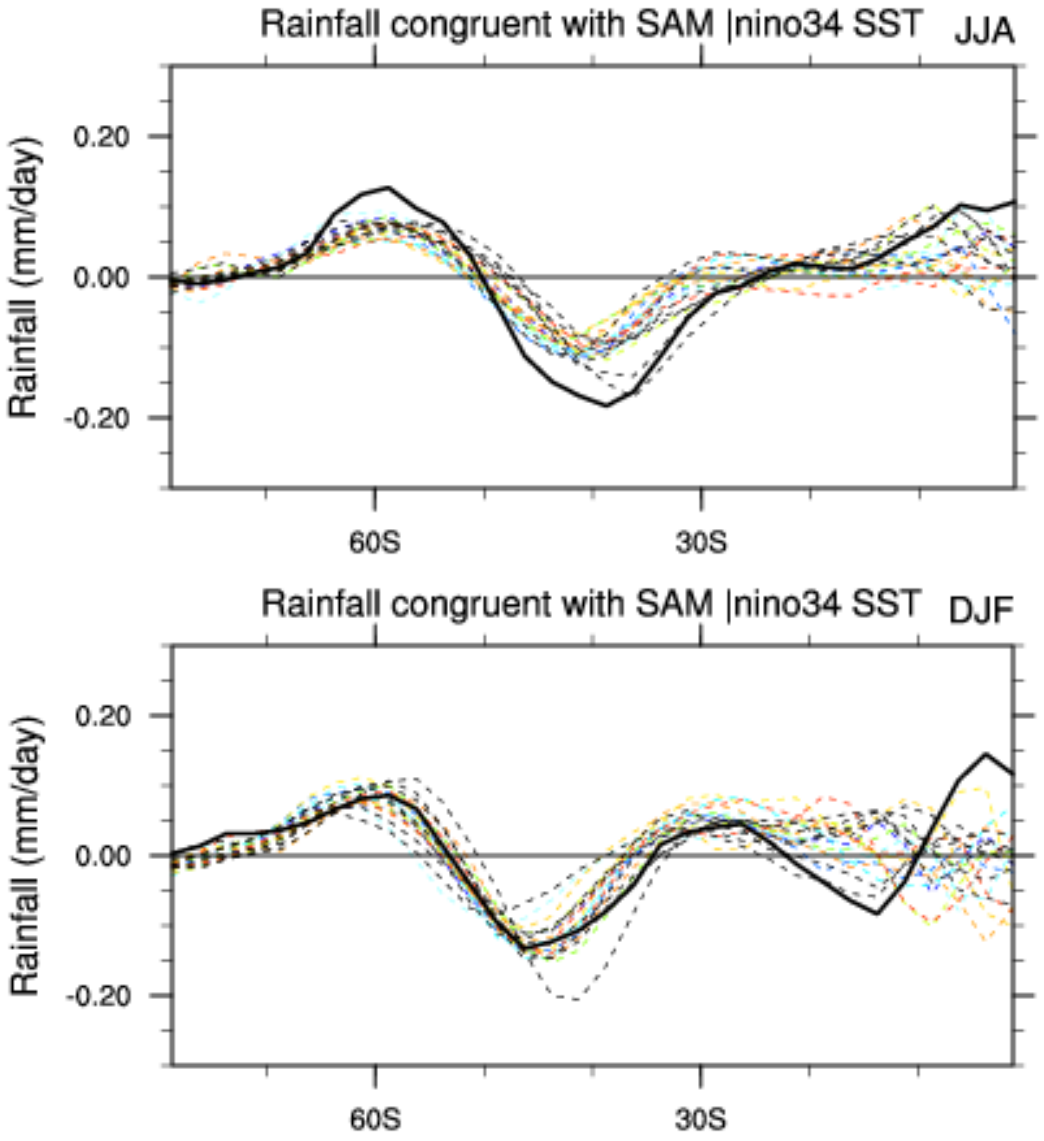

Figure 3.5: Rainfall regressed on the SAM index from which the influence of ENSO is removed in the observations (ERA-Interim; black solid line) and the CMIP5 historical runs (34 models; coloured dashed lines) in (a) JJA and (b) DJF. Nino3.4 SST index and Gong and Wang (1999) SAM index were used to represent ENSO and the SAM. Victoria is located between 34 and 38°S.

In the climate models with increasing greenhouse gases, the swing to the high phase of SAM is one of the most robust climate signals. Therefore, understanding climate models' capability to simulate the SAM and its teleconnection to SEA rainfall is important to interpret the future climate projected by the climate models. In Activity 2, the capability of CMIP5 models to simulate these seasonal variations of sub-tropical precipitation associated with the SAM was assessed. We conducted statistical analyses on the data from the 34 models with historical forcing from the CMIP5 archive that were available in the Bureau of Meteorology data store. The regression of zonal mean rainfall anomalies to the de-trended and ENSO-removed SAM index shows that CMIP5 models do capture the seasonality of sub-tropical rainfall response to the SAM (Figure 3.5).

In summer, sub-tropical rainfall increases responding to the positive phase of the SAM over 25-35°S whereas this sub-tropical wet response is absent in winter, which is consistent with the

observations. However, the dry response over the latitude band of 35-45°S during high SAM is underestimated in winter, and more importantly, there is a significant misrepresentation of rainfall response in the tropical-sub-tropical rainfall in summer in the CMIP5 models (i.e. the models depict too strong a rainfall increase at low latitudes during high SAM in summer). Further investigation suggests that these biases are likely due to the misrepresented teleconnection between the tropical Indian and western Pacific Ocean and the Southern Hemisphere extratropics. Therefore, projected climate is perhaps unreliable in the low latitudes in summer because the models are over-depicting the low latitude rainfall response to high SAM. Nonetheless, over the region that includes Victoria (~30°-40°S), the models capture the rainfall response to high SAM in both summer and winter reasonably well, but the underestimation of the dry condition associated with high SAM in the wintertime appears to leave some uncertainty in the intensity of dry condition projected for the future climate. Future work will be pursued to examine the impact of these biases on SEA rainfall in the future climate with increasing greenhouse gases.

We also evaluated the models' capability to simulate the seasonality of ENSO-SAM relationship because ENSO is an important driver of the SAM in austral spring to summer seasons (Lim et al. 2013). The seasonal variation of the ENSO-SAM teleconnection is not well simulated in the majority of the models (Figure 3.6), which is likely due to the models' inability to simulate the Indo-Pacific SST pattern associated with ENSO. Having considered the findings of VicCI research on the observed extreme dry/wet conditions over Australia in 1997, 2002 and 2010, model biases in the spatial structure and amplitude of ENSO and its teleconnection contribute to uncertainty for rainfall extremes of the future climate projected by these models.

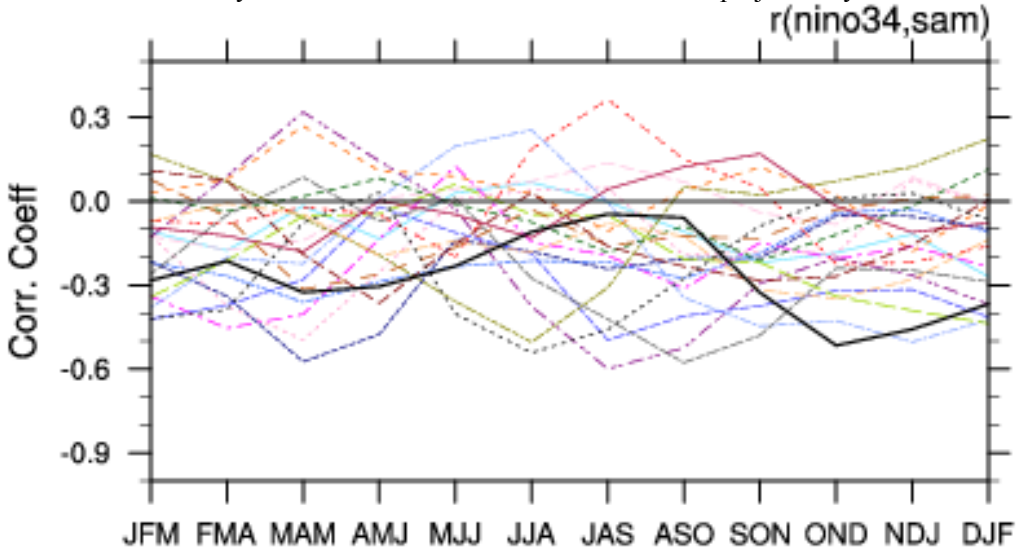

Figure 3.6: Correlation of ENSO and the SAM in the observations (black solid line) and the CMIP5 historical runs (coloured dashed lines.

Understanding the role of the SAM in the severe drought over eastern Australia in spring 2002 compared to the weaker response in spring 1997

In general, Australian springtime climate (September to November) is closely related to the occurrence of El Niño (e.g. McBride and Nicholls 1982) but especially sensitive to the flavours of El Niño (e.g. Wang and Hendon 2007). For instance, below average rainfall across Australia during El Niño is more strongly associated with central Pacific El Niños than with eastern Pacific El Niños (e.g. Wang and Hendon 2007, Lim et al. 2009). In particular, Wang and

Hendon (2007) showed that the massive 1997 El Niño, whose maximum SST anomaly occurred in the far eastern Pacific, produced a weak impact on Australian spring rainfall (Figure 3.7 left panels). By contrast, they showed that the relatively weak El Niño of 2002, as judged by the magnitude of the SST anomaly in the eastern equatorial Pacific (as monitored by the NINO3 index; e.g. Watkins 2003), resulted in a widespread devastating drought likely associated with the occurrence of a relatively strong positive SST anomaly just east of the date line (Figure 3.7 right panels). Motivated by the fact that Australian spring rainfall anomalies during 1997 and 2002 were so contrasting and perhaps opposite to intuition (i.e. one might have expected severe drought during 1997 and only minor impacts during 2002), the present study explores the causes and predictability of Australian spring rainfall for these two years using statistical techniques and conducting POAMA forecast sensitivity experiments.

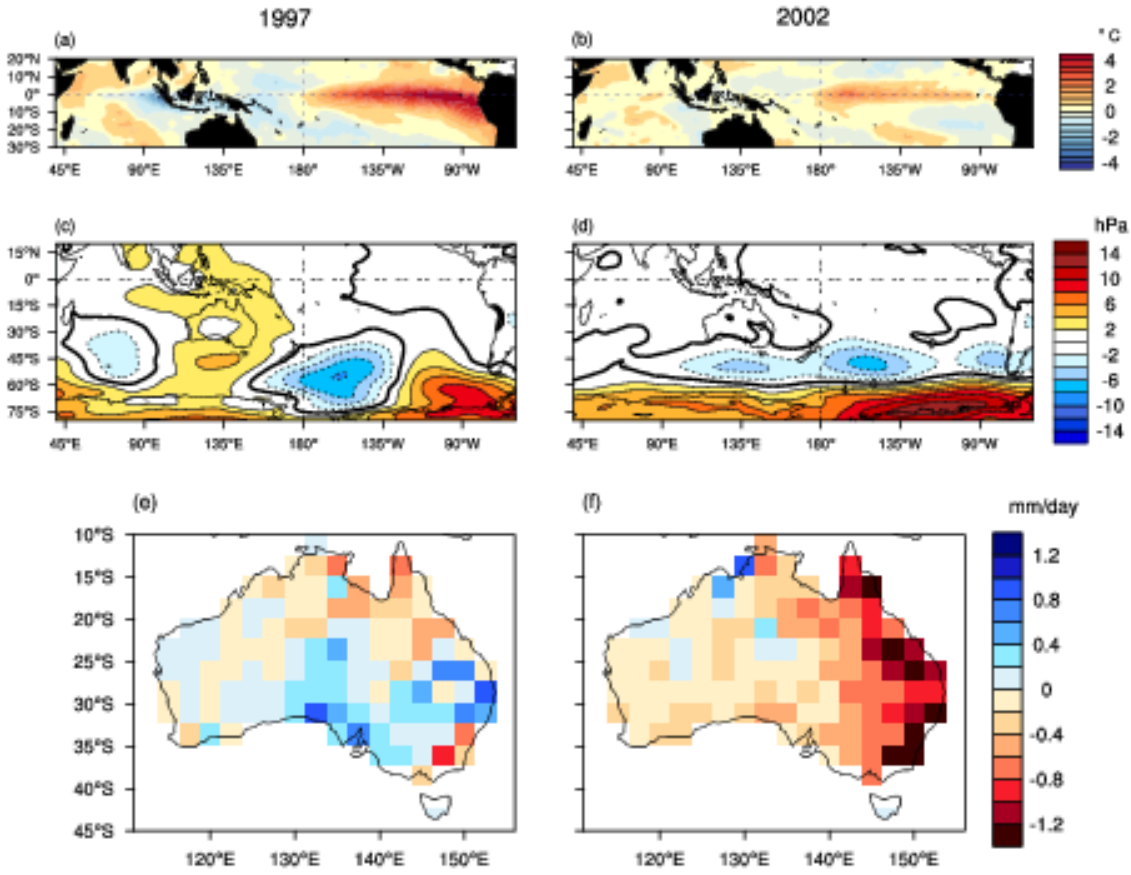

Figure 3.7: Observed anomalies of (a,b) SSTs, (c,d) MSLP and (e,f) Australian rainfall in 1997 (left) and 2002 (right) austral spring (September-October-November; SON) based on the climatology of 1982-2005. The colour shading interval is 0.5°C for SST anomalies, 2 hPa for MSLP anomalies, and 0.2 mm/day for rainfall anomalies (taken from figure 1 in Lim and Hendon, 2015).

POAMA is an atmosphere and ocean fully coupled forecast system. The atmospheric model of POAMA is the BoM's Atmospheric Model version 3 (BAM3; Colman et al. 2005). The ocean component of POAMA is the Australian Community Ocean Model version 2 (ACOM2) (Schiller et al. 2002, Oke et al. 2005). The atmosphere and ocean component models are coupled by the Ocean Atmosphere Sea Ice Soil (OASIS) software (Valke et al. 2000). In producing POAMA forecasts (P_ctrl), the atmosphere model is initialised with realistic atmospheric and land conditions generated from our nudging scheme called ALI, and the ocean model is initialised with realistic ocean conditions generated from an ocean data assimilation system called PODAS. Control forecasts consist of a 10 member ensemble that were initialized

on 1st of September 1997 and 2002 and are of 3 months duration. In order to understand the source of predictability and to elucidate the sensitivity of the seasonal forecasts to atmosphere and land initial conditions, four forecast sensitivity experiments were conducted – two coupled model experiments and two uncoupled model experiments (Table 3.1).

***Table 3.1**: Configuration of POAMA forecast experiments. Forecasts were initialized on the 1st of September 1997 and 2002 with the conditions generated from the BoM's forecast initialisation schemes shown in the table. Detailed descriptions of ALI, AMIP-style integration and PEODAS are provided in Section 2.*

	Coupled experiments			Uncoupled experiments	
	P_ctrl	P_aliAclimL	P_amipAL	FAMIP_psst	FAMIP_oisst
Atmosphere initialization	ALI	ALI	AMIP-style integration	ALI	ALI
Land initialization	ALI	ALI climatology	AMIP-style integration	ALI	ALI
Ocean initialization (coupled) /prescription (uncoupled)	PODAS	PODAS	PODAS	POAMA predicted monthly mean SSTs	Reynolds OI v2 monthly mean SSTs

First, to explore the impact of initial land surface conditions on the rainfall forecasts, we kept every initial condition the same as for P_ctrl except we initialize the land surface variables (soil moisture and temperature) with the climatological means of September 1st based on 1982-2005 that were produced from ALI. This experiment is referred to as P_aliAclimL (POAMA with ALI atmosphere and climatological land initial conditions). The upper layer soil moisture was observed to be below normal in the east but above normal in the west by the end of winter 1997, whereas it was strongly below normal across most of the continent by the end of winter 2002. Therefore, in the P_aliAclimL experiment, 1997 spring will start out with drier than observed soil conditions in the west and wetter than observed soil conditions in the east. Similarly, the P_aliAclimL experiment for 2002 will start out with wetter than observed soil conditions across most of the country.

To explore the sensitivity to realistic intraseasonal varying atmosphere/land initial conditions, we conducted an experiment whereby the atmosphere/land is initialized with the conditions that are reflective of the slowly varying boundary forcing but contains no realistic information about any intraseasonal variability, especially the SAM and the Madden-Julian Oscillation (MJO) which are known to directly affect Australian climate. These initial conditions were generated from an atmosphere model simulation forced with observed SSTs from June to August of 1997 and 2002 (i.e. AMIP (Atmosphere Model Intercomparison Project) type experiment). We refer to these forecasts as P_amipAL (POAMA with AMIP atmosphere and land initial conditions).
We also carried out two additional AMIP style experiments (i.e. SSTs are prescribed) to explore the response of Australian rainfall to observed and forecast SSTs of 1997 and 2002 SON. First, atmosphere-only (uncoupled) forecasts were made using the ALI atmosphere/land surface initial conditions but with the SSTs prescribed during the forecast to be the observed monthly mean SSTs (interpolated to the model time step) from Reynolds OI v2 SST analysis (Reynolds et al. 2002). We refer to these forecasts as FAMIP_oisst (Forecast AMIP with Reynolds OI SSTs).

Taking a step further, we created a similar ensemble of atmospheric forecasts but with the SSTs prescribed to be the predicted SSTs from the original hindcasts. We refer to these forecasts as FAMIP_psst (Forecast AMIP with POAMA SSTs). These experiments are designed to assess the sensitivity of prescribing SSTs rather than allowing full coupling as well as assessing the impact of SST forecast errors on the predicted rainfall anomalies.

From each of P_ctrl, P_amipAL, FAMIP_oisst and FAMIP_psst, a ten-member ensemble was produced for September, October and November for the period of 1982-2005, and the ensemble mean forecasts of the 3 month mean (SON) were computed for each year. Then, for each experiment the SON anomalies of 1997 and 2002 were computed with respect to the hindcast climatology consisting of three randomly chosen members. Thereby, systematic bias associated with model drift was removed from the forecasts (Stockdale et al. 1998). For P_aliAclimL, a ten-member ensemble of hindcasts for SON was generated only for 1997 and 2002, and their anomalies were obtained against the P_ctrl climatology. The design of experiments is summarized in Table 3.1.

The predictions of Australian rainfall are verified against observed behaviour based on the AWAP gridded monthly analyses of rainfall (0.25° lat x 0.25° lon, but interpolated onto the POAMA grids in this study; Jones et al. 2009). SST forecasts are verified against the Reynolds OI v2 SST analysis and MSLP forecasts are verified against the ERAI MSLP data (Dee et al. 2011).

Insight into the causes of these contrasting rainfall anomalies in these two years is provided by statistically reconstructing the rainfall anomalies. The reconstruction is based on multiple linear regressions using as predictors four climate indices that capture the large-scale oceanic and atmospheric circulation anomalies that are well known to affect Australian rainfall (e.g., Risbey et al. 2009). These include the time series of the first and second principle components of tropical Pacific SSTs (25°S-20°N,120°-295°E) that represent the variability of canonical eastern Pacific El Niño (SSTPC1) and central Pacific El Niño (SSTPC2), respectively; the Dipole Mode Index (DMI) that monitors the variability of the IOD; and the time series of the first principle component of MSLP over the Southern Hemisphere extratropics (20-75°S) that monitors the variability of the SAM (SAM index; SAMI, Figure 3.8). The time series of the four indices, their associated spatial patterns, and cross-correlations between the time series are presented in the Appendix of Lim and Hendon (2015).

The standardized amplitudes of the four predictor indices during 1997 and 2002 SON are displayed in Figure 3.8. SSTPC1 and the DMI show large amplitudes (2-3 standard deviations (σ)) in 1997 but much smaller amplitudes in 2002. However, SSTPC2, which depicts the central Pacific warming relative to the eastern and western Pacific basins, is strongly negative (-2σ) in 1997 but moderately positive in 2002. The SAM was extraordinarily strongly negative (-2σ) in 2002 but also significantly negative in 1997 (-1σ). The strongly negative occurrence of the SAM in 2002 has been attributed partly to the extraordinary strength of a rare sudden stratospheric warming (Newman and Nash 2005; Thompson et al. 2005).

The large negative amplitude of the SAM in 1997 is likely explained by the promotion of negative SAM by a cold tongue El Niño. However, the zonally symmetric component of the Southern Hemisphere extratropical circulation (i.e. the SAM) appears to be swamped by the zonally asymmetric component resulting from Rossby waves dispersing to high latitudes from the tropical Indian Ocean associated with the strong positive IOD during 1997 spring.

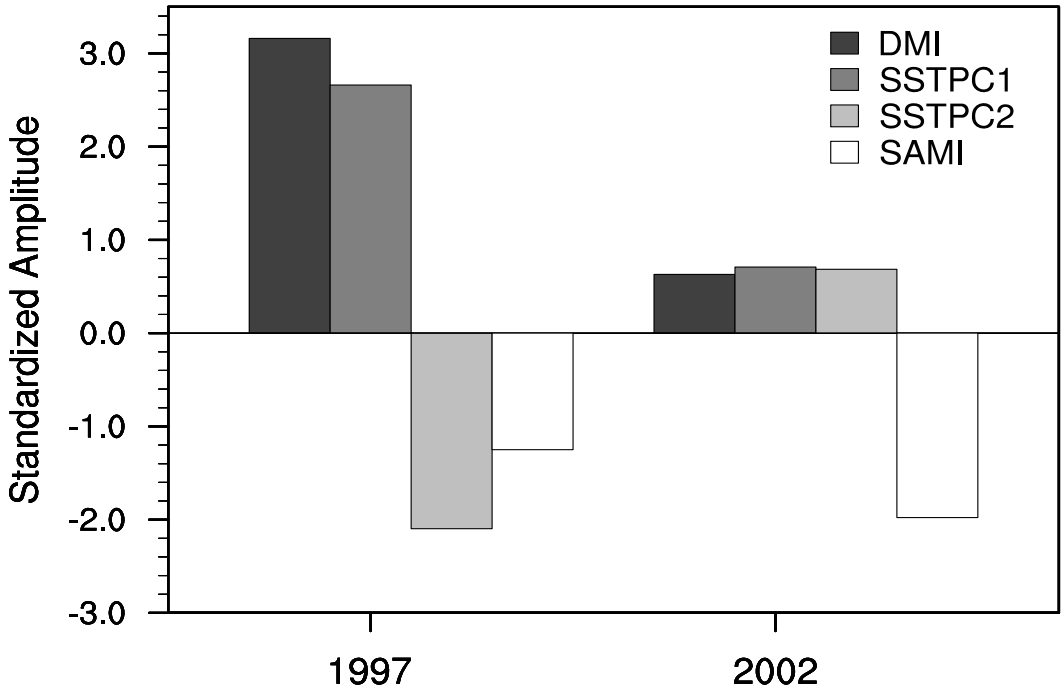

Figure 3.8: Amplitudes of climate indices in 1997 and 2002 SON (taken from figure 5 in Lim and Hendon, 2015). The time series of each index and the associated spatial pattern are presented in the figure A1 of Lim and Hendon (2015).

The reconstructed rainfall anomalies using these four indices reasonably well reproduce the main characteristics of observed rainfall anomalies across Australia (Figure 3.7 e,f), especially capturing that 1997 was not as dry as 2002 (Figures 3.9a,a'). In particular Western Australia and central eastern Australia are faithfully reconstructed to be wetter than normal whereas the northern end, the south east and the south west are reconstructed to be drier than normal in 1997. 2002 is reconstructed to be dry everywhere but especially in the east. Although the spatial patterns of rainfall anomalies are successfully depicted by this statistical reconstruction with the four predictors, the overall wetness of 1997 spring and the dryness of 2002 spring over the Australian continent are somewhat underestimated by this method.

Then, we repeated the multiple linear regression calculation but leaving one index out each time in order to see the sensitivity of the rainfall anomaly to the independent influence of each index. This exercise reveals that the large negative amplitude of SSTPC2 in 1997 was critical in suppressing the potentially severe dry response due to the record-breaking El Niño and IOD (Figure 3.10c), which confirms the findings of Wang and Hendon (2007). Likewise, the positive amplitude of SSTPC2 in 2002 is found to be an important cause of the extreme dry conditions in 2002 spring (Figure 3.10c'). However, a more important driver of the 2002 dry spring was the occurrence of negative SAM (Figure 3.10e'). In contrast, the negative SAM in 1997 seemed not to have played much of a role on the anomalous rainfall (Figure 3.10e). Finally, because SSTPC1 and the DMI strongly covary, the independent influence of the DMI appears not to be significant during both 1997 and 2002 (i.e. its omission does not make a noticeable difference from the original reconstruction as far as SSTPC1 is included in the reconstruction; Figure 3.10d,d').

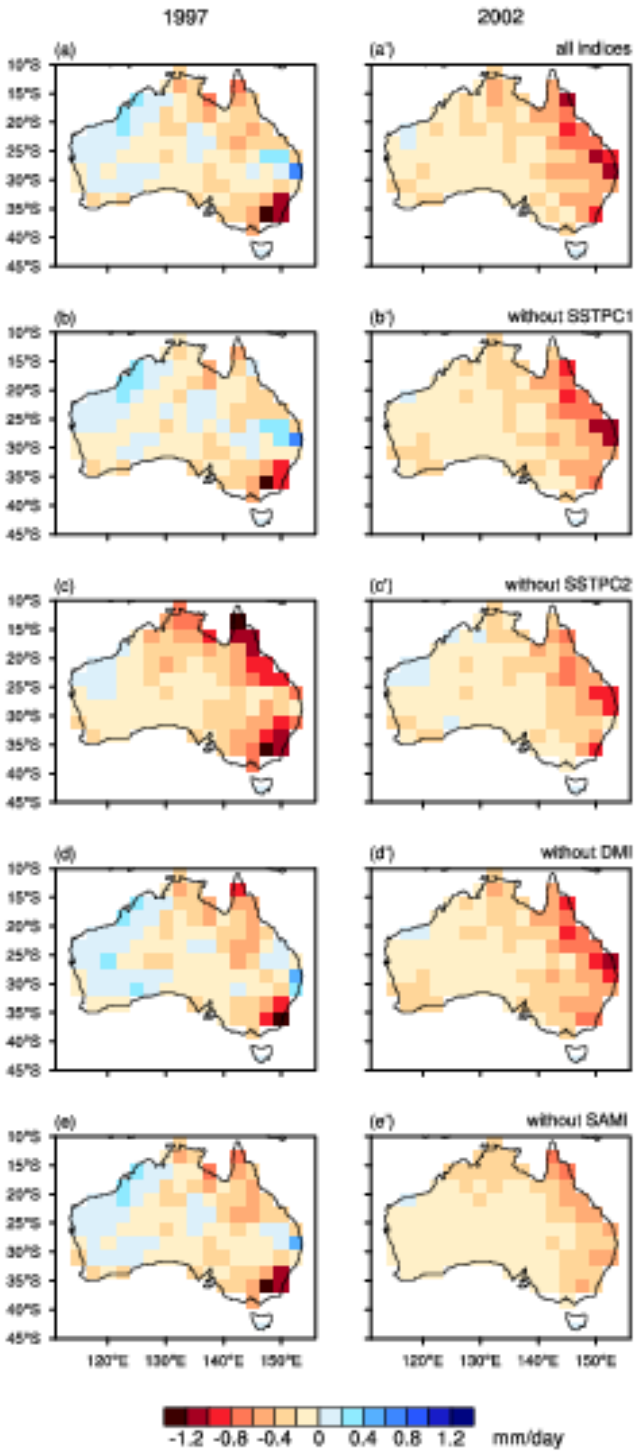

Figure 3.9: Left panels: (a) reconstructed rainfall anomalies with multiple linear regressions on SSTPC1, SSTPC2, DMI and SAMI for 1997 SON. (b)-(e) the same as (a) but each time leaving out a predictor – SSTPC1, SSTPC2, DMI and SAMI, respectively. Right panels: (a')-(e') same as (a)-(e) but for 2002. The colour shading interval is 0.2 mm/day (taken from figure 6 in Lim and Hendon, 2015).

The POAMA system demonstrates high skill in predicting the strong positive IOD and the strong eastern Pacific warming El Niño (i.e. large amplitudes of positive SSTPC1 and negative

SSTPC2) in 1997 (Figure 3.10). Similarly, the central Pacific warming El Niño (i.e. moderate positive amplitudes of SSTPC1 and SSTPC2) in 2002 is also well predicted (Figure 3.10). However, the occurrence of the weak positive IOD of 2002 is missed by the POAMA forecasts. The level of skill in predicting these tropical Indo-Pacific SST conditions is very similar between P_ctrl and P_amipAL, confirming the notion that atmospheric initial conditions do not play a primary role for predictability of ENSO. However, P_ctrl and P_amipAL demonstrate a substantial difference in the prediction of the magnitude of the negative SAM especially in 2002, which confirms that the occurrence of record strength negative SAM in 2002 was largely internal to the atmosphere.

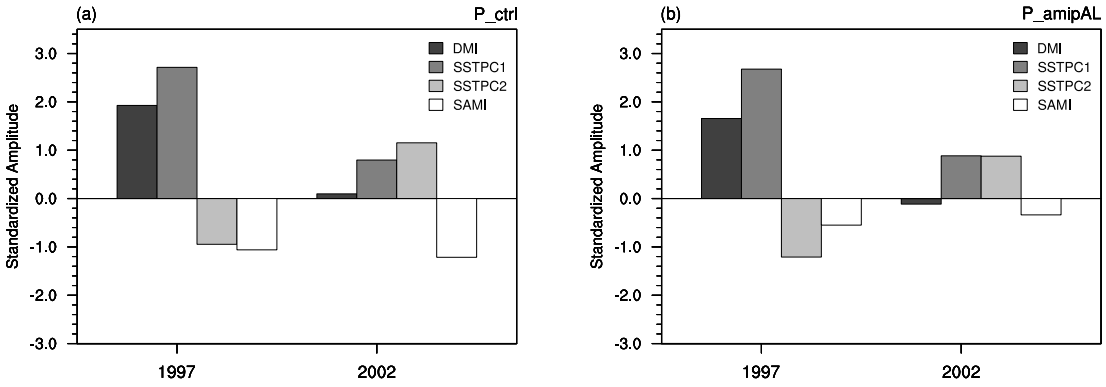

Figure 3.10: Predicted amplitudes of the DMI, SSTPC1, SSTPC2 and the SAMI in P_ctrl and P_amipAL experiments (taken from figure 8 in Lim and Hendon, 2015).

For Australian climate, P_ctrl predicts spring 1997 to be wetter than normal and 2002 to be drier than normal, although the forecasts tend to be somewhat wetter than the observed for both years (Figure 3.11a,b,a',b'). Interestingly, the forecasts from all the other four sensitivity experiments show 1997 to be not as dry as 2002 (Figure 3.11c-f,c'-f') despite the absence of realistic atmospheric or land information at the initial state in the coupled experiments and the absence of the atmospheric feedback to the ocean in the uncoupled experiments. Therefore, these results confirm that the source of the rainfall contrast between the two seasons was the difference in the tropical SSTs and that this rainfall contrast was predictable.

In detail, the rainfall forecasts initialized with climatological land surface conditions (P_aliAclimL) are reasonably similar to those with realistic land surface conditions (P_ctrl) in both 1997 and 2002 (Figures 3.11c, c'). The rainfall forecasts are found to be more sensitive to the atmospheric initial conditions than the initial soil moisture (Figures 3.11d, d'). The magnitudes of predicted rainfall anomalies are much smaller for the forecasts initialized with AMIP atmospheric conditions, which are balanced to the SSTs but do not contain realistic intra-seasonal variability, than for the forecasts initialized with the observed atmospheric initial conditions. In particular, the rainfall anomalies over the eastern states predicted in P_amipAL are significantly different from the original forecasts in P_ctrl at the 95% confidence limit for both years. A large portion of this difference stems from the first month of the forecasts for both 1997 and 2002 (not shown), which confirms that the atmospheric initial state matters for the evolution of the atmosphere up to a month time-scale and then the boundary forcing takes over (e.g. Hudson et al. 2013, Lim and Hendon 2015). Also, an important cause of the underestimation of 2002 drought in P_amipAL seems associated with the lack of skill in predicting the observed negative SAM (as shown in Figure 3.10b).

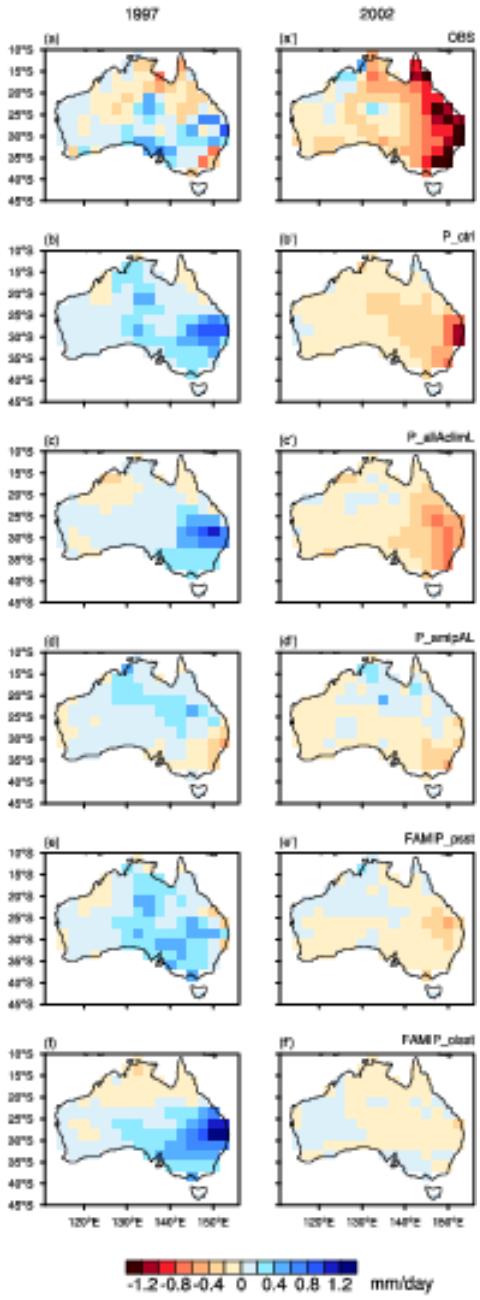

Figure 3.11: Left panels: (a) Observed and (b)-(f) predicted Australian rainfall anomalies in1997 SON. Right panels: (a')-(f') same as (a)-(f) but in 2002. Labels of each experiment are shown on the upper right corner of (b')-(f'). (b),(b') POAMA hindcasts with observed initial conditions of atmosphere, land and ocean; (c),(c') POAMA experiments with the same initial conditions as POAMA hindcasts except for the climatological land initial conditions; (d),(d') POAMA experiments with the same initial conditions as POAMA hindcasts except for the climatological land initial conditions and the atmospheric initial conditions consistent with SST conditions; (e),(e') POAMA experiments running the atmosphere model with prescribed SST that were predicted by POAMA; and (f),(f') The same experiments as (e),(e') but the atmosphere model with prescribed SST that were from the observation. The colour shading interval is 0.2 mm/day (taken from figure 9 in Lim and Hendon, 2015)

The 2002 rainfall forecast also shows high sensitivity to the atmosphere and ocean coupling. Although the dry condition is maintained in the east, the intensity is much weaker in the

experiment where the atmosphere is forced in uncoupled mode by the POAMA predicted SSTs from P_ctrl (FAMIP_psst; Figure 3.11e'). This sensitivity to coupling is statistically significant at the 95% c.l. The global MSLP and rainfall anomaly patterns from FAMIP_psst show that without proper air-sea interaction, there are significantly larger rainfall anomalies in the tropical eastern Indian Ocean and in the west coast of central Africa compared to the rainfall anomalies from P_ctrl. Hence a more zonally asymmetric wave pattern is found in the extratropical Indian Ocean (not shown). Consequently, the negative SAM is not predicted and the associated Australian rainfall response is weak in FAMIP_psst. The inability to predict the negative SAM of 2002 spring and the associated rainfall is also found in the experiment where the atmosphere is forced by the observed SSTs. In FAMIP_oisst, the hemispheric scale rainfall anomaly related to the SAM is absent; therefore Australia is predicted to be substantially less dry in FAMIP_oisst than in P_ctrl. It should be reiterated here that the atmosphere and land initial conditions used for FAMIP_psst and FAMIP_oisst were identical to those used for P_ctrl, yet Australia was significantly less dry in the two AMIP-type experiments than in P_ctrl. Therefore, these results suggest that the model's ability to simulate the negative SAM was important to the prediction of the extraordinarily dry conditions over eastern Australia in 2002 spring. It is interesting to learn from FAMIP_psst and FAMIP_oisst that realistic representation of air-sea coupled processes is important to the skilful predictions of the SAM and its associated regional climate impacts. This connection between air-sea coupling and improved prediction of the SAM needs further study. On the other hand, air-sea coupling does not seem to make a noticeable difference to the prediction of Australian rainfall for 1997 spring (Figure 3.11e).

To summarize, the near normal Australian rainfall anomaly in 1997 spring resulted from the far eastward shift of the maximum SST warming by El Niño in the eastern Pacific, although above-normal rainfall in the southern part of central and eastern Australia was likely due to atmospheric processes that were skilfully captured in the POAMA model by the use of the realistic atmosphere initial conditions of the 1st of September 1997. In comparison, the drier than normal conditions during 2002 spring resulted from the occurrence of a central Pacific El Niño event which maximum SST warming was placed close to the date line. However, the extremity of the dryness of 2002 spring was significantly contributed to by the occurrence of record strength negative SAM. The forecast experiments that were unable to predict the large negative excursion of the SAM were unable to predict the strength of the drought in 2002. Realistic atmospheric initial conditions and good representation of air-sea interaction are found to be important for the skilful prediction of the strong negative SAM during spring 2002.

Conclusions and future perspectives

The calculation of the MMC in isentropic streamfunction is a complex calculation, and current results based on monthly quantities do not fully capture the 'geostrophic' part of the isentropic flow which is dominant in the extratropics. Investigation is still ongoing to explore further the issue using daily quantities to obtain more accurate results.

The calculations using monthly data do seem to agree with what is expected regarding inter-annual variability. In response to El Niño, a narrowing and intensification of the tropics and the Hadley cell is observed. In terms of the SAM response, the variability appears correct: the storm track is further poleward during the positive phase. Over the longer term, computed trends indicate changes to the MMC. The outflow regions of the upper arm of the Hadley cell may be changing. In the Southern Hemisphere, the sub-tropical 'downward' branch appears to be moving more poleward. The calculations suggested that the biggest changes may lie in MAM, although an expansion in most seasons is seen. These results are subject to change, particularly

in the extratropics, because of the largely missing 'geostrophic' component of the MMC which is currently under investigation.

In Activity 2 the link between the Southern Annular Mode (SAM) and sub-tropical rainfall via atmospheric circulation in CMIP5 simulations with historical forcing was analysed. It was found that the climate models skilfully simulate the relationship of high SAM and increased rainfall in the subtropics in summer, which would bring above normal rainfall to Victoria, but the absence of this relationship in winter is linked to the expanded dry zone over Victoria to the north of Victoria. However, the dry response over the latitude band of 30-35S to high SAM is underestimated in winter, and more importantly, there is a significant misrepresentation of rainfall response in the tropical-sub-tropical rainfall in summer in the CMIP5 models. Also, the seasonality of ENSO-SAM relationship is not well simulated in the majority of the models, which is likely due to the models' inability to simulate the Indo-Pacific SST pattern associated with ENSO. Therefore, future study will focus on understanding sources of these biases and the impact of these biases on SEA rainfall in the simulations with historical forcing and increasing greenhouse gases.

In addition, the study on the comparison of1 997 and 2002 spring rainfall over Australia revealed that not only the El Niño, whose maximum warming was shifted to the date line, but also the record strength of the negative SAM, played a key role in the severity of the drought experienced in eastern Australia in 2002. In 1997 spring, which was expected to be very dry due to the record strength of El Niño, the rainfall amount over eastern Australia was near average due to the near normal SST anomaly over the central Pacific Ocean and weather noise. These results were found by both the statistical method and dynamical model experiments, which provides robustness to the findings.

The outcomes of Activity 2 have important implications for predicting current and future climate. The strong influence of the SAM on south-eastern Australian rainfall means that limited predictability of the SAM on a seasonal timescale (e.g. Lim et al. 2013) places a strong constraint on predictability of rainfall. From a climate change perspective, a robust finding of projected future climate in response to increased greenhouse gases is a promotion of high SAM in all seasons (e.g. Yin 2005; Gillet et al. 2013). The emergence of this upward trend of the SAM in winter in the future climate would then result in an expanded sub-tropical dry zone in winter and so a drier Victoria in winter (e.g., Scheff and Frierson 2012). The emergence of high SAM thus would mean a further contribution to any ongoing drying trend for south-eastern Australia, such as that resulting from a local poleward expansion of the subtropics and associated intensification of the sub-tropical ridge. By contrast, the upward trend of the SAM in summer would result in a poleward shift of the sub-tropical dry zone away from Victoria with a poleward shift of the wet-topics into Victoria and so we can expect increased warm season (spring-summer-autumn) rainfall in the future climate.

Following on from these implications, we will continue to investigate the linkage between the SAM and Australian climate in the present and future climate by assessing the CMIP5 models for their capability to simulate the seasonality of the response of the SAM to ENSO (strong in summer and weak in winter). We will explore the relationship between the misrepresentation of the SAM-rainfall teleconnection and biases in the model's mean state, especially the separation of the sub-tropical and high latitude jets. If a systematic relationship is found, we can use this information to put more faith in the projections for the response to CO2-induced high SAM for those models with reduced biases.

PROJECT 5: CRITICAL ASSESSMENT OF CLIMATE MODEL PROJECTIONS FROM A RAINFALL PERSPECTIVE

Bertrand Timbal[1], Dewi Kirono[2] and Louise Wilson[2]

[1]: R&D Branch, Bureau of Meteorology
[2]: CSIRO, Ocean and Atmosphere

Key Findings

- Following on from the analysis of Australian STR and its relationship with Victorian rainfall in climate models, this year, influence from the tropical sea surface temperatures (SSTs) to Australia's north was examined. It was found that while the CMIP5 models capture a part of the observed relationship between tropical SSTs and SEA rainfall with a reasonable annual cycle, the magnitude of the correlation varies strongly from one model to the next and is weaker than observed (significantly so except for a few models). In that respect, while models' future warming projected onto the tropical tripole varies considerably amongst models, it does not relate as expected to the range of rainfall projections across Victoria.
- The relationship between SEA rainfall and a tropical tripole index, which has been observed to vary markedly on decadal timescale, appears stable in response to external anthropogenic forcings. While the magnitude of the relationship within individual models can differ for different 50 year periods, the full ensemble mean shows a remarkably stable picture for the past and current centuries; suggesting no change in the magnitude of this relationship due to response to anthropogenic forcing.
- State of the art, nation-wide climate change projections being delivered jointly by the CSIRO and the Bureau of Meteorology for the needs of Natural Resource Management (NRM) groups have been analysed to provide a summary of climate projections for the state of Victoria. Information in the IPCC Fifth Assessment report and recent research have been summarised for climate model performance and the projected future of the main drivers of Victorian climate. The NRM results relevant to the state of Victoria are to be synthesised into a single report.
- The Millennium drought had the longest spell of months during which no 'wet' month occurred within 121 months. The CMIP5 models reproduce such a spell, but not of this duration. Multi-models average of the longest spell during the 20th century is only 54 months. For the 21st century, half of the models indicate spells that might occur with a duration of 60 months or more.

Background

Climate projections from climate models are showing some consistent behaviour (e.g. dry to the south and wet to the north across SEA) and some inconsistent behaviour (the degree of future rainfall change). Some of this uncertainty is linked to the models' ability to represent important teleconnections (e.g. the impact of the SAM on the HC) and key modes of climate variability (e.g. the tropical influences of the Pacific vs. Indian oceans) identified through SEACI research as being important for SEA rainfall. In order to provide guidance as to which models to use for projecting future climate (with a particular focus on subsequent impacts on water availability), we need to assess individual models for the capability to simulate these key teleconnections and modes of climate variability.

Objectives

1. Understand the source of spread in rainfall projections by evaluating model projections of tropical sea surface temperatures and their association with Victorian rainfall

2. Evaluate CMIP5 models ability to capture extended dry spells such as Millennium drought. Explore the risk for SEA to experience such a spell in the future.

Activity 1: Climate model's ability to capture tropical sea surface temperature changes and associated rainfall in Victoria

Combining the tropical influences of the Pacific and Indian oceans, Timbal and Hendon (2011) developed a tripole based index to maximise the amount of SEA rainfall inter-annual variability captured by a simple Sea Surface Temperature (SST) based index. Using this index, it was shown that the tropical modes of variability did not explain the rainfall reduction during the Millennium drought except during the worsening of the drought at the end, and in particular during the spring season. On the contrary, the post 2009 recovery was strongly driven by tropical modes of variability. The influence of the tropics on SEA and Victorian rainfall in turn is important for streamflows across the State. Annual composites of streamflows based on the tripole index show a sizeable difference between positive and negative tripole years (Timbal et al. 2015, Fiddes and Timbal, 2015). It is of interest to determine if global climate models can capture the same association and, if so, how their results vary into the future. Further details can be found in Timbal et al. (2015).

Data and method

We analyse rainfall variations using the Australian Bureau of Meteorology's current operational high-resolution monthly rainfall analyses, generated as part of the Australian Water Availability Project (AWAP) (Jones et al. 2009). south-eastern Australia (SEA) rainfall is defined as rainfall over the continent south of 33.5°S and east of 135.5°E (the area outlined by the red box in the middle panel of Figure 5.1). We used Hadley Centre/UK Meteorological Office SST (HadISST) analyses from 1870 to 2014 interpolated onto a 1° by 1° grid (Rayner et al., 2003).

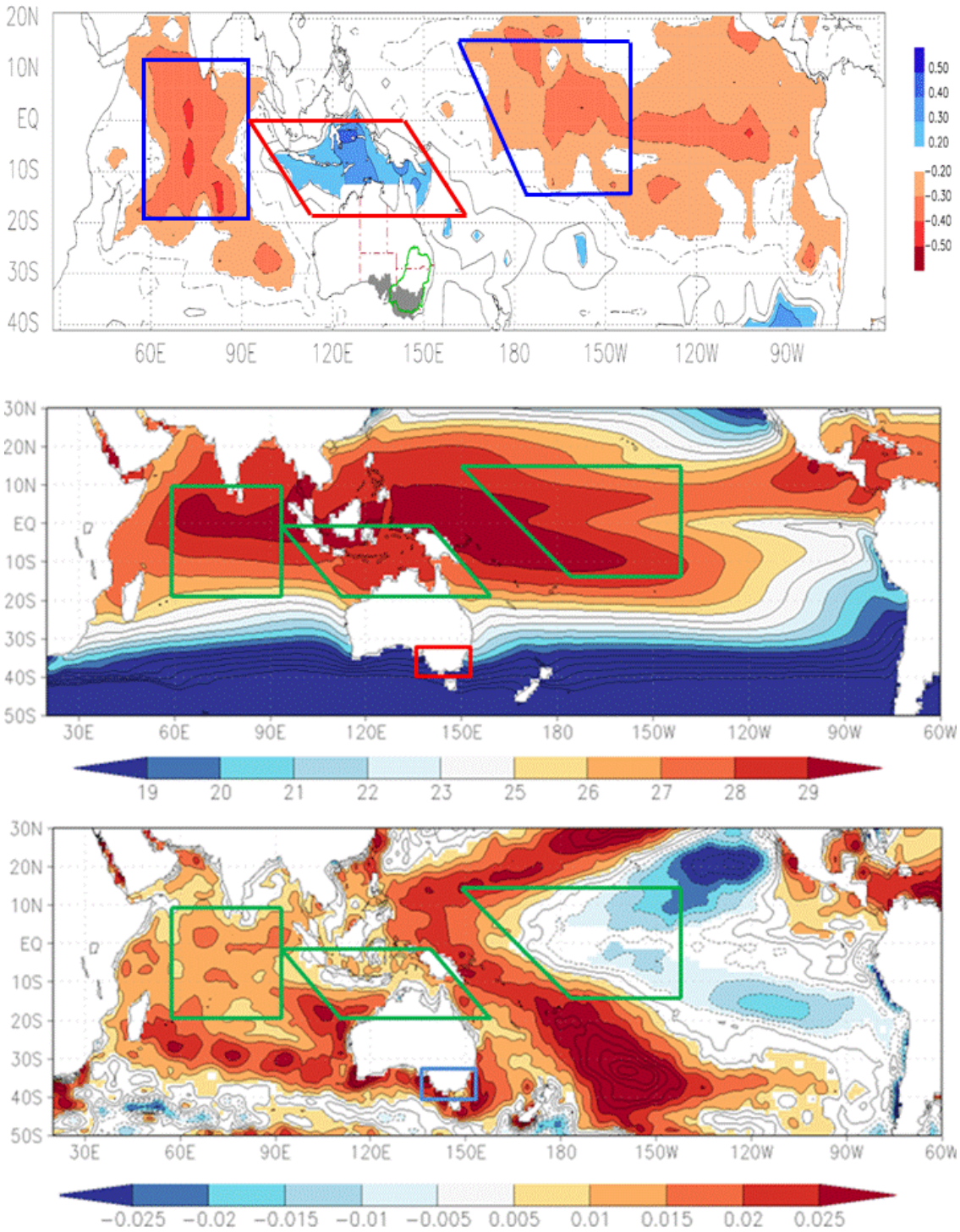

Figure 5.1: The 'tri-polar' index (tripole) is formed by subtracting the mean SST over the central-western Indian Ocean and the central Pacific Ocean blue boxes in top panel from the SST in the red box to the north of Australia. These boxes were defined as regions where the correlation of tropical SST with the time series of rainfall in SEA (red box in middle panel) was in excess of ±0.2. Correlations are shown in top panel (from Timbal and Hendon, 2011). The middle panel is the annual mean Sea Surface Temperature (in °C) and the lower panel is the linear trends (in °C/year) computed using Reynolds dataset from 1985 to 201.

The extra-tropical teleconnectivity with SEA rainfall is evaluated using the method developed by Timbal and Hendon (2011). They developed a 'tri-polar' index (tripole) by examining the spatial distribution of the correlation of tropical SST with the time series of rainfall in SEA and observed three regions of significant correlation (in excess of ±0.2); these regions define the tripole index (see top panel in Figure 5.1). The tripole is computed as the difference between the mean SST north of Australia (extending from the eastern Indian Ocean and across the Maritime Continent) minus the average of the SST over the central-western Indian Ocean and the central Pacific Ocean (see boxes in Figure 5.1).

Monthly climate model data is from the Coupled Model Intercomparison Project Phase 5 (CMIP5) (Taylor et al. 2012). The required data to conduct this analysis was available from 29 models. In the set of national projections delivered by CSIRO and BoM (2015), rainfall projections based on RCP8.5 use 39 models (Table 3.3.2 in CSIRO and BoM, 2015). Therefore, while providing a large sample of the uncertainties attached to the CMIP5-based projections for rainfall, the model ensemble in this study does not represent the full details of existing model projections and results found here may not be perfectly comparable to the full ensemble. The future reconstructed pathway of emissions chosen is RCP8.5.

Results

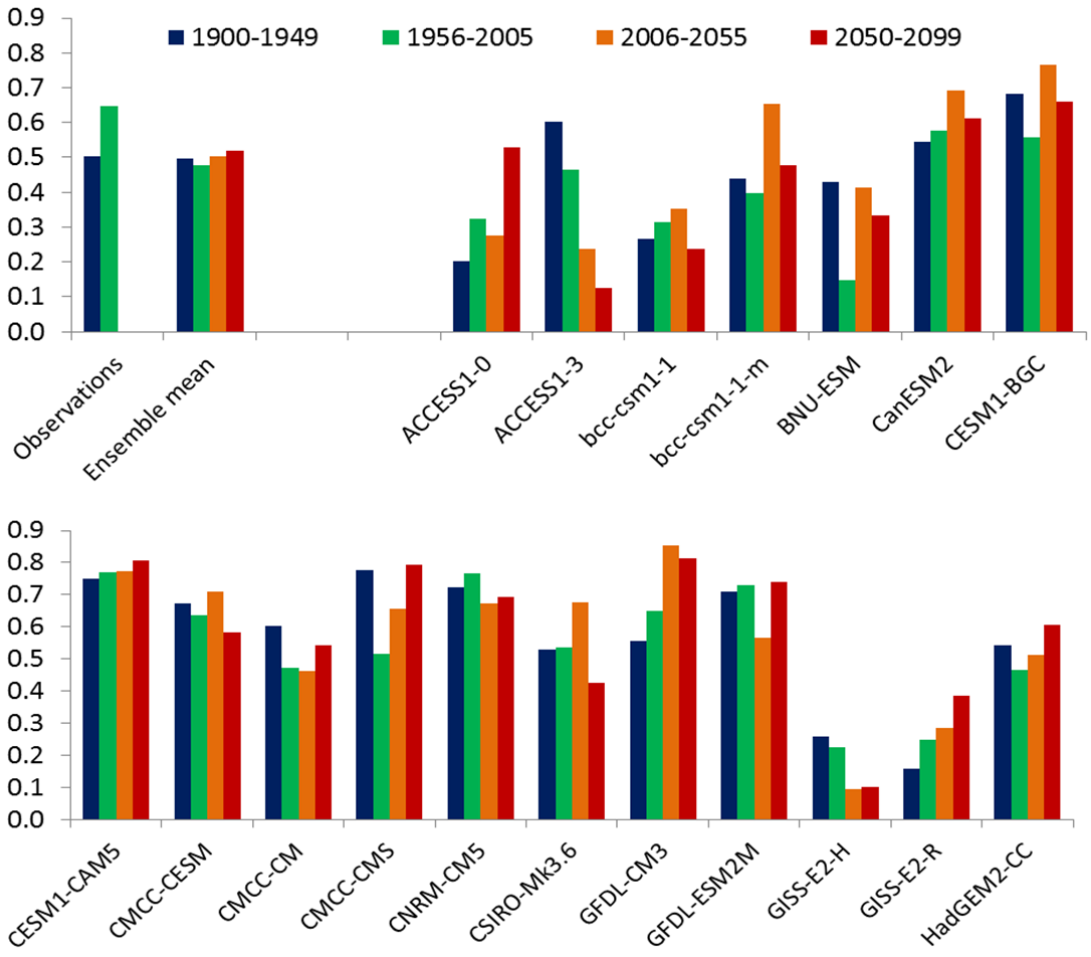

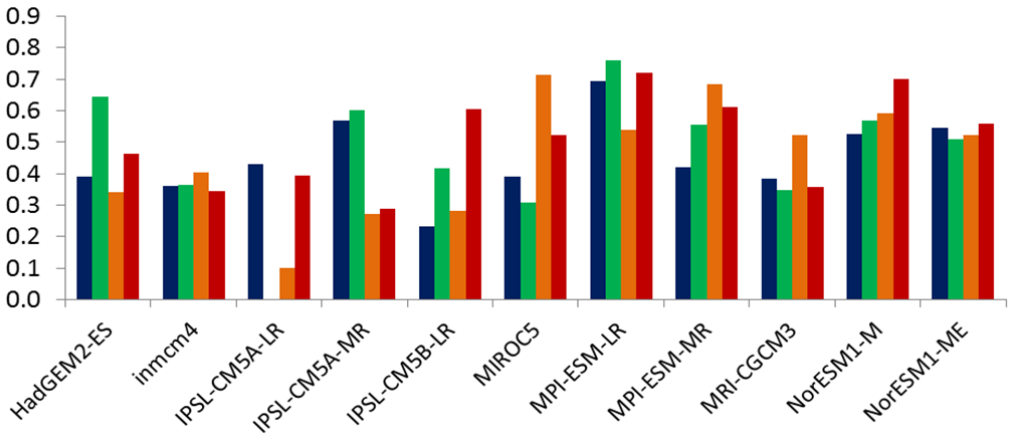

Figure 5.2 Correlation coefficients between July to November mean tripole index and SEA rainfall computed for 50 year periods for the observations (past climate only), the CMIP5 ensemble mean and the individual models.

It was found that while the CMIP5 models generally capture the observed relationship between tropical SSTs and SEA rainfall, and match the shifts in that relationship through the annual cycle, the magnitude of the correlation varies from one model to the next. The relationship in the models is often slightly weaker than observed, though some individual models do have a relationship as strong as or stronger than observed (Figure 5.2).

Table 5.1: Correlation coefficients through the scatter across the 29 individual CMIP5 modelled quantities (indicated in the two left columns, note 'STD' is standard deviation) averaged over period of time indicated in the third column and for different seasons (columns 4 to 9). [Bracketed correlation values indicate results when one outlier model is excluded; the model excluded is not the same in all cases.] Correlation coefficients above 0.37 (0.47) are significant at the 95% (99%) level and are indicated in italics (bold).

Correlated quantities			Season					
Variable 1	Variable 2	Period considered	Annual	JASON	AMJJASO	SON	DJF	Cool-Warm
STD SEA Rainfall	STD Tripole	1900-2005	*0.44*	**0.48**	**0.47**	0.40	0.19	0.03
		1976-2005	*0.43*	**0.55**	**0.48**	**0.47**	0.18	-0.04
	Corr. Coef. SEA rainfall vs Tripole	1976-2005	*0.43*	**0.51**	**0.48**	**0.49**	0.01	-0.14
SEA Rainfall trends	Tripole trends	1976-2005	0.27 *(0.37)*	0.34 *(0.46)*	*0.41* **(0.52)**	**0.47** **(0.62)**	0.00 (0.07)	0.36 (0.36)
	Corr. Coef. SEA rainfall vs Tripole	1976-2005	-0.08	-0.12	-0.13	-0.02	-0.02	-0.20

A positive correlation between the tripole and SEA rainfall means that high SEA rainfall is associated with warm SSTs to the north of Australia (relative to the SSTs to the north-east and north-west). The correlation coefficients for the July to November averaged SEA rainfall and tripole for 50 year periods are shown in Figure 5.2. In the observations there is a marked difference between 1900-1949 (r = 0.50) and 1956-2005 (r = 0.65) correlation values. The difference is even larger when annual values are considered (r = 0.33 and 0.66 respectively). The correlation values over the same 50 year periods from individual CMIP5 models can differ by a similar amount to observed (although both negative and positive shifts are seen), but the correlations averaged over the model ensemble show no indication of a systematic shift either in the past century or in the 21st century under RCP8.5 pathways. Thus it appears that shifts in the strength of the relationship between tropical variability and SEA rainfall are due to internally generated decadal variability, with no tendency due to anthropogenic forcing towards a reduction or an increase in the strength of the relationship during the 21st century.

The internal relationship between aspects of variability of SEA rainfall and the tripole for each model was explored using the scatter plot from all the models (e.g. Figure 5.3), with results summarised in Table 5.1. The standard deviation (STD) of the SEA rainfall was compared with the STD of the tripole and in general higher rainfall variability is associated with higher variability in the tripole. This indicates that interannual variability in SEA rainfall varies with the tropical SSTs. The strength of the correlation between SEA rainfall and the tripole also indicates whether SEA rainfall has high interannual variability, with a stronger correlation associated with higher SEA rainfall variability.

The association between the trends in SEA rainfall trends over the last 30 years and the Tripole trends from each model is also significant and positive in spring, meaning strong upward trends in rainfall are associated with strong warming to the north of Australia.

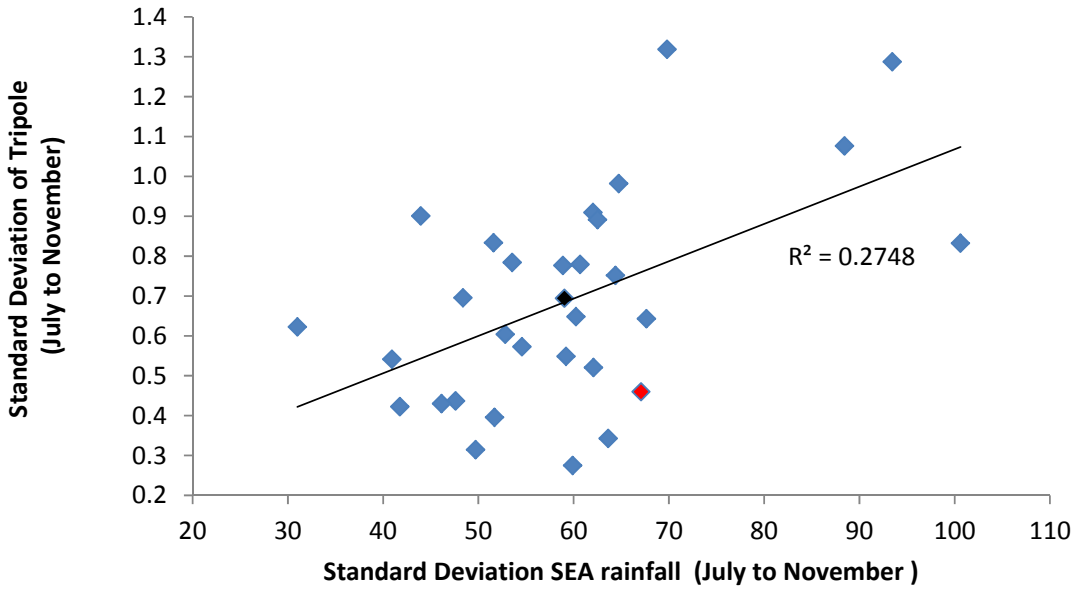

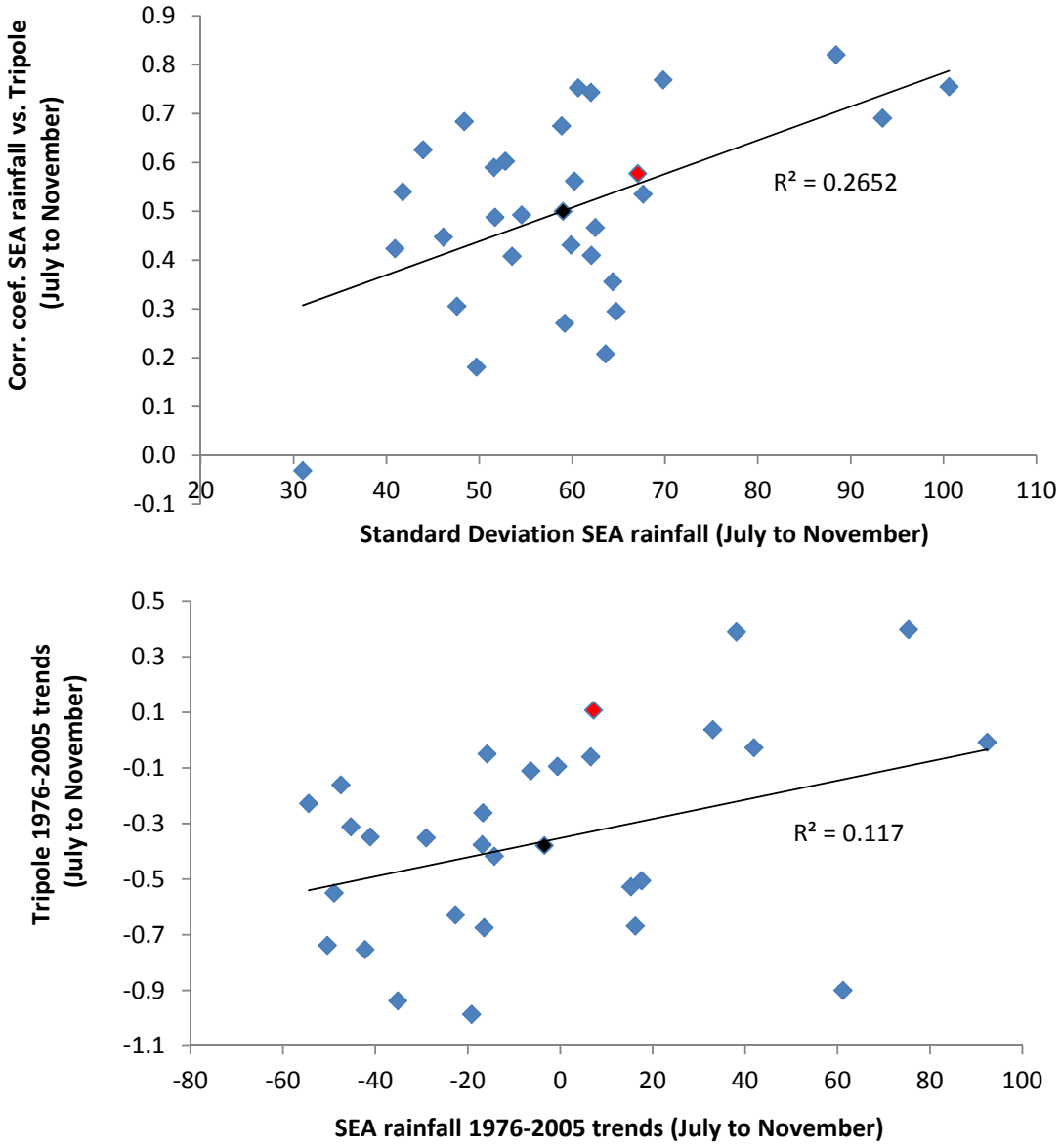

Figure 5.3 Scatter plots of individual CMIP5 models metrics, relating: standard deviation of July to November SEA rainfall and tripole index (top panel), standard deviation of July to November SEA rainfall with the strength of the SEA rainfall-tripole relationship (middle panel) and July to November SEA rainfall linear trends and tripole trends (lower panel). All quantities are computed on the last 30 years of the current climate simulations (1976-2005). In all panels, the ensemble mean is shown with a black symbol and the observations with a red symbol, linear lines of best fit and square correlation are displayed.

In the next year of the project, similarly the association between future trends in SEA rainfall over the 21st century and Tripole trends from each model will be investigated to explore what part of the SEA rainfall range is due to individual models spatial warming in the tropical oceans.

Activity 2: Length of dry spells in CMIP5

Introduction

SEA has experienced many major droughts including the "Federation drought' (~1895-1903), the "World War II drought" (~1939-1945) and the "Millennium drought" (~1997-2009). In terms of rainfall decline, each of these droughts has been different in its severity, spatial signature, seasonality and seasonal rainfall make-up (Verdon-Kidd and Kiem, 2009). In terms of decline in runoff, the Millennium drought was more severe, with a greater reduction in annual runoff compared to historical droughts with similar low mean annual rainfall (Ballard et al. 2014, Potter et al., 2011) and this has placed enormous pressure on water resources.

Potter and Chiew (2011) describe possible reasons for the greater reduction in runoff in SEA during the Millennium drought in comparison to other long periods of drought. These include changes in the dominant hydrologic processes; the higher proportional reduction in autumn and winter rainfall - which in turn has high impact on the runoff since most of the SEA runoff occurs in the winter months; changes in the daily rainfall distribution and rainfall sequencing; and a decrease in interannual variability as well as a lack of high rainfall years (e.g. Verdon-Kidd and Kiem, 2009; Potter and Chiew, 2009; Potter et al. 2011; Timbal, 2010).

With regard to the lack of high rainfall years, Timbal (2010) shows that during the Millennium drought there was a 15 years in a row of no wet months (defined as months with monthly total rainfall in excess of the 90th percentile for that calendar month). The lack of wet months in a very long period of time is expected to decrease mean runoff, and potentially depleting surface and groundwater reservoirs (Potter and Chiew, 2011). Thus, from a hydrological point of view, the continuous non-existence of wet months for a prolonged period of time can be very critical.

In this study, the length of time with no 'wet' months in SEA is examined, in CMIP5 models' simulations of both the 20th and 21st centuries.

Data and Methods

Following Timbal (2010), we calculated the areal mean monthly rainfall for SEA (defined as mainland Australia south of 33.5^{o}S and east of 135.5^{o}E) for both the observed and modelled rainfall data. The source of the observed monthly rainfall data is the Australian Water Availability Project (AWAP) gridded climate datasets of the Australian Bureau of Meteorology (Jones et al., 2009). Meanwhile the modelled rainfall from a set of 32 Global Climate Models (GCMs) available, at the time of the study, in the World Climate Research Programme's (WCRP's) Coupled Model Intercomparison Project phase 5 (CMIP5) multi-model dataset. The historical simulations span the years 1900-2005, while the 21st century simulations span 2006-2100. Future simulations forced under the 'business as usual' emission scenario of RCP8.5 were used.

Wet months were defined as months above the 90th percentile. Based on the 1900-1999 climatology of each model, the 90th percentile of rainfall for each model's month of the year was calculated.

Two tiers of model evaluation were conducted. One was to compare a model's rainfall monthly mean and interannual variability against observations (six matrices in total). The second was to test a model's ability in reproducing the observed length of no-wet months. The interannual variability matrices are the standard deviation, coefficient of variation, the 90th and 10th percentiles, and the interannual range (defined as the difference between the 90th and 10th divided by the median). For each of the six matrices we calculate the coefficient correlation (R) between the model and the observations. In doing so, each R is calculated based on twelve data

points, where a positive value of *R* indicates better model performance and vice versa. A subsequent ranking process is performed for each of the matrices. Then, the average of all six matrixes is calculated for each model and assigned as a model's final rank.

Results

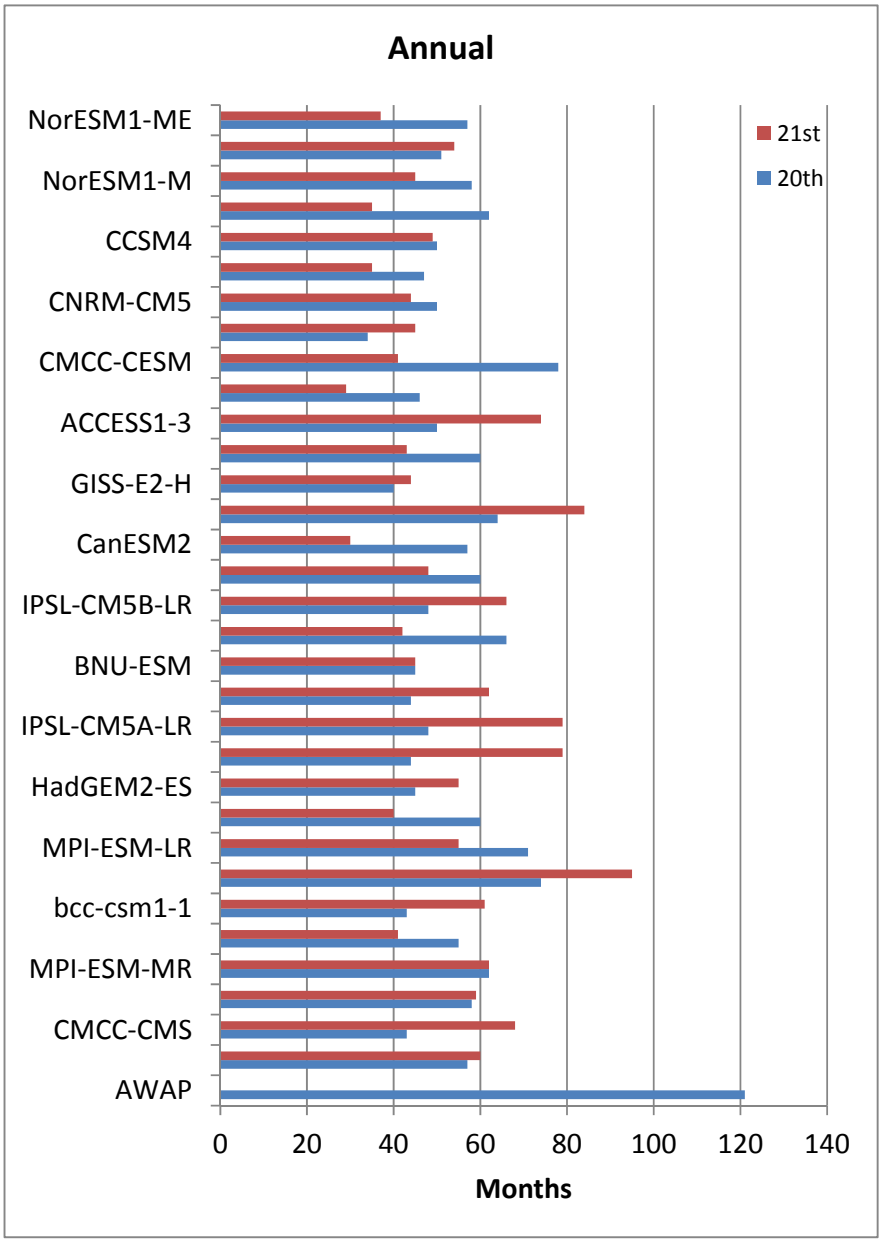

Figure 5.4 The longest spell of months in south-east Australia during which no wet month occurred. Observed from AWAP is at the bottom, at 121 months. Blue bars represent the 20th century while red bars represent the 21st century. The models are ordered according to their rank (see Table 5.3), with MIROC5 and NorESM1-ME each as the top and the bottom rank, respectively.

Table 5.3 *Number of prolonged no-wet period of different lengths in the 20th Century (1900-2009) and in the 21st Century (2010-2099). Model is ordered according to its rank.*

Models	Model ranking	At least 5 years (60 months) in a row		At least 4 years (48 months) in a row		At least 3 years (36 months) in a row		Longest dry period (in months)*	
		20th	21th	20th	21th	20th	21th	20th	21st
AWAP (Obs)		1	-	1	-	2	-	121	-
MIROC5	1	0	0	1	1	3	1	57	60
CMCC-CMS	2	0	1	0	3	2	5	43	68
GFDL-CM3	3	0	0	2	1	4	4	58	59
MPI-ESM-MR	4	1	2	2	2	2	3	62	62
MRI-CGCM3	5	0	0	2	0	4	1	55	41
bcc-csm1-1	6	0	1	0	1	1	2	43	61
IPSL-CM5A-MR	7	1	1	1	3	4	5	74	95
MPI-ESM-LR	8	2	0	2	3	5	6	71	55
CMCC-CM	9	1	0	2	0	7	1	60	40
HadGEM2-ES	10	0	0	0	1	4	1	45	55
MRI-ESM1	11	0	0	0	0	2	3	44	79
IPSL-CM5A-LR	12	0	1	0	3	3	8	48	79
HadGEM2-CC	13	0	1	0	3	4	7	44	62
BNU-ESM	14	0	0	0	0	3	4	45	45
MIROC-ESM	15	1	0	2	0	4	1	66	42
IPSL-CM5B-LR	16	0	2	0	3	2	7	48	66
inmcm4	17	1	0	2	1	4	1	60	48
CanESM2	18	0	0	1	0	4	0	57	30
GFDL-ESM2M	19	2	2	3	2	5	11	64	84
GISS-E2-H	20	0	0	0	0	4	7	40	44
ACCESS1-0	21	1	0	1	0	1	1	60	43
ACCESS1-3	22	0	1	1	2	4	7	50	74
FGOALS-s2	23	0	0	0	0	3	0	46	29

CMCC-CESM	24	1	0	2	0	4	1	78	41
GISS-E2-R	25	0	0	0	0	0	3	34	45
CNRM-CM5	26	0	0	1	0	1	1	50	44
GFDL-ESM2G	27	0	0	0	0	2	0	47	35
CCSM4	28	0	1	1	1	2	1	50	49
CESM1-CAM5	29	1	0	2	0	6	1	62	35
NorESM1-ME	30	0	1	0	0	5	1	58	45
CESM1-BGC	31	0	0	2	1	5	2	51	54
NorESM1-M	32	0	0	1	0	3	2	57	37
Multi-models mode		**0**	**0**	**0**	**0**	**4**	**1**	**57**	**45**
Multi-models average		**0.4**	**0.4**	**1.0**	**1.0**	**3.3**	**3.1**	**54.0**	**53.3**

Overall, the multi-model ensemble reproduces the rainfall observed mean and interannual variability of each of the 12 months very well (not shown here). However, at an individual level, some models perform poorly. Based on the six matrices applied here, MIROC5 is in the top rank while the NorESM1-M performs the least well (see Table 5.3).

The longest period of no-wet months in each century in the models is far shorter than that seen during the Millennium drought (Figure 5.4). It must be noted that the 121 months shown as observed differs from the value in Timbal (2010) due to a different data set being used. With the new dataset there is now 1 wet month in those 15 years. That said, the 121 months is far longer than any no-wet spell simulated by these models. The longest modelled event is 78 months (shown by the CMCC-CESM model), whereas the multi-model average of longest events is 54 months. Noteworthy is that most models' longest period in each century is actually longer than the second longest observed event happening in 1942-1946, roughly at the end of the World War II drought. Figure 5.4 also indicates no clear association between the model's longest event and model's rank.

Table 5.3 shows the number of events when no wet month occurs for various lengths of time. The multi-model average suggests that the frequency of occurrence through the 21st century is projected to be similar to that in the 20th century. For example, the modelled frequencies of the 21st century events that have duration of at least 5 and 4 years will be around 0.4 times and 1.0 times in 90 years respectively - which are similar frequencies to those modelled for the 20th century.

Conclusions and future perspectives

The analysis of the impact of the tripole on SEA rainfall is being taken further by investigating the dual role of tropical warming and STR changes to try to better explain model rainfall projection uncertainties. The relationship between SEA rainfall and Tripole, which has been observed to vary markedly on decadal timescales, appears stable in response to external anthropogenic forcings. An unexpected result was a change in sign in the association between the Tripole and SEA rainfall in the future as compared to the last 30 years, with declines in SEA

rainfall while the Tripole was trending upward. It was found that six models had a spurious upward jump at the transition between historical forcing and RCP8.5 at 2005, from which the models then simulate a steady downward trend in the Tripole which likely colours all other associations. Further analysis will likely focus on models that capture the transition from the 20th century to the 21st century correctly. Combining these results with those from the STR analysis of the previous year will also form part of the work in the coming year.

The observed 121 months with no occurrence of a wet month is far longer than any no-wet month spell simulated by the 32 CMIP5 models examined. Most models only show a spell of less than 60 months. However, half of the models indicate that similar spells may occur in the future. This warrants further analysis to see if the future spells can be associated with large-scale factors that drive the SEA's rainfall. Since the rainfall contribution to SEA's water resources varies during the cool and warm season, a similar dry spell analysis focussing on these cool and warm seasons may also be warranted.

A new small component of the project next year will aim to provide updated monitoring of SEA rainfall anomalies over the last 20 and 30 years and the implications for defining a new baseline for water managers.

PROJECT 6: CONVECTION-RESOLVING DYNAMICAL DOWNSCALING

Marie Ekström, CSIRO Land and Water

Key Findings

- Model simulations using the selected 6 WRF configurations were completed for all case study periods. An evaluation of daily rainfall patterns in the fine resolution domain against observed gridded rainfall data showed a somewhat better performance (as judged by spatial skill metrics) by simulations using microphysics scheme WDM6 in combination with the planetary boundary layer scheme MYNN.
- The results are promising, but the fine resolution set-up is resource intensive, implying that with limited computing resources, important choices are required with regard to simulation period and extent of spatial domain. For the final year of the project, a multi-year example is scheduled to investigate if very fine resolution convective permitting simulations are computationally justified from a water resource perspective.

Background

Within the Victorian Climate Initiative (VicCI), we are interested in understanding future impacts on runoff, as changes in runoff are directly relevant to management of water supply in the state of Victoria. Simulations of future climate are generated by global climate models (GCMs) that typically operate on scales of 100-250 km. This scale is considered much too coarse for most hydrological applications (*Fowler et al.*, 2007); hence there is a need to translate the climate change signal in the GCM output to a finer resolved regional signal. Numerous methods exist that attempt to bridge this scale-gap and they are all referred to as 'downscaling' methods.

In Project 6, we are assessing the value of fine grid-scale resolution dynamical downscaling for the purpose of downscaling rainfall to provide input to hydrological impact models. The term 'dynamical downscaling' denotes methods that use a numerical model to simulate the dynamical response at a finer resolution than the GCM (*Laprise*, 2008). There are several different approaches to dynamical downscaling; the most common is the use of a Limited Area Model (LAM), which is given input from a 'host' GCM along its lateral and lower model domain boundaries.

Output from dynamical downscaling is attractive to users of downscaled data, as it gives a dynamical response to a wide range of variables for a defined spatial and temporal domain. There are however a number of drawbacks with the method, such as their heavy usage of computation and data storage resources. This means that dynamical downscaling is usually run only for a selection of host GCMs and emission scenarios, which limits their ability to represent uncertainty in these components. Further, the models themselves are not perfect so will contain a model-bias relative to the observed real climate (*Foley*, 2010).

In Project 6, we are interested in quantifying the value of dynamical downscaling conducted on a fine resolution (10-12 km) versus operating the LAM at a very fine resolution (<3 km). These resolutions relate to the spatial scales where a dynamical model is able to resolve convective motions in the atmosphere (<3 km) and the finest resolution whereby it is advisable to use parameterised convection (>10 km). Operating the model at the finer scale is much more expensive in computing terms, hence there needs to be good justification for conducting

downscaling at very fine resolutions. This is especially true in a climate change context as downscaling outputs are typically of the order of multiple decades. The motivation to use fine resolution convection-resolving models for downscaling across Victoria is based on reported improved skill by these types of experiments to represent the spatial and temporal characteristics of rainfall events (*Kendon et al.*, 2012); a characteristic that could improve projections of future runoff.

The potential added value of using very fine resolution downscaling across Victoria is assessed through a hind-cast study, where a LAM is configured to produce output at the two scales of interest using input data from a re-analysis data set (based on observations) rather than output from a GCM. The use of re-analysis data as input means that it is possible to evaluate the skill of the LAM against historical observed data. This study will provide guidance on whether output from fine resolution simulations leads to significantly different (and improved) runoff projections relative to somewhat less computationally expensive model resolutions.

In year one of VicCI, model configurations and experiments were designed to identify an application-appropriate configuration of WRF to be used for a multi-year experiment in the final year of VicCI. Initially, 8 different configurations were chosen based on peer-review literature, WRF model documentation and limited testing of the model itself.

The WRF model is highly configurable and for this reason it is necessary to test the suitability of different application-relevant physics options. Of particular interest were complex microphysics (mp) schemes (generates the grid-resolved rainfall) and the proposed ensemble included four of the more complex micro physics (mp) schemes: the WRF double moment 6-class scheme (WDM6) (*Lim and Hong*, 2010), the Thompson scheme (*Thompson et al.*, 2008), the Milbrandt scheme (*Milbrandt and Yau*, 2005), the NSSL scheme (*Mansell et al.*, 2010). These mp schemes were used in combination with two different planetary boundary layer schemes (which together with the surface physics scheme governs the mixing of surface fluxes into the boundary layer): the pbl scheme Mellor-Yamada Nakanishi and Niino Level 2.5 (MYNN) (*Nakanishi and Niino*, 2006) and Yonsei University (YSU) (*Hong et al.*, 2006).

In discussion with VicCI partners in DELWP and Bureau of Meteorology, a case study domain was selected, taking into consideration guidance on areas most relevant from a water supply perspective as well as overlap with regions covered by radar products (see Figure 6.1). The case study periods were also identified through discussions with VicCI partners but also through visual inspection of daily rainfall maps and synoptic charts for the 2010-2011 period and a consideration of flood events as noted in the Victorian Government review of the 2010-11 Flood Warnings and Response (*Comrie*, 2011). The resultant time periods were 8th to 21st of August 2010, 6th to 19st October 2010 and 31th January to 13th of February 2011. The two week periods represente a cold season (April to October), shoulder season and warm season (November to March) respectively.

The motivation and selection of model physics options as well as case studies for project 6 are documented in detail in the publically available CSIRO Land and Water report (*Ekstrom*, 2014).

Objectives

1. Finalise ensemble selection of model configurations; address cause for potential spurious rainfall pattern in test runs conducted in year 1 (Activity 1 and 2); and
2. Assessing skill in simulation of daily rainfall by the selected physics configurations (Activity 3).

Activity 1 and 2: 'Analyse output from WRF' and 'Investigate cause for spurious patterns in the high resolution inner most domain'

In the documentation for model physics selection for Project 6 (*Ekstrom*, 2014), it was noted that the innermost fine resolution modelling domain (2km grid cell resolution) showed striation in rainfall output that could imply strong influence of noise. These results appeared in daily rainfall patterns of Case study 1 (8th to 21st August 2010), and it was suggested that simulations of Case study 2 and 3 were not completed until some model modifications were implemented to reduce the potential noise influence.

Since model runs were completed and analysis conducted, the US National Centre for Atmospheric Research (NCAR) put out two model revisions since version 3.5, which was used for Project 6 simulations. In April 2014, version 3.6 was released, soon followed by version 3.6.1 in August 2014. The latter was used for year two WRF simulations in VicCI. In addition to using a revised model version, three modifications were made to WRF in order to minimise potential for growth of noise in simulations and to make the model more suitable to regional climate change experiments. These were:

- With the model upgrade to v3.6, code deficiencies associated with the diffusion scheme were addressed, which allowed the selection of a more complex treatment of diffusion terms ('diff_op't set to 2 instead of 1). 'diff_opt=2' was the preferred option in v3.5 runs, but proved unstable over complex terrain causing simulations to terminate before completion. Hence, was replaced with a less complex option (diff_opt=1). With WRF version 3.6/3.6.1 installed in April/August 2014, 'diff_opt=2' proved stable and was used for subsequent simulations.
- The switch in setting can have large impacts on simulations in complex terrain, as the simpler approach (Option 1) tells WRF to conduct horizontal diffusion of mixing terms along model levels. In complex terrain, this setting cause horizontal diffusion to occur up or down sloped terrain (thus mixing vertically rather than horizontally). Option 2 enables horizontal diffusion to take place in 'physical space', using a vertical correction that involves more grid points than that used by Option 1.
- Raising the model ceiling from 50mb to 10mb. This means that the simulated model domain extends into the stratosphere, including the maximum ozone concentration level. Raising the ceiling means that more fields are used from ERA interim giving a fuller representation of the atmosphere (highest input field from ERA interim is 1 mb). This modification is not crucial for a 2 week simulation using ERA interim as lateral and lower boundary input, but is implemented for improved simulations of regional climate in a climate change context.
- With increase of model height, an increase in model levels from 40 to 51 was implemented. 51 levels being the number of levels used by WRF in a typical regional climate case.

Activity 3: Complete case studies as informed by Activity 1 and 2.

In year two, selected physics configurations are assessed using three two week case studies for a simulation window located within the state of Victoria. We note that when upgrading the model version to 3.6.1, the mp scheme NSSL failed hence leaving an ensemble of 6 members. As described in the background section, the spatial domain was identified in consultation with stakeholders and research partners, bearing in mind criteria for selecting robust model simulation domains and limitations imposed by computing resources (storage and time). The

chosen structure is a nested configuration (model domains of 50, 10 and 2 km respectively) with the innermost grid focusing on a region about 450 by 600 km stretching from just east of the Great Dividing Range towards east of (but not including) the Grampians national park. In a north-to-south direction, the innermost domain encompass' the southern coastline and the State boundary towards New South Wales (Figure 6.1). On this Figure, the differences between red and black liens are the buffer zones which comprised about 10 grid points in all cases.

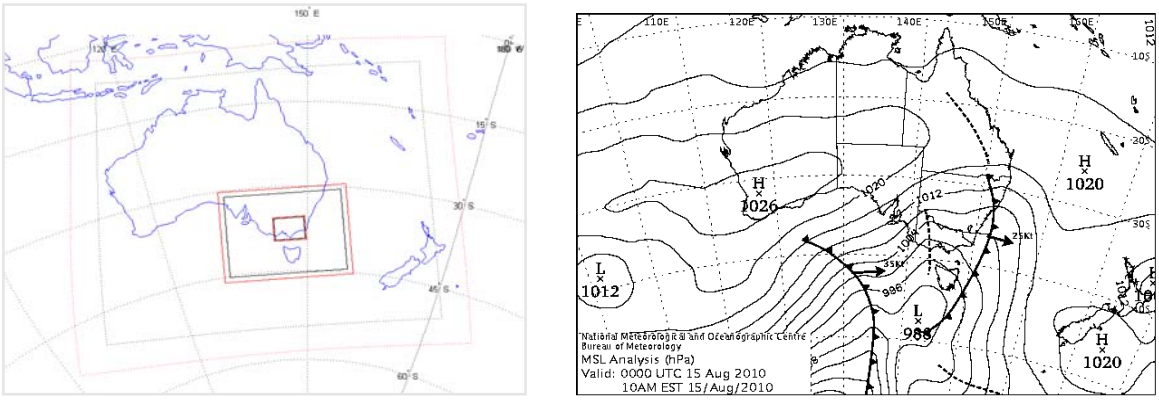

Figure 6.1: Spatial extent of the three model domains D01, D02 and D0, in decreasing size (left panel). The red lines denote the outer boundaries and the black lines the model domains (excluding the relaxation zone where information from bordering nests is blended). Mean sea level pressure analysis (00UTC) from the 15th of August 2010 (C1 case) (right panel: source the Australian Bureau of Meteorology online analysis chart archive).

The three case study periods capture a cold season period (8th to 21st of August 2010, C1), a shoulder season period (6th to 19th of October 2010, C2), and a warm season period (31st January to 13th February 2011, C3), each including several rainfall events (Figure 6.1 illustrating the passage of rain bearing cold fronts across Victoria on the 15th of August 2010).

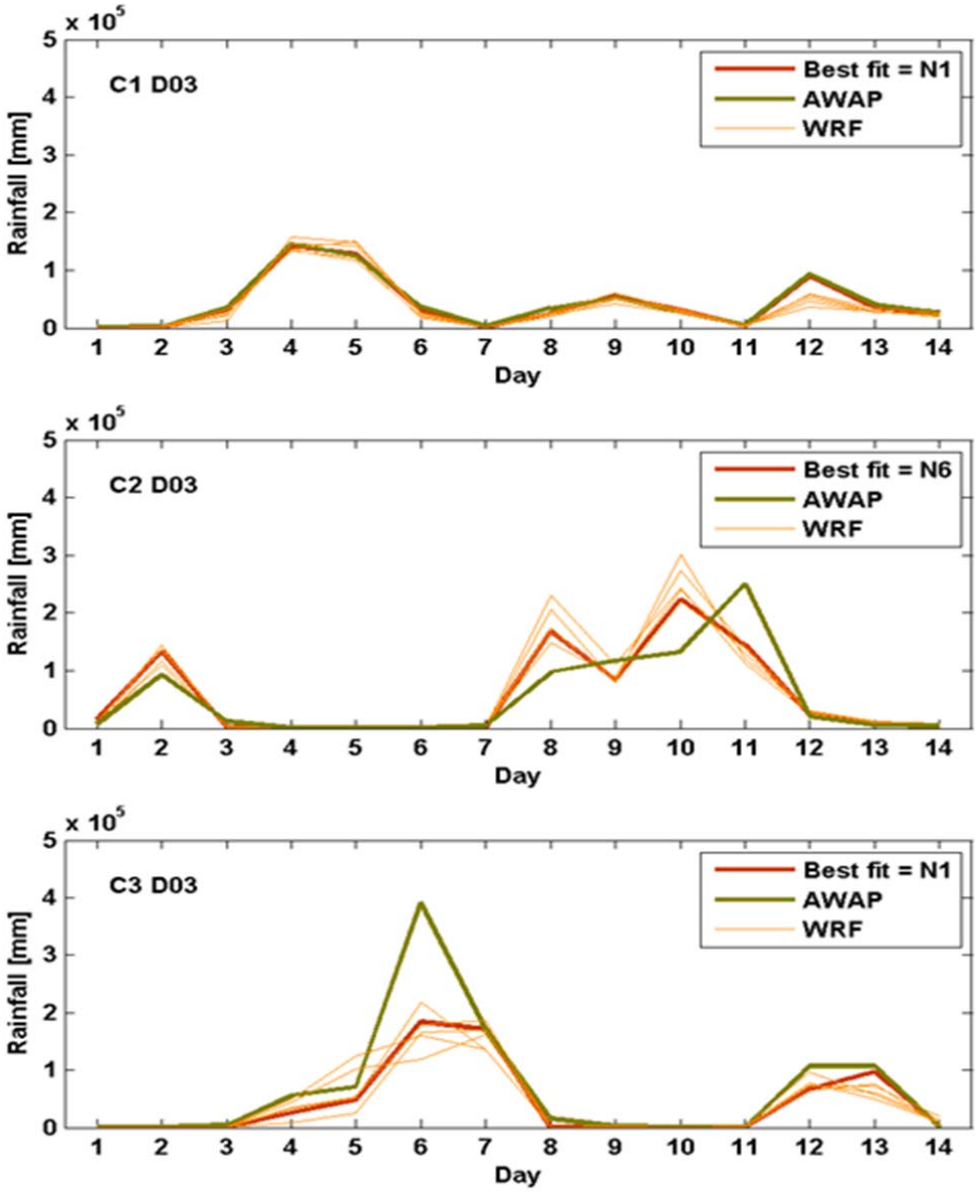

Figure 6.2: Rainfall totals (mm/day, note the 10^5 multiplier) within domain D03 for AWAP (green) and WRF simulations (orange). The best fit ensemble member (using mean absolute error, as calculated between observed and simulated data) is shown in red and identified in top right legend. The panels show the cold season case (C1, top), the shoulder season case (C2, middle) and the warm season case (C3, bottom. NB: N_i is the ensemble member with temporal evolution most similar to AWAP (see text for details) (taken from Ekström, 2015).

Focusing on skill in the inner domain (2 km), the simulated daily rainfall fields are assessed against observed gridded rainfall data from the Australian Water Availability Project (AWAP; (*Jones et al.*, 2009), see Figure 6.2 for daily totals relative to AWAP for the three case study periods and Figure 6.3 for example of simulation of daily rainfall for the 11th of August 2010. Analysis focuses on metrics quantifying spatial characteristics rather than skill on grid point level, such as variography (*Lepioufle et al.*, 2012) and the Fractions Skill Score (*Mittermaier and Roberts*, 2010; *Roberts*, 2008) a spatial matching statistics (for a given percentile). The variography also focuses on spatial detail rather than point-to-point skill. In the former,

parameters of the experimental semi-variogram can be used to describe the dissimilarity between data points as a function of distance, and in the latter, skill is assessed across a predefined 'neighbourhood' or window rather than for co-located grid points.

All configurations showed skilful estimation of rainfall across the study region with some differences in terms of spatial configuration (spatial variance and positioning of the event) and daily grid cell magnitudes. Considering all metrics used, one configuration was selected as producing rainfall fields with spatial and temporal characteristics somewhat more 'similar' to observed data compared to other configurations, viz. the configuration using mp scheme WDM6 in combination with the PBL scheme MYNN. It is worth noting that it is difficult to pinpoint why a particular configuration perform better: humidity, heat and velocity variables on different pressure levels were investigated but no clear explanation stood out. To say something with statistical significance would require a larger sample which is beyond the limited time frame of the project. The primary focus is the scale difference and this is being investigated by doing longer run (5 years), from which reasonable statistics should emerge. This configuration will be used for the second WRF experiment intended for the third year of VicCI, whereby a multi-year simulation using one configuration will be used to assess if very fine resolution convective permitting simulations are computationally justified from a water resource perspective.

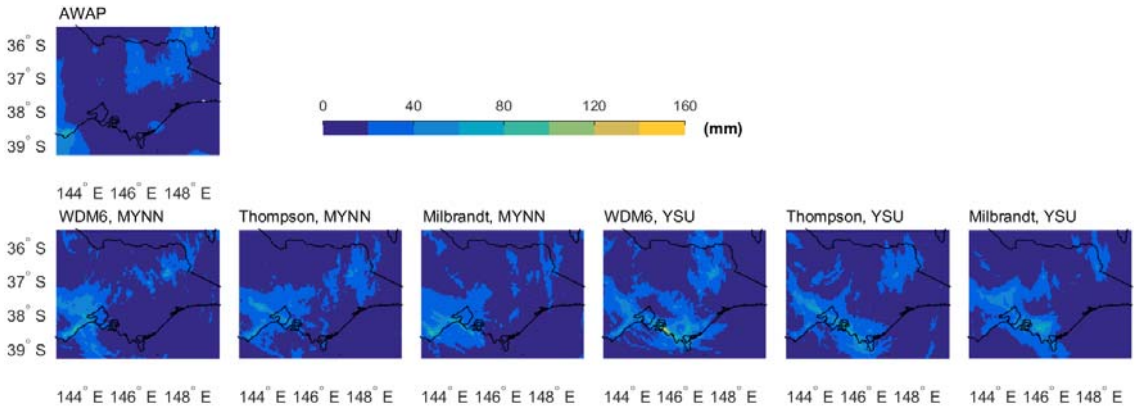

Figure 6.3: Observed (AWAP, top panel) and simulated (lower panel) rainfall fields for the 11th of August 2010 day 4 in the cold season case study (C1). Figure titles note microphysics scheme and planetary boundary layer scheme.

Conclusions and future perspectives

In Project 6 the relative value of very fine resolution convective-resolving downscaling versus fine resolution downscaling with parameterised convection is assessed. This work is expected to lead to the provision of improved regional rainfall simulations and hence runoff projections for Victoria.

Suspected spurious simulated rainfall patterns identified in year one were addressed in part by model upgrade but also through some modification of model dynamics and model structure settings. With noted modifications in place, case study experiments were initiated. For consistency, case study one was re-run with revised model settings.

Model ensemble results were evaluated with focus on the innermost domain with a view to choose an application-appropriate model for a multi-year simulation in year three of VicCI. Using mainly measures of spatial skill, an assessment suggested that the model configuration with strongest similarity to observed characteristics in terms of spatial variability and spatial

dependence was WDM6 MYNN. In year three, the multi-year experiment will be conducted and followed by an analysis of output of the 2 and 10 km fields to assess whether there are quantifiable differences in rainfall simulations that are of significant importance when downscaling for the purpose of water resource impact and adaptation work.

PROJECT 7: IDENTIFICATION OF IMPROVED METHODOLOGIES FOR WATER AVAILABILITY PROJECTIONS

Bertrand Timbal[1], Nick Potter[2], Jin Teng[2], Sonya Fiddes[1, 3]
[1]: R&D Branch, Bureau of Meteorology

[2]: CSIRO Land and Water

[3]: The University of Melbourne

Key Findings

- A proof-of-concept of the ability to produce values of catchment-scale monthly streamflow from rainfall and temperature fields was demonstrated in the first year of the program. That simple method was extensively tested across a diverse set of catchments (in terms of size, elevation, mean streamflow, mean runoff). The method was updated with the inclusion of ten year antecedent rainfall which a small improvement consistent across almost all catchments. The reconstruction was able to capture the long-term trends and the depth of the Millennium Drought well, something which has proven difficult to achieve with many hydrological models. Having now demonstrated the performance of the simple method across a diverse set of catchments, we are now confident that the streamflow projections delivered with this approach will be meaningful. Hence it was decided to use this combination when applied to downscaled GCM outputs. Two variations of the linear reconstruction of streamflows were applied to the 22 available downscaled CMIP5 GCMs.
- The transfer of the above statistical relationship to data from climate models was challenged by climate model biases even when these models are statistically downscaled (i.e. modelled historical rainfall does not typically match observed values). A number of calibration techniques were applied and the most successful used. Projections for 27 catchments across Victoria have been generated using the downscaling of 22 GCMs from the CMIP5 database and using two emission pathways (RCP 8.5 and RCP 4.5). In all cases two sets of streamflow projections were generated with and without temperature. The influence of temperature appeared to be very small during the validation phase, furthermore future projections show there is very little difference in these two sets of projections despite the strong projected warming in the 21st century.
- As part of the validation of the simple approach across Victorian selected catchments, a further analysis of the drivers of the declining trend in streamflow from 1977-2012 at 27 catchments across the State was conducted. The response of streamflow across the State is strongly related to the mean runoff rather than to the pattern of rainfall reduction. The elasticity term varied from catchment to catchment. In terms of large-scale climate forcings, strong correlations were found during the cool season with the sub-tropical ridge intensity and, to a lesser extent, with its position. Tropical modes of variability are important in catchments other than those on the southern flank of the Great Dividing Range; however, they do not explain the streamflow reduction during the Millennium Drought. Instead they continue to relate well to high and low streamflow years (albeit relative to lower mean streamflows) since the mid-1990s.
- Bias correcting dynamically downscaled rainfall improves bias considerably, but the non-stationarity of bias remains an issue, and could result in over prediction of rainfall for projections into a future drier climate. Consistent with other studies, bias from hydrological models is much smaller than bias from downscaling.

- Downscaling can introduce bias into rainfall estimates in two ways, namely the bias inherent in GCM data, and also bias introduced from the scale mismatch between GCM and point or gridded rainfall data. An experiment was devised to isolate the magnitude of this scaling effect in relation to the overall bias by aggregating observed (SILO) rainfall data to GCM scale, and then applying empirical scaling to the aggregated data. The results showed that the scale effect by itself produces little bias (with the largest relative biases in SON rainfall and the number of dry days) and this suggests that most of the error from empirical downscaling comes from the GCM itself rather than the downscaling method.
- Observed periods of low and high rainfall over the last 25 years do not match between the NCEP/NCAR reanalysis data and SILO observations. As such, it is difficult at present from this study to draw firm conclusions on choice of downscaling methods for Victorian hydroclimate projections. Ideally, the experiments should be repeated with actual large-scale data that match the observed climatic variability, rather than the NNR reanalysis data.

Background

The aim of this project is to provide information about model behaviour and methodological choices that can improve the reliability and usefulness of runoff projections for mid- to long-term future time horizons (2030 and 2090), which are needed for the next round of strategic planning for urban water supplies in 2016. Two research activities were planned for this year to explore the different aspects of modelling techniques.

Objectives

1. Apply the simple methods previously derived to relate gridded rainfall to streamflow across Victorian catchments to data outputs from climate model simulations and produce streamflow projections.
2. Compare bias-correction methodologies using available climate change data sets in order to investigate the effect of bias correction on hydro-climate projections, and describe their strengths and weaknesses in the context of VicCI.

Activity 1: Future streamflow projections reconstructed using rainfall and temperature

Introduction

The rationale, method and catchments used in this study were reported in last year's VicCI Annual Report (Murphy et al. 2014). Here we report on further work: 1) improvement to the method and additional insight gained by analysing the results and 2) the application of the method to downscaled climate models. The topography and exposure of each catchment was found to influence the relationship between streamflow, runoff and rainfall. Figure 7.1 shows the catchments considered in this study.

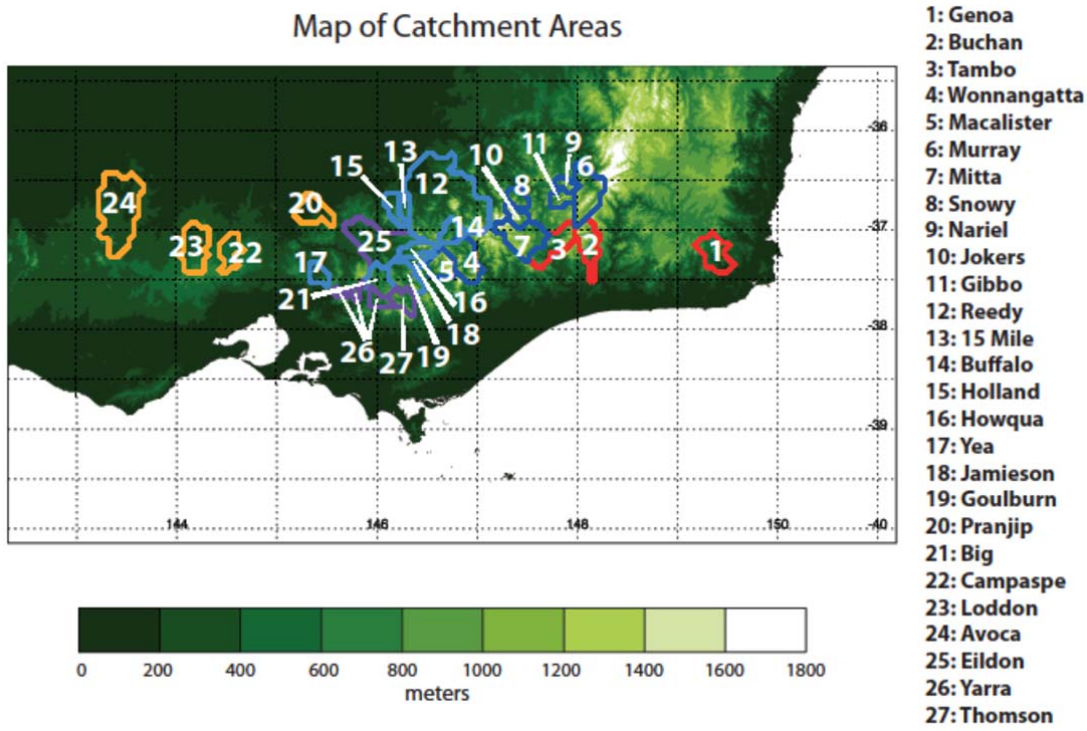

Figure 7.1: Topographical map of the catchment boundaries. Red boundaries signify the east subregion, the alps are shown in dark blue, the western slopes light blue, the far west in yellow and the Melbourne water catchments previously analysed in purple (taken from Figure 1 in Fiddes and Timbal, 2015).

Empirical computation for future streamflow

The empirical computation developed in Timbal et al. (2015) and updated in (Fiddes and Timbal 2015) was further tested this year, and found to be robust. It is a simple approach which only requires 30 years of streamflow observations in order to be developed for any catchment within Australia. The version including all timescales from the current month to the preceding 10 years was chosen for use with output from climate models:

$$R2=a+bx1+cx2+dx3+ex4+fx5$$

In this empirical computation of the monthly streamflow (R2), the following quantities are used:

$x1$ = current month's rainfall

$x2$ = previous month's rainfall

$x3$ = current month's temperature

$x4$ = previous 12 month's total rainfall

$x5$ = previous 120 month's total rainfall

Although temperature was not found to influence the results in the current climate greatly, it was believed that this should be included under potentially warmer climates of the future. Comparison will be made of versions of the statistical model both including and removing the temperature component.

The development of the empirical computation of streamflow for use with GCM outputs required an extra calibration step to remove the biases present in each climate model (in simulating historical rainfall) even following on from the statistical downscaling of the climate model outputs.

For the rainfall data, correction of both the monthly mean and the variance was needed. This was done as per the formulae below, where P = monthly precipitation, M = monthly mean precipitation, σ = the standard deviation. Subscript c = the calibrated precipitation, 1 being the first stage, m = uncorrected model data, a = AWAP data.

(1) $$P_{c_1} = P_m \times \frac{M_a}{M_m}$$

(2) $$P_{c_2} = \left[P_{c_1} - M_{c_1}\right] \times \frac{\sigma_a}{\sigma_m} + M_{c_1}$$

This method initially corrects the monthly mean across the annual cycle by multiplying the model precipitation timeseries by the ratio of the monthly AWAP/model mean (1). It then subtracts the new annual cycle from the new timeseries and multiplies the anomalies by the ratio of the AWAP/model standard deviation in order to correct the variance, and finally adds the annual cycle back in (2). This was performed for each catchment and model individually, for each month of the year.

By doing this the variance went from being only 35% of that of the AWAP rainfall for the same time period to 105%, and the mean from 81% to 100%. Furthermore, the shape of the annual cycle now matched the AWAP annual cycle.

The calibration for the model temperature was simpler as the mean was already being reproduced well (100%), hence only the variance needed attention. Here, T = maximum temperature and M = monthly mean maximum temperature. The method used was essentially the same as correcting the precipitation variance, as seen by (3), where the anomalies were corrected without causing much change to the mean. After this correction, the temperature variance went from 128% to 105%, and the mean remained the same.

(3) $$T_c = \left[T_m - M_m\right] \times \frac{\sigma_a}{\sigma_m} + M_m$$

Rainfall and maximum temperature from each climate model were downscaled using the statistical BOMSDM method, and then calibrated using the above equations and then R2 was calculated. Relevant data were available from 22 GCMs in the CMIP5 suite. Once the calibration is applied, different statistical models exist for each climate model. In addition, two empirical computations of streamflow were considered, one with and one without the monthly temperature included. The multi-model mean streamflow reconstructed (averaged across all climate model used) using this method was now 104% of the mean streamflow reconstructed using AWAP data, and 85% of the variance (see Figure 7.2 for each individual model). The

inclusion of temperature had no effect, but, may well have an effect in future. The new, calibrated, empirical computation of streamflow also needed to be constrained to remove the possibility of negative streamflow. This new method was applied to data from 22 GCMs across 27 catchments and the raw outputs were provided to DELWP as Excel spreadsheets.

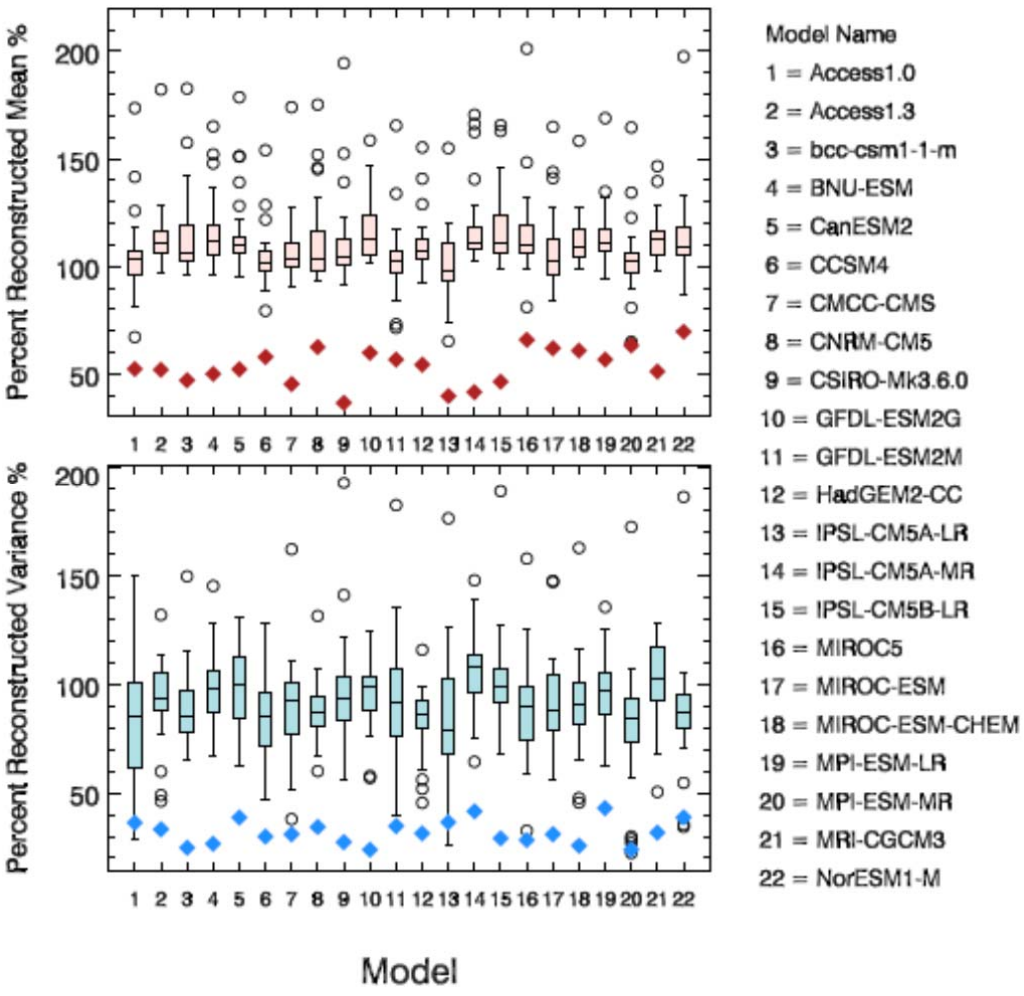

Figure 7.2 Box plots drawn from the 27 catchments of the percentage of reconstructed mean (top) and variance (bottom) catchment streamflow shown for each climate model. Boxplots indicate the 25th – 75th percentile via the box, the median is shown by the horizontal line within each box, the whiskers indicate the maximum or minimum of the data or 1.5 times the 25th or 75th percentile (whichever is smaller) and the open circles show the outliers of the data series. The filled diamonds indicate the mean percentage of reconstructed mean (red) or variance (blue) before calibration was performed. The corresponding models are listed on the right.

Analysis of observed streamflow variability

Further work was done to better understand the state-wide variability in streamflow and runoff. This analysis is being reported in Fiddes and Timbal (2015, submitted to Climate Research). Critical insight into observed variability of rainfall and streamflow across Victoria during the last 30 years is described here as per the submitted article.

Considering the Millennium Drought event (MD, 1997-2009), the annual depth of the Millennium Drought anomalies as a percentage of the 1977-2012 mean are shown in (Figure

7.3). Regional averages are provided (Table 7.1) for both the annual mean and a seasonal (cool and warm) breakdown of streamflows.

Table 7.1: *1997-2009 Millennium Drought anomalies shown as a* ***percentage*** *from the 1977-2012 mean for the annual mean, cool season (May-November for streamflow and April-October for rainfall) and warm season (December-April for streamflow and November-March for rainfall) of AWAP rainfall and observed streamflow (taken from Table 2 in Fiddes and Timbal, 2015).*

	Rainfall			*Streamflow*		
	Annual	*Cool*	*Warm*	*Annual*	*Cool*	*Warm*
East	-9.9	-8.7	-11.1	-42.0	-39.6	-49.4
Alpine	-11.9	-10.8	-14.0	-20.9	-19.3	-28.1
West Alps	-13.0	-12.3	-14.9	-34.3	-33.4	-43.2
Far West	-14.5	-16.6	-13.9	-75.6	-75.6	-77.6
Melbourne	-14.0	-13.8	-14.8	-30.7	-30.2	-33.2
Average	-12.6	-12.0	-14.1	-31.2	-30.0	-38.2

Catchments in, or in close vicinity to the GDR experienced a lesser decline in annual streamflow over this 13 year time period than those in the east and far west of Victoria with a strong correlation (R = 0.86) between the Millennium drought anomaly of streamflow and the catchment's runoff (or streamflow intensity) (Figure 7.3b). The Avoca catchment experienced the largest deficit, an 87% reduction in mean streamflow. The Mitta Mitta and Jokers Creek catchments have experienced less than a 20% deficit over the Millennium Drought whilst the majority of streamflow anomalies are significantly different to the mean at the 90% level of confidence (Figure 7.3a) as one would expect due to the widespread nature of the Millennium Drought across south-eastern Australia.

Literature has noted that generally, deficits in streamflow are typically 2-3 times greater than that experienced by rainfall in Australia (e.g. Chiew 2006).This study finds that on average, the streamflow Millennium Drought anomaly was 2.5 times greater than that of the rainfall anomaly for Victorian's catchments considered here, which is less than what was found for the MDB (CSIRO 2010). The spatial variably of this ratio across the State is large. Here, it is again highlighted that the catchments further from the Alps experienced the biggest differences between the rainfall Millennium Drought anomalies to that of the streamflow response. This elasticity can be explained in part by the characteristics of the catchment itself (i.e. a log relationship with the runoff), and the variability of rainfall to a lesser degree.

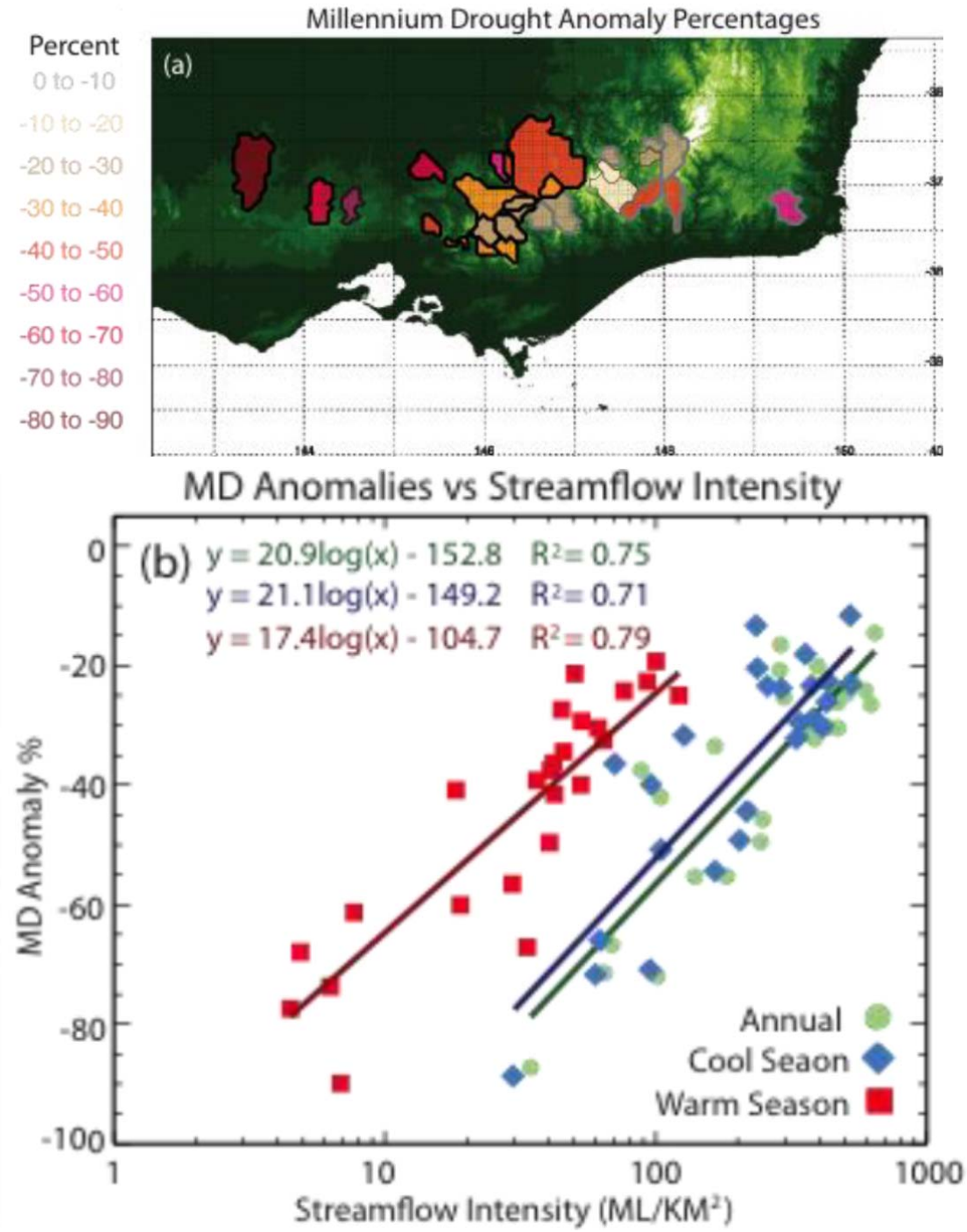

Figure 7.3:1977-2012 reduction in streamflow during the Millennium Drought (as a percentage of the 1977-2012 mean streamflow), for the mean annual observed streamflow (a). Statistical significance is shown by the catchment outlines: bold black indicates significance to the 95th percentile; bold grey indicates significance to the 90th percentile, no bold indicates non-significant trends. Additionally, the relationship of the trends (percent) across the 27 catchments to the (log transformed) runoff (mm), (b) is shown for the annual mean and the cool (May to November) and warm (December to April) seasons. The slopes of the lines of best fit and the squared correlation coefficients of these relationships are indicated.

Application to downscaled GCM data and future projections of streamflow

Future projections of streamflow were generated across Victoria for the 27 catchments and using two emission scenarios (RCP4.5 and RCP8.5). These results were provided to the DELWP to help inform water mangers about long-term risks due to on-going climate change.. These results will be analysed further in the final year of the program and compared to other approaches (past work or work under development by other research groups) to provide a perspective on this simple approach. In this year's report, only a brief summary of the results is provided.

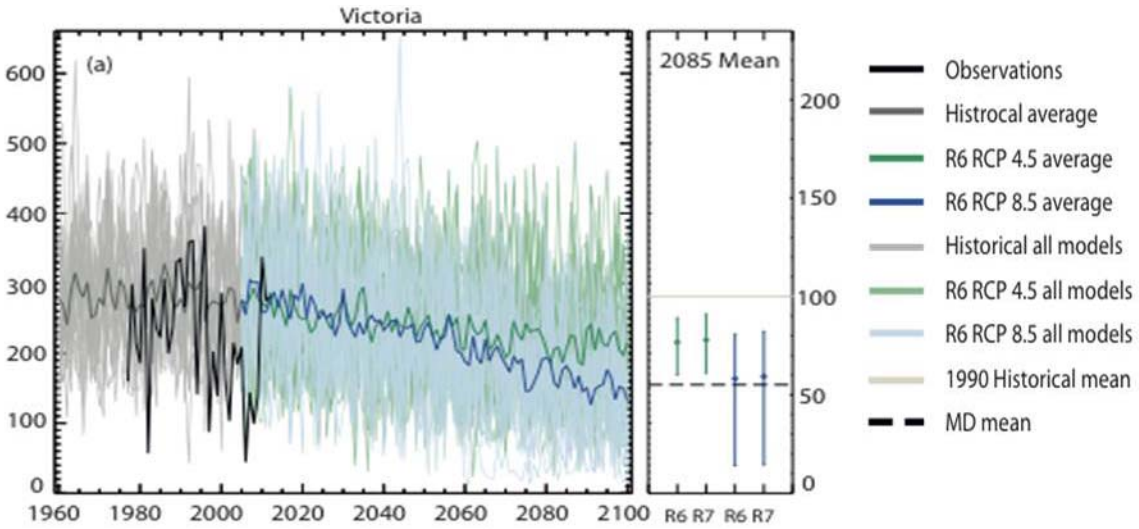

Figure 7.4: Projected inflow time series for Victoria from 1960-2100 using this model. Observed inflow is plotted in black. The model mean projections are as follows: historical 1960-2005 (grey) and 2005-2100 RCP 4.5 (green) and RCP 8.5 (blue). The lighter shades are the individual model projections. The box on the right shows the 2085 mean (2075-2100) for two versions of the statistical model for RCP 4.5 (green) and RCP 8.5 (blue), with the 1990 historical (1975-2005) mean (light grey solid line) and the observed mean of the 1997-2009 MD (black dashed line).

Results averaged across the 27 catchments studied indicate that by 2050, streamflows will be 16%-22% less than the 1986-2005 average (Figure 7.4). By 2085 this increases to 25%-43%, which for the catchments within the influence of the Great Dividing Range is equivalent to the streamflow reductions experienced during the MD. These projections are difficult to compare to those provided as part of the SEACI work (http://www.seaci.org) as spatial, temporal scales method differ. For the far west and east catchments, although the model results indicate that the 2085 inflow reductions will not be as severe as those in the MD, it is worth noting for this part of the State the empirical reconstructions are less skilful. In this study, the effect of temperature on streamflow was analysed by using reconstructions with and without maximum temperature in the statistical model. The streamflow responses to temperature appear to differ across subregions. For the catchments in the vicinity of the Alps, temperature did not seem to play a large role in the streamflow reconstructions but that is not the case in other catchments further away from the GDR. This is interesting, as during the validation of the method, no significant difference was found between reconstructions with or without temperature, indicating that the different results found here may be linked to the higher temperatures expected by the end of the century. That small and spatially variable effect of the temperature effect is rather uncertain, as future projected temperature lie outside of the past observed range (this is not the case for rainfall as future projections rarely exceed in severity the MD deficit which the statistical model were successfully tested against). A larger effect of temperature through increased PET cannot be discarded based on this study alone.

Activity 2: Bias correction and hydro-climate projections

Introduction

Hydrological impact studies typically require downscaling of future projections from the larger GCM spatial resolution (~100km × 100km) to a finer spatial resolution (~5km × 5km) in order to provide regionalised climate information (Ekström et al. 2015). Due to their finer resolution, downscaled projections are considered more usable for hydrological models that simulate processes on much finer scales than GCMs. Downscaling involves many fundamentally different approaches to achieve a finer resolved climate projection (e.g. Fowler et al. 2007; Chen et al. 2011; Ekström et al. 2015). A fundamental assumption for all statistical downscaling methods is that any derived relationships remain constant into the future. Of course, without, or even with the benefit of, additional knowledge (such as may be derived from physically based climate models), this assumption is difficult to verify (Giorgi 2008).

Last year's effort focused on (i) reviewing the application of different bias correction techniques and (ii) evaluating four bias correction methods applied to dynamically downscaled outputs from the Weather Research and Forecasting (WRF) model (Evans and McCabe 2010) and the follow on impacts on runoff for 8 Victorian catchments. Dynamical downscaling provides localised climate information using a physically based method. However, bias can be high using these methods (e.g. Wilby et al., 2000; Piani et al., 2010; Teng et al., 2015) owing to model assumptions and the fact that such methods are not explicitly calibrated to station data. However, dynamical downscaling methods may be better suited to explore the effect of changes in hydroclimatic processes than scaling or statistical methods. It is recognised that success in downscaling is dependent on the skill of GCMs in reproducing relevant climate characteristics (Ekström et al, 2015). Although a range of bias correction methods were developed, correcting bias using two climatically different time periods, in which the bias itself was different, resulted in over- and under-estimation, respectively, of the downscaled rainfall relative to observations (Teng et al., 2015).
This year we investigated strengths and weaknesses of downscaling methods focusing on 26 Victorian catchments. Also, a draft scoping study outlining methods for the delivery of runoff projections for Victoria was commenced.

Study area and data

From the available gauged streamflow data, 26 catchments were selected (Table 7.2) so that the overlapping time period of the data was the longest. SILO gridded data (Jeffrey et al., 2001) was used as observational rainfall and potential evapotranspiration data.

Table7.2: Selected streamflow gauging stations used in the study.

ID	Name	Area (km2)
401012	Murray River at Biggara	1257.3
401210	Snowy Creek at Below Granite Flat	415.7
401217	Gibbo River at Gibbo Park	389.8
405215	Howqua River at Glen Esk	374.0
221210	Genoa River at The Gorge	844.1
222206	Buchan River at Buchan	850.2
223202	Tambo River at Swifts Creek	899.3
224206	Wonnangatta River at Crooked River	1099.5
225219	Macalister River at Glencairn	570.4

401212	Nariel Creek at Upper Neriel	251.6
401216	Big River at Jokers Creek	356.8
403213A	Fifteen Mile Creek at Greta South	230.9
403222	Buffalo River at Abbeyard	415.0
404207	Holland Creek at Kelfeera	448.0
405217	Yea River at Devlins Bridge	360.6
405218	Jamieson River at Gerrang Bridge	364.2
405219	Goulburn River at Dohertys	700.2
405226	Pranjip Creek at Moorlim	749.4
405227	Big River at Jamieson	626.9
406213	Campaspe River at Redesdale	633.8
407215	Loddon River at Newstead	1028.5
408200	Avoca River at Coonooer	2677.3
MW19	GRACEBURN	26.2
MW13	MAROONDAH	102.1
MW22	O'SHANNASSY	118.9
MW29	UPPER YARRA	326.4

We use NCEP/NCAR reanalysis (NNR) data (Kalnay et al. 1996) as the 'GCM climate model' data to be downscaled. Many studies have attempted to rank or filter GCMs according to pre-defined climatic or hydrological metrics (e.g. Kirono and Kent 2011; CSIRO 2012; Grose et al. 2015; McMahon et al. 2015).

Although this is an important strand of work, particularly in order to reduce the uncertainty of hydroclimatic projections for particular geographical or climatic areas, this is not the main focus of the present study. As such, we took the NNR data to be representative of climate model data and that can also be directly compared with finer scale SILO gridded data as described above. This enables us to better identify the impacts of the downscaling methods, independent of any consideration of GCM errors.

There are five netCDF4 grid cells covering the study area (Figure 7.5). The variable prate (precipitation rate) from the NNR data set gives six-hourly average rates measured in units of kg m^{-1} s^{-1} at the times 00:00, 06:00, 12:00 and 18:00 UTC. SILO data on the other hand is daily accumulations from 09:00 local Australian time to 09:00 the next day. Since Victoria is located in time zone GMT+10 hours, we convert each value of prate from the NNR data to mm m^{-2} (commensurate with SILO) by assuming the instantaneous rate occurs over the entire six-hour period, and aggregating each UTC day. In this way, the NNR data accumulated to daily scale are only one hour out from the SILO data (two hours during daylight savings time).

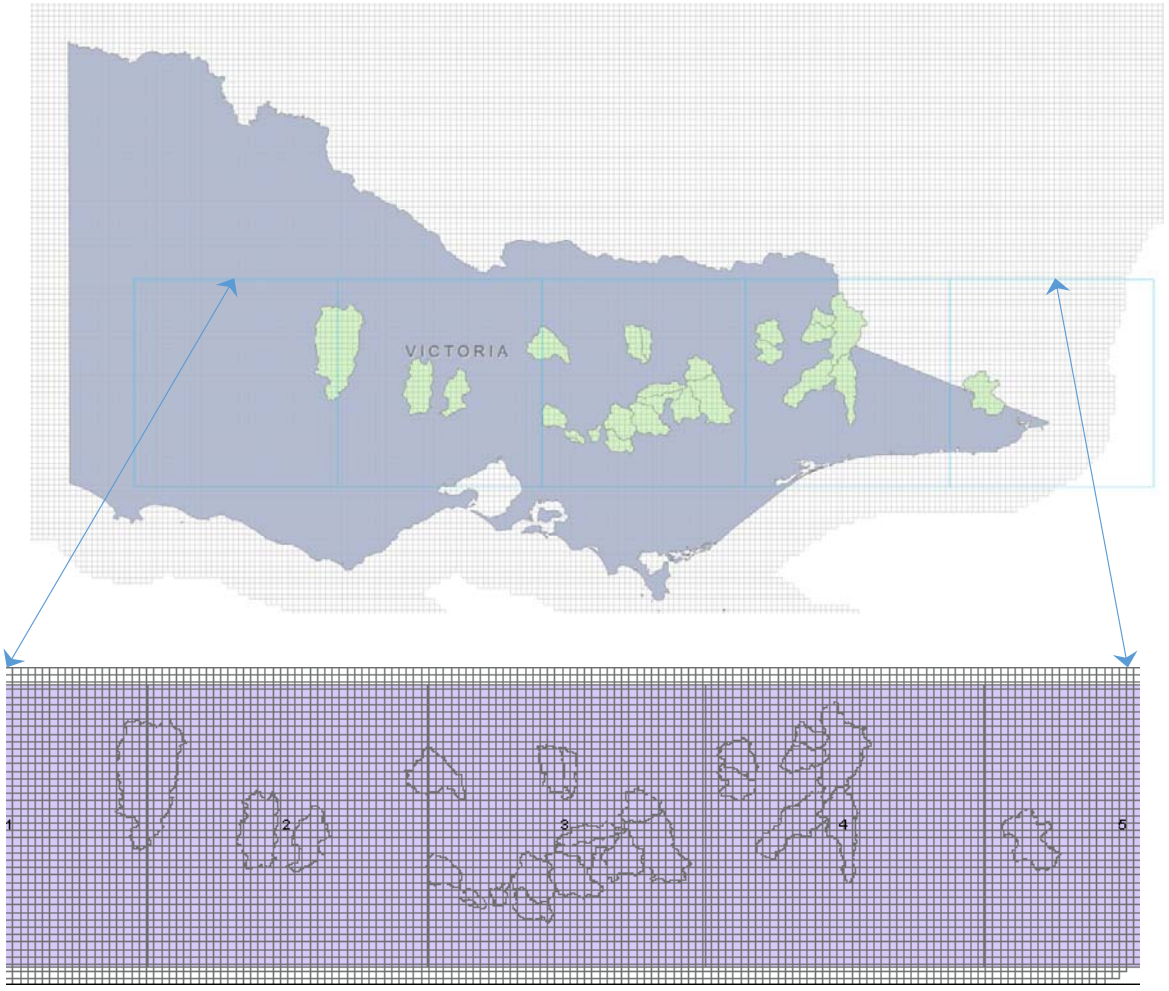

***Figure 7.5**: Location of the catchments in the study area overlaid with the netCDF4 grid cells containing NNR data (large grid) and SILO grid cells (small grid). Inset is expanded to make the smaller grid clearer.*

Method

To assess different downscaling methods, we devised seven different experiments for generating local climate input data for rainfall-runoff modelling:

1. SILO observations (baseline/control)
2. Dynamically downscaled (raw) WRF rainfall, using lateral boundary conditions from the NNR data (Teng et al. 2015).
3. Bias-corrected WRF rainfall
4. Empirically downscaled (seasonal linear scaling) reanalysis data
5. Empirically downscaled (seasonal linear scaling) SILO aggregated to GCM scale

6. Reanalysis data bias-corrected to SILO observations

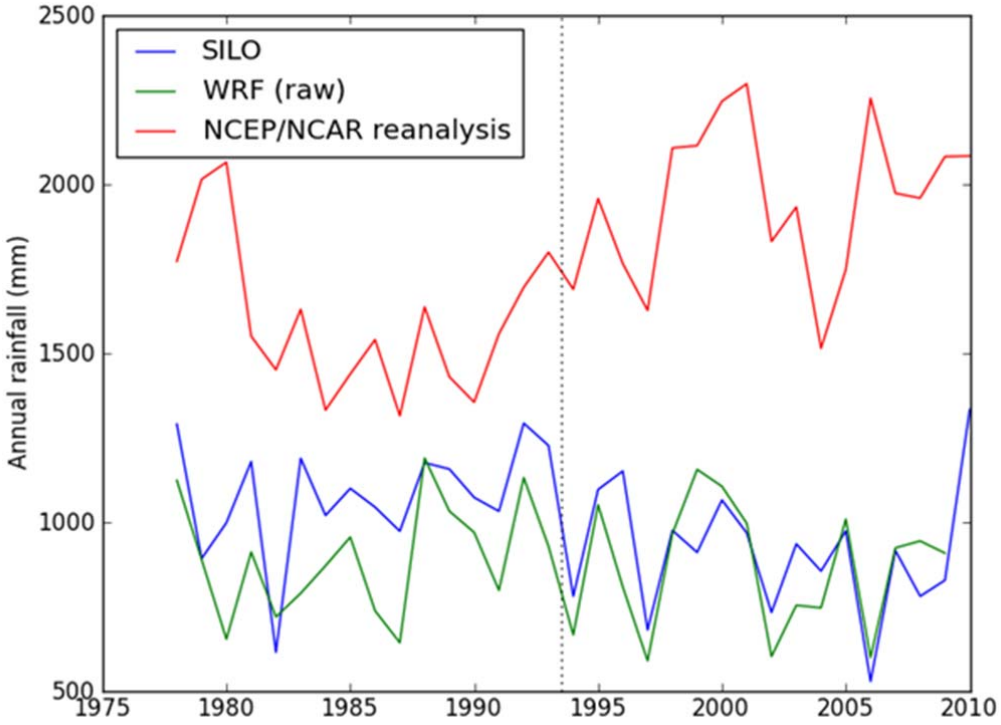

***Figure 7.6**: SILO, WRF, and NNR rainfall averaged over the study region (catchment averaged for SILO and WRF, average of five grid cells for NNR). Observations in the second ('future') period are relatively drier (reflecting the Millennium Drought), although not for the NNR data.*

The study period (1978–2009) was divided into two time periods: 1978–1993 (relatively wetter) and 1994–2009 (relatively drier). Thus the effect of bias correcting in climatically different time periods can be studied using the split sampling approach. The regionalised SILO rainfall has a severe drought corresponding to 1982, followed by relatively wet period until the start of the Millennium Drought. However, the NNR data has a significantly lower rainfall period over the entire 1980s (Figure 7.6). As such, the NNR data is actually wetter during the second time period. This is consistent with earlier analysis of the NNR data where it was shown that large-scale rainfall events (i.e. not the part computed from the convective parameterisation) trended upward across most of the South-Eastern part of Australia (Timbal et al. 2006) in contrast to observations.

Results – Rainfall

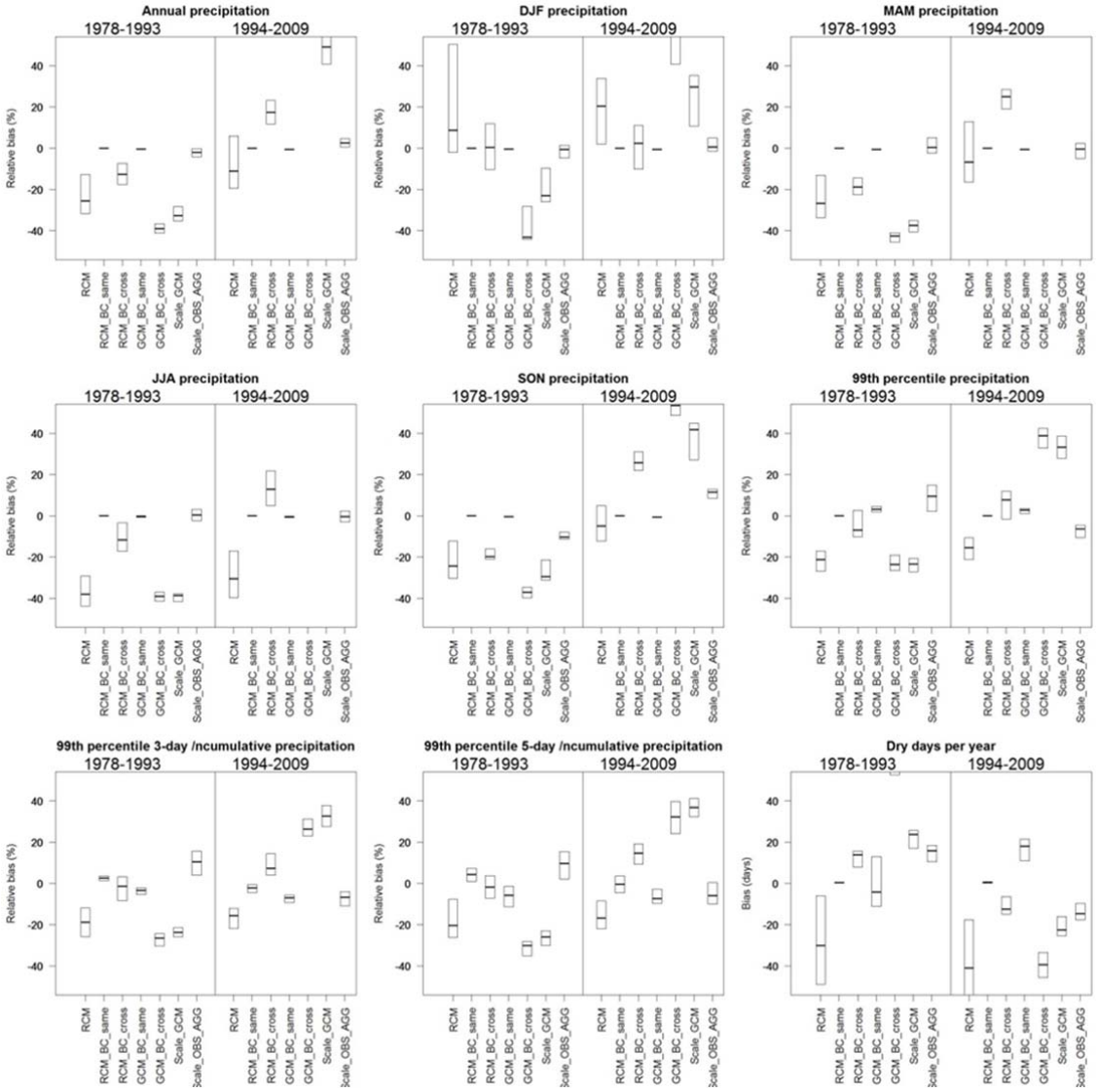

***Figure 7.7**: Performance of downscaling methods for rainfall metrics. Here the experiments are labelled as: 2 (dynamic downscaling) "RCM"; 3 (bias-corrected dynamic downscaling) "RCM_BC"; 4 (empirically scaled reanalysis) "Scale_GCM"; 5 (empirically scaled aggregated SILO) "Scale_OBS_AGG"; 6 (bias corrected reanalysis) "GCM_BC". Biases are relative to the observational baseline (experiment 1), with positive biases indicating overprediction. For the bias correction experiments, "same" and "cross" refer to the bias-correction relationship – "same" indicates that the same time period was used, whereas "cross" uses the relationship from the other time period.*

Figure 7.7 shows interquartile range of the rainfall statistics for each downscaling method and the two time periods. The raw WRF rainfall data shows a negative bias in annual rainfall, and this is also seen in Figure 7.6. However, there is a less bias in the later (drier) period. This pattern is repeated in each season except DJF, in which WRF over predicts rainfall slightly.

Again, the later period has less bias than the earlier period (in absolute terms). Large rainfall amounts and rainfall accumulations are slightly under predicted too. The number of dry days is under predicted in both time periods.

The "RCM_BC_same" and "GCM_BC_same" statistics all have zero bias for the annual and seasonal rainfall means, by construction (i.e. these are bias corrected to the observed SILO distributions in each time period). There is a slight tendency for over prediction of 99th percentile rainfall, but interestingly bias-corrected RCM slightly over-predicts 3-day and 5-day high rainfall accumulations, whereas bias-corrected GCM slightly under-predicts this. The number of dry days is generally under-predicted with bias corrected GCM, but well predicted with bias corrected RCM. Overall, these two methods work well, but require the 'future' distribution of rainfall for bias correction, which is generally not available.

Using cross-period distribution for bias correction, i.e. using the relationship between 'historical' observed and 'historical' RCM/GCM rainfall distributions to correct for biases does significantly worse. Bias-corrected RCM rainfall is under predicted during the wet period and over predicted during the dry period. This occurs annually and for all seasons except DJF, in which rainfall is on average bias free. This effect is similar for GCM rainfall bias-corrected using cross-period distributions, except amplified. The DJF season is also under/over-predicted. This effect was referred to as 'non-stationarity of bias' by Teng et al. (2015) – briefly, when bias is not a constant proportion of mean rainfall across two periods with different climatic conditions, bias correction will tend to over-correct and under-correct depending on the relative size of the bias. This is also evident in the bias for high rainfall and dry days: cross-period bias-corrected RCM and GCM high rainfall is under predicted in wet periods and over predicted in dry periods; dry days are over predicted in wet periods and under predicted in dry periods.

Out of all experiments, the empirically scaled reanalysis data (experiment 5; "Scale_GCM") performs the worst overall. Annual rainfall, as well as seasonal rainfall is significantly over-predicted during the second period and under-predicted during the first period. Similarly, high-rainfall amounts, rainfall accumulations are over-predicted in the second period, and dry days are under-predicted in the second period (and these effects are reversed for the first period). The poor performance of this experiment is presumably due to the fact that reanalysis data simulate the second period as much wetter than the first period, in contrast to the observational data. This highlights the necessity of carefully choosing the appropriate dataset in performing these experiments and indicates that using the latest available products (i.e. AWAP for observed rainfall) and ERA interim reanalyses is likely to yield to better results.

Out of all experiments, the empirically scaled aggregated observations do the best. The bias in annual precipitation is close to zero, as is the bias in all seasons, except for SON. This could be a result of a greater proportion of convective rainfall events occurring in this season, which is smoothed out by the aggregation process. High rainfall events have only a small bias too, but slightly over predicted during the first period, and under predicted during the second period. The largest relative bias is for the number of dry days, and this may indicate a significant difference between the rainfall characteristics in the two time periods.

Of course, using aggregated observational data in this way assumes that the aggregated data represents a 'perfect' simulation (at the GCM spatial scale), and is not intended to be a feasible downscaling option for future rainfall projections. Instead, this experiment shows that the scale effect, or smoothing out of climate variability over GCM grid cells, by itself has little effect on errors in downscaling, with the largest errors in SON and for the number of dry days. In reality, however, GCMs are not parameterised to capture smaller-scale climate heterogeneity that we see in observational data, and instead model the grid cell as a climatic unit. This experiment can

also be considered as providing an indication of the smallest errors possible in downscaling GCM data.

Results – Runoff

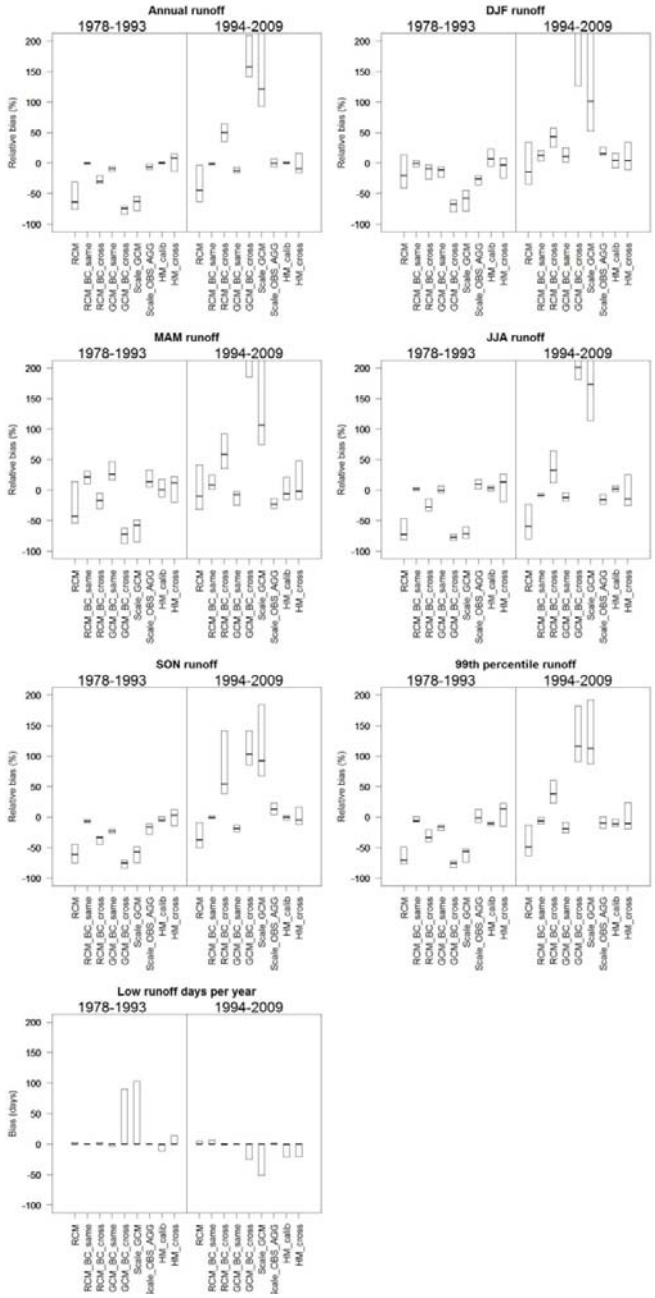

***Figure 7.8**: Performance of downscaling methods for runoff metrics. Here the experiments are labelled as in 7.6 with the addition of two additional experiments, which represent validated runoff from a hydrological model using observed data calibrated to the same time period ("HM_calib") and the other time period ("HM_cross").*

Runoff modelled from raw RCM data has a similar pattern to that observed for rainfall (see Figure 7.8). Specifically, runoff is generally under-predicted, and this bias is around twice the size of the bias in rainfall. Runoff in DJF is under-predicted, even though rainfall in DJF is over-predicted, and this is probably because rainfall in DJF contributes to a relatively small proportion of overall runoff in south-eastern Australia. These biases are relatively smaller in the second period.

For both the bias-corrected GCM and RCM rainfall using the same period for bias correction ("same"), the resulting runoff typically has a non-zero bias. This bias is relatively small, and there is no discernible seasonal pattern to this. The biases in seasonal runoff generally follow the biases in seasonal rainfall, although the errors are amplified as the rainfall biases propagate through the rainfall-runoff model. Overall, the errors in bias-corrected RCM runoff are much smaller than the errors in bias-corrected GCM runoff, and this reflects the better modelling of finer scale variability by the RCM compared to the GCM.

The runoff resulting from empirically scaled reanalysis data is heavily biased. Runoff is over-predicted in the second period (in the order of 100–200%) and under-predicted in the first period (in the order of 50–100%), and this reflects the bias in rainfall.

Runoff from the empirically scaled aggregated SILO data performs very well, with little to no bias for the runoff metrics examined. The largest errors are in DJF and MAM, and this is most likely due to the fact that out of all seasons, SON rainfall is the most biased. When this error is passed through the hydrological model, soil-moisture levels may be incorrectly modelled, which result in biased runoff during DJF and MAM. However, runoff in these seasons constitutes a relatively small proportion of annual runoff, and this means that the bias in DJF and MAM does not affect bias in annual runoff to a great extent.

To put the bias resulting from downscaling in perspective to the 'standard' bias coming from hydrological modelling, we have also included the error bars from hydrological model calibration (HM Calib) and cross-validation (HM Cross) for comparison. The errors from HM_Calib are generally very small, which reflects the relatively high performance of the chosen hydrological model (GR4J) in calibrating. The HM_Cross errors are slightly larger but still considered small for most of the runoff characteristics.

Conclusions and future perspectives

This year, two lines of investigation were undertaken with a view to developing improved methodologies for future water availability projections. This work will allow the delivery of a range of water availability projections of varying methodological complexity which will provide a robust understanding of impacts of climate change on water availability across Victoria.

A simple statistical method to describe monthly streamflow based on linear regression of rainfall and temperature was further tested. It was applied to 27 catchments across Victoria with most catchments showing satisfactory results. Application of the method to downscaled GCM data was then tested and a number of issues resolved. Overall, the results from this method indicate that whilst catchments across Victoria will respond differently to the effects of climate change, the majority of catchments are projected to see reductions of inflow similar to those experienced during the MD by the end of the century, severely limiting Victoria's water capacity if it were to rely on rainfall alone. Further assessment of the results from GCMs will be done in the upcoming year, with a view to providing confidence bounds on the projections. Comparison with other methods will be done if those results are available.

Bias correcting dynamically downscaled rainfall (with WRF) in Activity 2 reduces bias considerably, but the non-stationarity of bias effect identified by Teng et al. (2015) means that bias corrected WRF rainfall could be over-predicted when projected into a drier future climate. Empirically downscaling 'perfect' GCM results, examined by downscaling observed rainfall data aggregated to GCM scale, suggests that the scale effect (i.e. the loss of fine scale information at the larger spatial scale) by itself produces little bias, with the exception of SON rainfall and the number of dry days. This result indicates that most of the error from empirical downscaling comes from the GCM itself rather than the downscaling method.

It is clear from the results that the use of NNR reanalysis data to calculate change factors and bias-correction parameters presents a serious problem. This is due to the fact that the periods of low and high rainfall do not match between NNR and SILO (Figure 7.6). As such, it is difficult at present from this study to draw firm conclusions on choice of downscaling methods for Victorian hydroclimate projections. Ideally, the experiments should be repeated with actual GCM data that match the observed climatic variability, rather than the NNR reanalysis data.

REFERENCES

Abram, N. J., M. K. Gagan, J. Cole, W. S. Hantoro, and M. Mudelsee, 2008: Recent intensification of tropical climate variability in the Indian Ocean. *Nat. Geosci.*, **1**, 849–853, doi:10.1038/ngeo357

Annamalai, H., S. P. Xie, J. P. McCreary, and R. Murtugudde, 2005: Impact of Indian Ocean sea surface temperature on developing El Niño. *J. Climate*, **18**, 302–319, doi:10.1175/JCLI-3268.1

Arfken, G., 1985: Helmholtz's Theorem. §1.15 in *Mathematical Methods for Physicists, 3rd ed*. Orlando, FL: Academic Press, pp. 78-84

Ballard, C., N. Garland, and J. Foreman, 2014: Management of drought in the southern Murray-Darling Basin, Australia, from 1996/1997 to the present. Irrigation and Drainage, 63, 254-262

Cai, W., and T. Cowan, 2008: Evidence of impacts from rising temperature on inflows to the Murray Darling Basin. Geophysical Research Letters, 35(7)

Cai, W., P. v. Rensch, T. Cowan, and H.H. Hendon, 2011: Teleconnection pathways for ENSO and the IOD and the mechanism for impacts on Australian rainfall. *J. Climate.*, **24**, 3910-3923. doi: 10.1175/2011JCLI4129

Cai, W., W, P. van Rensch, T. Cowan, H. H. Hendon, 2012: An asymmetry in the IOD and ENSO teleconnection pathway and its impact on Australian climate. *J.Climate*, 25, 6318-6329

Chen, J., Brissette, F. P., and R. Leconte, 2011: Uncertainty of downscaling method in quantifying the impact of climate change on hydrology, J. Hydrol., 401, 190–202, doi:10.1016/j.jhydrol.2011.02.020

Chowdary, J.S., S.P. Xie, H. Tokinaga, Y.M. Okumura, H. Kubota, N. Johnson,and X.T. Zheng, 2012: Interdecadal variations in ENSO teleconnection to the Indo–western Pacific for 1870–2007. *J. Climate*, **25**, 1722–1744, doi:10.1175/JCLI-D-11-00070.1

Colman, R., L. Deschamps, M. Naughton, L. Rikus, A. Sulaiman, K. Puri, G. Roff, Z. Sun, and G. Embery, 2005: BMRC Atmospheric Model (BAM) version 3.0: Comparison with mean climatology. BMRC Research Report No. 108, Bureau of Meteorology Research Centre, 32 pp (http://www.bom.gov.au/bmrc/pubs/researchreports/researchreports.htm)

Comrie, N. 2011: Review of the 2010–11 Flood Warnings & Response Rep., 235 pp, Melbourne, Victoria, Australia

CSIRO, 2010: Climate variability and change in south-eastern Australia: A synthesis of findings from Phase 1 of the South Eastern Australian Climate Initiative (SEACI). May 2010, Canberra, Australia, 30 pp, http://www.seaci.org

CSIRO, 2012: Climate and water availability in south-eastern Australia: A synthesis of findings from Phase 2 of the South Eastern Australian Climate Initiative (SEACI), CSIRO, Australia, September 2012, 41 pp, http://www.seaci.org

CSIRO and Bureau of Meteorology 2015: Climate Change in Australia Information for Australia's Natural Resource Management Regions: Technical Report, CSIRO and Bureau of Meteorology, Australia

Dee, D.P., S.M. Uppala, A.J. Simmons, P. Berrisford, P. Poli, S. Kobayashi, U. Andrae, M.A. Balmaseda, G. Balsamo, P. Bauer et al, 2011: The ERA-Interim reanalysis: configuration and performance of the data assimilation system. *Q. J. R. Meteorol. Soc.*, **137**, 553-597. doi: 10.1002/qj.828

Ekstrom, M., 2014: Test of WRF physics schemes for Project 6 of the Victorian Climate Initiative: An outline of selected physical parameterisation schemes and other runtime optionsRep., 36 pp, CSIRO Water for a Healthy Country Flagship, Australia

Ekström, M., 2015: Metrics to identify meaningful downscaling skill in WRF rainfall patterns, submitted to Enviromental modelling and software

Ekström, M., Grose, M. R. and P.H. Whetton, 2015: An appraisal of downscaling methods used in climate change research. *WIREs Clim. Change, 6*, 301–319, doi:10.1002/wcc.339
England, M.H. et al., 2014: Recent intensification of wind driven circulation in the Pacific and the ongoing warming hiatus. *Nature Clim. Change.* doi: 10.101038/NCLIMATE2106

Evans, J. P. and M.F. McCabe, 2010: Regional climate simulation over Australia's Murray–Darling basin: a multitemporal assessment, J. Geophys. Res., 115, D14114, doi:10.1029/2010jd013816

Fiddes, S and B. Timbal, 2015: Assessment and reconstruction of catchment streamflow in response to rainfall variability across Victoria, accepted, *Clim. Res.*

Foley, A. M., 2010: Uncertainty in regional climate modelling: A review, Progress in Physical Geography, 34(5), 647-670

Fowler, H. J., Blenkinsop, S., and C. Tebaldi, 2007: Linking climate change modelling to impacts studies: recent advances in downscaling techniques for hydrological modelling, Int. J. Climatol., 27, 1547–1578, doi:10.1002/joc.1556, 2007.

Gillett, N. P., J. C. Fyfe, and D. E. Parker, 2013: Attribution of observed sea level pressure trends to greenhouse gas, aerosol, and ozone changes, *Geophys. Res. Lett.*, **40**, 2302–2306, doi:10.1002/grl.50500

Giorgi, F., 2008: Regionalization of climate change information for impact assessment and adaptation. *Bulletin - World Meteorological Organization,* 57, available at: http://www.wmo.int/pages/publications/bulletinarchive/archive/57_2_en/giorgi_en.html

Grose, M. et al. 2015: Southern Slope Cluster Report, Climate Change in Australia Projections for Australia's Natural Resource Management Regions: Cluster Reports, eds. Ekström, M. et al., CSIRO and Bureau of Meteorology, Australia

Grose, M., B. Timbal, L. Wilson, J. Bathols and D. Kent, 2015: The subtropical ridge in CMIP5 and implications for projections of rainfall in southeast Australia, *Australian Meteorological and Oceanographic Journal*

Haagenson P, M.A. Shapiro, 1979: Isentropic trajectories for derivation of objectively analysed meteorological parameters. NCAR Tech Note NCAR/TN-149+STR, (December 1979), 30 pp

Held, I. M. and T. Schneider, 1999: The surface branch of the zonally averaged mass transport circulation in the troposphere. *J .Atmos. Sci.*, **56**, 1688-1697

Hendon, H. H., D. W. J. Thompson, and M. C. Wheeler, 2007: Australian rainfall and surface temperature variations associated with the Southern Hemisphere annular mode. *J. Climate*, **20,** 2452–2467

Hendon, H. H., E.-P. Lim and H. Ngyuen, 2014: Variations of Subtropical Precipitation and Circulation associated with the Southern Annular Mode, *J. Climate*, **27**, 3446-3460

Hong, S.-Y., Y. Noh, and J. Dudhia, 2006: A new vertical diffusion package with an explicit treatment of entrainment processes, Monthly Weather Review, 134(9), 2318-2341

Hudson, D., A. G. Marshall, Y. Yin, O. Alves, and H. H. Hendon, 2013: Improving intraseasonal prediction with a new ensemble generation strategy. *Mon. Wea. Rev.*, **141**, 4429-4449

Huffman, G.J, R.F. Adler, D.T. Bolvin, G. Gu, 2009: Improving the Global Precipitation Record: GPCP Version 2.1. *Geophys. Res. Lett.*, **36**, L17808, doi: 10.1029/2009GL040000

Hurrell, J.W., Hack, J.J., Shea, D., Caron, J.M. and J. Rosinski, 2008: A new sea surface temperature and sea ice boundary data set for the Community Atmosphere Model. *J.*

Ihara, C., Y. Kushnir, and M. A. Cane, 2008: Warming trend of the Indian Ocean SST and Indian Ocean dipole from 1880 to 2004. *J. Climate*, **21**,2035–2046, doi:10.1175/2007JCLI1945.1

Imielska A., 2011: Seasonal climate summary southern hemisphere (summer 2010–2011): second wettest Australian summer on record and one of the strongest La Niña events on record. *Australian Meteorological and Oceanographic Journal,* **61**: 241–251

Jeffrey, S.J., Carter, J.O., Moodie, K.B. and A.R. Beswick, 2001: Using spatial interpolation to construct a comprehensive archive of Australian climate data. Environmental Modelling & Software 16, 309–330

Kendon, E. J., N. M. Roberts, C. A. Senior, and M. J. Roberts, 2012: Realism of Rainfall in a Very High-Resolution Regional Climate Model, Journal of Climate, 25(17), 5791-5806

Jia, X., J.-Y. Lee, H. Lin, H. Hendon, and K. Ha, 2014: Interdecadal change in the Northern Hemisphere seasonal climate prediction skill: part II. Predictability and prediction skill, *Clim. Dyn.,* **43**, 1611-1630, doi:10.1007/s00382-014-2084-x

Jones, D., W. Wang, R. Fawcett, 2009: High-quality spatial climate datasets for Australia. *Australian Meteorological and Oceanographic Journal*, **58**(12), 233 – 248
Jones, R.N., C.K. Young, J. Handmer, A. Keating, G.D. Mekala and P. Sheehan: Valuing adaptation under rapid change, National Climate Change Adaptation Research Facility, Gold Coast, 184 pp

Kalnay, E., M. Kanamitsu, R. Kistler, W. Collins, D. Deaven, L. Gandin, M. Iredell, S. Saha, G. White, J. Woollen, Y. Zhu, M. Chelliah, W. Ebisuzaki, W. Higgins, J. Janowiak, K.C. Mo, C. Ropelewski, J. Wang, A. Leetmaa, R. Reynolds, R. Jenne, and D. Joseph, 1996: The NCEP/NCAR 40-year reanalysis project, *Bull. Amer. Meteor. Soc., 77*, 437-470

Kiem, A. S., S. W. Franks, and G. Kuczera, 2003: Multi-decadal variability of flood risk. *Geophys. Res. Lett.*, **30**, No. 2, 1035, doi:10.1029/2002GL015992

King, A. D., L. V. Alexander, and M. G. Donat, 2013: Asymmetry in the response of eastern Australia extreme rainfall to low-frequency Pacific variability. *Geophys. Res. Lett.*, **40**, 1-7, doi:10.1002/grl.50427

Kirono, D.G.C. and D.M. Kent, 2011: Assessment of rainfall and potential evaporation from global climate models and its implications for Australian regional drought projection. *Int. J. of Climatol.*, 31, 1295–1308, doi:10.1002/joc.2165

Kosaka, Y. and S.-P. Xie, 2013: Recent global-warming hiatus tied to equatorial Pacific surface cooling. *Nature*, **501**, 403-407

Kumar, A., B. Jha, and M. L'Heureux, 2010: Are tropical SST trends changing the global teleconnection during La Niña? Geophys. Res. Lett., **37**, L12702, doi:10.1029/2010GL043394

Laprise, R., 2008: Regional climate modelling, Journal of Computational Physics, 227(7), 3641-3666

Lepioufle, J. M., E. Leblois, and J. D. Creutin, 2012: Variography of rainfall accumulation in presence of advection, Journal of Hydrology, 464, 494-504

Lim, E.-P., H. H. Hendon, D. Hudson, G. Wang and O. Alves 2009: Dynamical forecast of inter-El Niño variations of tropical SST and Australian spring rainfall. *Mon. Wea. Rev.* **137**, 3796-3810

Lim, E.-P., H. H. Hendon and H. A. Rashid, 2013: Seasonal predictability of the Southern Annular Mode due to its association with ENSO. *J. Climate*, **26**, 8037–8054

Lim, E.-P. and H. H. Hendon, 2015: Understanding the contrast of Australian springtime rainfall of 1997 and 2002 in the frame of two flavors of El Niño. *J. Climate*, **28**, 2804-2822

Lim, E.-P., H. H. Hendon, M. Zhao and Y. Yin, 2015: Inter-decadal variations in the linkages between ENSO, IOD and south-eastern Australian rainfall in the past 30 years (under internal review)

Lim, K.-S., and S.-Y. Hong, 2010: Development of an Effective Double-Moment Cloud Microphysics Scheme with Prognostic Cloud Condensation Nuclei (CCN) for Weather and Climate Models, Monthly Weather Review, 138(5), 1587-1612

Lucas, C., H. Nguyen and B. Timbal, 2012: An observational analysis of Southern Hemisphere tropical expansion. *J. Geophys. Res.*, **117**, D17112, doi:10.1029/2011JD017033

Lucas, C., H. Nguyen and B. Timbal, 2014: The expanding tropics: A critical review of the observational and modelling studies. WIRes *Climate Change*, **5**, 89-112. doi:10.1002/wcc.251

Lucas, C. and H. Nguyen, 2015: Regional characteristics of tropical expansion and the role of climate variability. *J. Geophys. Res. Atmos.*, **120**, doi:10.1002/2015JD023130

Luo, J.-J., and Coauthors, 2015: Current status of intraseasonal-seasonal-to-interannual prediction of the Indo-Pacific climate. Chapter 1 in The Indo-Pacific Climate Variability and Predictability (eds. Yamagata, T. and Behera S.), Asia-Pacific Weather and Climate book series, the World Scientific Publisher (in press)

Mansell, E. R., C. L. Ziegler, and E. C. Bruning, 2010: Simulated Electrification of a Small Thunderstorm with Two-Moment Bulk Microphysics, Journal of the Atmospheric Sciences, 67(1), 171-194

McBride, J. L., and N. Nicholls, 1983: Seasonal relationships between Australian rainfall and the Southern Oscillation. *Mon. Wea. Rev.*, **111**, 1998–2004

McMahon, T.A., M.C. Peel, and D.J. Karoly, 2015: Assessment of precipitation and temperature data from CMIP3 global climate models for hydrologic simulation. *Hydrol. Earth Syst. Sci., 19*, 361–377, doi:10.5194/hess-19-361-2015

Meyers, G.A., P.C. McIntosh, L. Pigot and M.J. Pook, 2007: The years of El Niño, La Niña and interactions with the tropical Indian Ocean. *J. Climate*, **20**, 2872-2880

Milbrandt, J. A., and M. K. Yau, 2005: A multimoment bulk microphysics parameterization. Part II: A proposed three-moment closure and scheme description, Journal of the Atmospheric Sciences, 62(9), 3065-3081

Mittermaier, M., and N. Roberts, 2010: Intercomparison of Spatial Forecast Verification Methods: Identifying Skillful Spatial Scales Using the Fractions Skill Score, Weather and Forecasting, 25(1), 343-354

Murphy, B., Timbal, B., Hendon, H. and Ekstrom, M. (Eds), 2014: Victorian Climate Initiative: Annual Report 2013-14. CAWCR Technical Report, **76**, 143pp

Nakanishi, M., and H. Niino, 2006: An improved mellor-yamada level-3 model: Its numerical stability and application to a regional prediction of advection fog, Boundary-Layer Meteorology, 119(2), 397-407

Newman, P. and E. R. Nash 2005: The Unusual Southern Hemisphere stratosphere winter of 2002. *J. Atmos. Sci.*, **62**, 614-628

Nguyen, H., Evans A., Lucas C., Smith I., Timbal B., 2013: The Hadley circulation in reanalyses: climatology, variability and expansion., *J. Climate*, **26**, 3357-3376. doi:10.1175/JCLI-D-12-00224

Nguyen H., C. Lucas, A. Evans, B. Timbal, L. Hanson, 2015a: Expansion of the Southern Hemisphere Hadley cell in response to greenhouse gas forcing. *J. Clim*ate, DOI: 10.1175/JCLI-D-15-0139.1

Nguyen H., Hendon H.H., Lim E.P., Lucas C., Maloney E. and B. Timbal, 2015b: Regional impacts of Hadley Circulation expansion in the Southern Hemisphere. In Prep. for J. Clim.

Oke, P. R., A. Schiller, D. A. Griffin, and G. B. Brassington, 2005: Ensemble data assimilation for an eddy-resolving ocean model of the Australian region. *Q. J. Roy. Met. Soc.*, **131**, 3301-3311.

Oort AH, JJ Yienger, 1996: Observed interannual variability in the Hadley circulation and its connection to ENSO. *J. Clim* **9**:2751-2767

Parker, D., C. Folland, A. Scaife, J. Knight, A. Colman, P. Baines, and B. Dong, 2007: Decadal to multidecadal variability and the climate change background. *J. Geophy. Res.*, **112**, D18115, doi:10.1029/2007JD008411

Piani, C., Weedon, G. P., Best, M., Gomes, S. M., Viterbo, P., Hagemann, S., and J.O. Haerter, 2010: Statistical bias correction of global simulated daily precipitation and temperature for the application of hydrological models, J. Hydrol., 395, 199–215, doi:10.1016/j.jhydrol.2010.10.024

Potter, N. J., F. H. S. Chiew, and A. J. Frost, 2010: An assessment of the severity of recent reductions in rainfall and runoff in the Murray–Darling Basin. Journal of Hydrology, 381, 52-64

Potter N.J. and F.H.S. Chiew, 2011: An investigation into changes in climate characteristics causing the recent very low runoff in southern Murray-Darling Basin using rainfall-runoff models. Water Resources Research, 47, W00G10

Potter N.J., C. Petheram and L. Zhang, 2011: Sensitivity of streamflow to rainfall and temperature in south-eastern Australia during the Millennium drought. In: MODSIM2011 (Editors: F Chan, D Marinova and RS Anderssen), 19th International Congress on Modelling and Simulation, Modelling and Simulation Society of Australia and New Zealand, December 2011, pp. 3636–3642, www.mssanz.org.au/modsim2011/I6/potter.pdf

Power, S., T. Casey, C. Folland, A. Colman, and V. Mehta, 1999: Interdecadal modulation of the impact of ENSO on Australia. *Climate Dyn.*, **15**,319–324, doi:10.1007/s003820050284

Power, S., M. Haylock, R. Colman, and X. Wang 2006: The predictability of interdecadal changes in ENSO activity and ENSO teleconnections. *J. Climate*, **19**, 4755-4771

Rayner, N. A., Parker, D. E., Horton, E. B., Folland, C. K., Alexander, L. V., Rowell, D. P., Kent, E. C., Kaplan, A., 2002: Global analyses of sea surface temperature, sea ice, and night marine air temperature since the late nineteenth century. *J. Geophys. Res.,* **108**, No. D14, 4407 10.1029/2002JD002670

Risbey, J.S., M.J. Pook. P.C. McIntosh, M.C. Wheeler, and H.H. Hendon, 2009: On the remote drivers of rainfall variability in Australia . *Mon. Wea. Rev.* , DOI 10.1175/2009MWR2861.1
Roberts, N., 2008: Assessing the spatial and temporal variation in the skill of precipitation forecasts from an NWP model, Meteorological Applications, 15(1), 163-169

Saji, N., B. N. Goswami, P. N. Vinayachandran, and T. Yamagata, 1999: A dipole mode in the tropical Indian Ocean. *Nature*, **401**, 360–363

Scheff, J., and D. Frierson, 2012: Twenty-first-century multimodel subtropical precipitation declines are mostly midlatitude shifts. *J. Climate*, **25**, 4330–4347

Schiller, A., J. S. Godfrey, P. C. McIntosh, G. Meyers, N. R. Smith, O. Alves, G. Wang, and R. Fiedler, 2002: A New Version of the Australian Community Ocean Model for Seasonal Climate Prediction. CSIRO Marine Research Report No. 240

Schneider, T., 2006: The general circulation of the atmosphere. *Ann. Rev. Earth Planet. Sci.*, **34**, 655-688

Schneider T, Smith KL, O'Gorman PA, Walker CC., 2006: A climatology of tropospheric zonal-mean water vapour fields and fluxes in isentropic coordinates. *J. Climate*, **19**, 5918-5933.

Schwendike, J., P. Govekar, M. J. Reeder, R. Wardle, G. J. Berry, and C. Jakob, 2014: Local partitioning of the overturning circulation in the tropics and the connection to the Hadley and Walker circulations, J. *Geophys. Res. (Atmos.)*, **119**, 1322–1339, doi:10.1002/2013JD020742

Taylor, K. E., R. J. Stouffer, et al., 2012: An Overview of CMIP5 and the Experiment Design. Bulletin of the American Meteorological Society 93(4): 485-498

Teng, J., Potter, N.J., Chiew, F.H.S., Zhang, L., Wang, B., Vaze, J., and J.P. Evans, 2015: How does bias correction of regional climate model precipitation affect modelled runoff?, *Hydrol. Earth Syst. Sci.*, 19, 711-728, doi:10.5194/hess-19-711-2015

Thompson, D.W.J., M.P. Baldwin, and S. Solomon, 2005: Stratosphere-troposphere coupling in the Southern Hemisphere. *J. Atmos. Sci.*, **62**, 708-715

Thompson, G., P. R. Field, R. M. Rasmussen, and W. D. Hall, 2008: Explicit Forecasts of Winter Precipitation Using an Improved Bulk Microphysics Scheme. Part II: Implementation of a New Snow Parameterization, Monthly Weather Review, 136(12), 5095-5115

Timbal, B., 2010: A discussion on aspects of the seasonality of the rainfall decline in South-Eastern Australia. CAWCR Research Letters, 4, 20-27

Timbal, B., J. Arblaster and S. Power, 2006: Attribution of the late 20th century rainfall decline in South-West Australia. *J. of Climate*, **19(10)**, 2046-2062
Timbal, B. et al. 2015: Murray Basin Cluster Report, Climate Change in Australia Projections for Australia's Natural Resource Management Regions: Cluster Reports, eds. Ekström, M. et al., CSIRO and Bureau of Meteorology, Australia

Timbal, B., M. Griffith, and K.S. Tan, 2015: Rainfall and streamflow in Greater Melbourne catchment areas: variability and recent anomalies, Clim. Res., 63, 215-232, doi:10.3354/cr01296

Timbal, B., M. Griffith, M. and K.S. Tan, 2015a: Rainfall and streamflow in Greater Melbourne catchment areas: variability and recent anomalies, Clim. Res., doi:10.3354/cr0129

Timbal, B. and H. Hendon, 2011: The role of tropical modes of variability in recent rainfall deficits across the Murray-Darling Basin. Water Resources Research, 47, W00G09, 10.1029/2010wr009834

Timbal B, L. Wilson L and D. Kirono, 2015b: Understanding Victorian rainfall projection uncertainties: the influence of tropical warming patterns. To be submitted to the Journal of Climate

Townsend R.D., D.R. Johnson., 1985: A diagnostic study of isentropic zonally averaged mass circulation during the First GARP Global Experiment. *J. Atmos. Sci.*, **42**, 1565-1579

Ummenhofer, C., A. Sen Gupta, Y. Li, A. S. Taschetto, and M. H. England, 2011: Multi-decadal modulation of the El Niño–Indian monsoon relationship by Indian Ocean variability. *Environ. Res. Lett.*, **6**, 034006, doi:10.1088/1748-9326/6/3/034006

Valke, S., L. Terray, and A. Piacentini, 2000: The OASIS coupled user guide version 2.4, Technical Report TR/ CMGC/00-10, CERFACS

Verdon-Kidd, D. and A. Kiem, 2009: Nature and causes of protracted droughts in southeast Australia: Comparison between the Federation, WWII, and Big Dry droughts. Geophysical Research Letters, 36, doi:10.1029/2009GL041067

Wang, G., O. Alves, and N. Smith, 2005: BAM3.0 tropical surface flux simulation and its impact on SST drift in a coupled model. BMRC Research Rep. 107, 30 pp

Wang, G. and H.H. Hendon, 2007: Sensitivity of Australian rainfall to inter-El Niño variations. *J. Climate*, **20**, 4211–4226

Watkins, A.B., 2003: Seasonal climate summary southern hemisphere (spring 2002): the El Niño reaches maturity and dry conditions dominate Australia. *Aust. Met. Mag.* **52**, 213-226

Weller, E., W. Cai, Y. Du, and S.-K. Min, 2014: Differentiating flavors of the Indian Ocean Dipole using dominant modes in tropical Indian Ocean rainfall. *Geophys. Res. Lett.*, **41**, doi:10.1002/2014GL062459

Wilby, R. L., Hay, L. E., Gutowski, W. J., Arritt, R. W., Takle, E. S., Pan, Z., Leavesley, G. H., and M.P. Clark, 2000: Hydrological responses to dynamically and statistically downscaled climate model output, Geophys. Res. Lett., 27, 1199–1202

Yin, J., 2005: A consistent poleward shift of the storm tracks in simulations of 21st century climate. *Geophys. Res. Let.*, **32**, L18701,doi:10.1029/2005GL023684

Zhao, M., H. H. Hendon, O. Alves, G. Liu and G. Wang 2015: Weakened El Niño predictability in the early 21st Century, *submitted to Nature Geoscience*

GLOSSARY

Cool season

For rainfall it is defined as the seven months from April to October (inclusive); for streamflow it is defined from May to November and corresponds to the main filling period.

CMIP3- CMIP5

CMIP3 refers to the third Coupled Model Intercomparison Project, or more typically, the global climate models involved in this project. They are also the models used in the IPCC Fourth Assessment Report. CMIP5 refers to the fifth Coupled Model Intercomparison Project, or more typically, the global climate models involved in this project. They are also the models used in the IPCC Fifth Assessment Report. Note that to make the numbers line up with the IPCC Assessment Reports, there was no CMIP4.

Downscaling

Commonly, so called downscaling methods are used to derive estimates of local scale climate variables from large-scale global climate model outputs. These methods are typically classed as either statistical or dynamical, where the former includes regression or weather pattern based relationships between large and local scale variables and the latter refers to the use of a fine-scale regional climate model.

El Niño – Southern Oscillation (ENSO)

The El Niño – Southern Oscillation is a Pacific wide oscillation; it can be in an El Niño, La Niña or neutral state. El Niño conditions tend to bring drier conditions to south-eastern Australia, while La Niña conditions tend to bring wetter conditions; they tend to occurs every 2 to 5 years. It is quantified using the several measures, most commonly used in that report are SST anomalies across Equatorial Pacific Basin (NINO3 or NINO3.4).

Hadley circulation - Hadley cell (HC)

The Hadley circulation is the large-scale atmospheric circulation that transports heat from the tropics to the sub-tropics. The Hadley cell is the name given to each of the two cells of the Hadley circulation, typically the southern hemisphere cell as used in this report.

Indian Ocean Dipole (IOD)

The Indian Ocean Dipole is a coupled ocean-atmosphere climate mode that occurs inter-annually in the tropical parts of the Indian Ocean. When the western Indian Ocean is warmer than the eastern part of the ocean, it is termed a positive IOD and it tends to bring drier conditions to south-eastern Australia. The opposite phase is termed a negative IOD and tends to bring wetter conditions to south-eastern Australia. It is quantified using the dipole mode index (DMI) based on the measured difference between sea-surface temperature in the western (50°E to 70°E and 10°S to 10°N) and eastern (90°E to 110°E and 10°S to 0°S) equatorial Indian Ocean.

Interdecadal Pacific Oscillation (IPO)- Pacific Decadal Oscillation (PDO)

The Interdecadal Pacific Oscillation is the Pacific-wide manifestation of the Pacific Decadal Oscillation (PDO). It is an El Niño-like pattern of sea surface temperature that varies on decadal time scales. The IPO has a positive phase, when temperatures in the equatorial eastern Pacific are above normal and the trade winds are relaxed, that was last active from 1977 to 1998; and a negative phase, when temperatures in the equatorial eastern Pacific are colder than normal and the trade winds are enhanced, that has been the active from 1999 to 2014. The phase modulates the relative frequency of El Niño and La Niña events and their predictability. The Pacific Decadal Oscillation—related to the IPO but defined based on surface temperatures across the North Pacific region.

Mean meridional circulation (MMC)

The mean meridional circulation refers to the overall atmospheric circulation of the Earth, transporting heat and moisture from the tropics towards the poles. It includes the Hadley circulation.

NINO, NINO3.4 and NINO4

One measure of the state of the ENSO based on the sea-surface temperature in the central Pacific Ocean and used to indicate whether it is in an El Niño, La Niña, or neutral state.

Reanalysis dataset

These are synthesised assimilation of historical datasets that aim to describe the state of the climate system in a consistent manner.

Southern Annular Mode (SAM)

The Southern Annular Mode is the leading mode of climate variability over the Southern Ocean, controlling passage of westerlies and embedded frontal weather systems. It is measured by the strength of westerly winds across southern Australia based on the difference between the surface pressure at 40 and 65°S. Positive SAM phases typically result in weaker westerly winds and therefore drier conditions across the western part of south-eastern Australia in winter. In summer, the main impact is an increase in easterly winds, leading to wetter conditions across the eastern part of south-eastern Australia.

Sub-tropical ridge (STR)

The region of high pressure that exists across the mid-latitudes resulting from the descending branch of the Hadley circulation; in this report three different measures of the subtropical ridge are considered: global across the entire southern hemisphere, regional (60°E to 175°W) and local (140°E to 150°E). The first two are computed using re-analyses while the last one can either be computed using reanalyses or MSLP observations from the Bureau of Meteorology.

Teleconnection

A statistical association between climate variables at widely separated geographical locations. For example, the rainfall pattern associated with El Niño sea surface temperature anomalies in the Pacific.

Warm season

For rainfall it is defined as the five months from November to March (inclusive), for streamflow it is from December to April.

Walker circulation

The atmospheric circulation that occurs across the tropical Pacific Ocean with air rising above warmer ocean regions (normally in the west), and descending over the cooler ocean areas (normally in the east). Its strength fluctuates with that of the Southern Oscillation.

Water availability

For the purposes of this report, water availability is synonymous with surface water runoff or streamflow from mid-sized catchments (50–2000 km^2).